AD-A054 466 XEROX CORP/ELECTRO-OPTICAL SYSTEMS PASADENA CALIF F/G 13/1
THERMAL ENERGY STORAGE DEMONSTRATION UNIT FOR VUILLEUMIER CRYOG--ETC(U)
OCT 77 R RICHTER F33615-75-C-2045
UNCLASSIFIED 2340-F AFAPL-TR-77-65 NL

1 OF 2
AD A054466

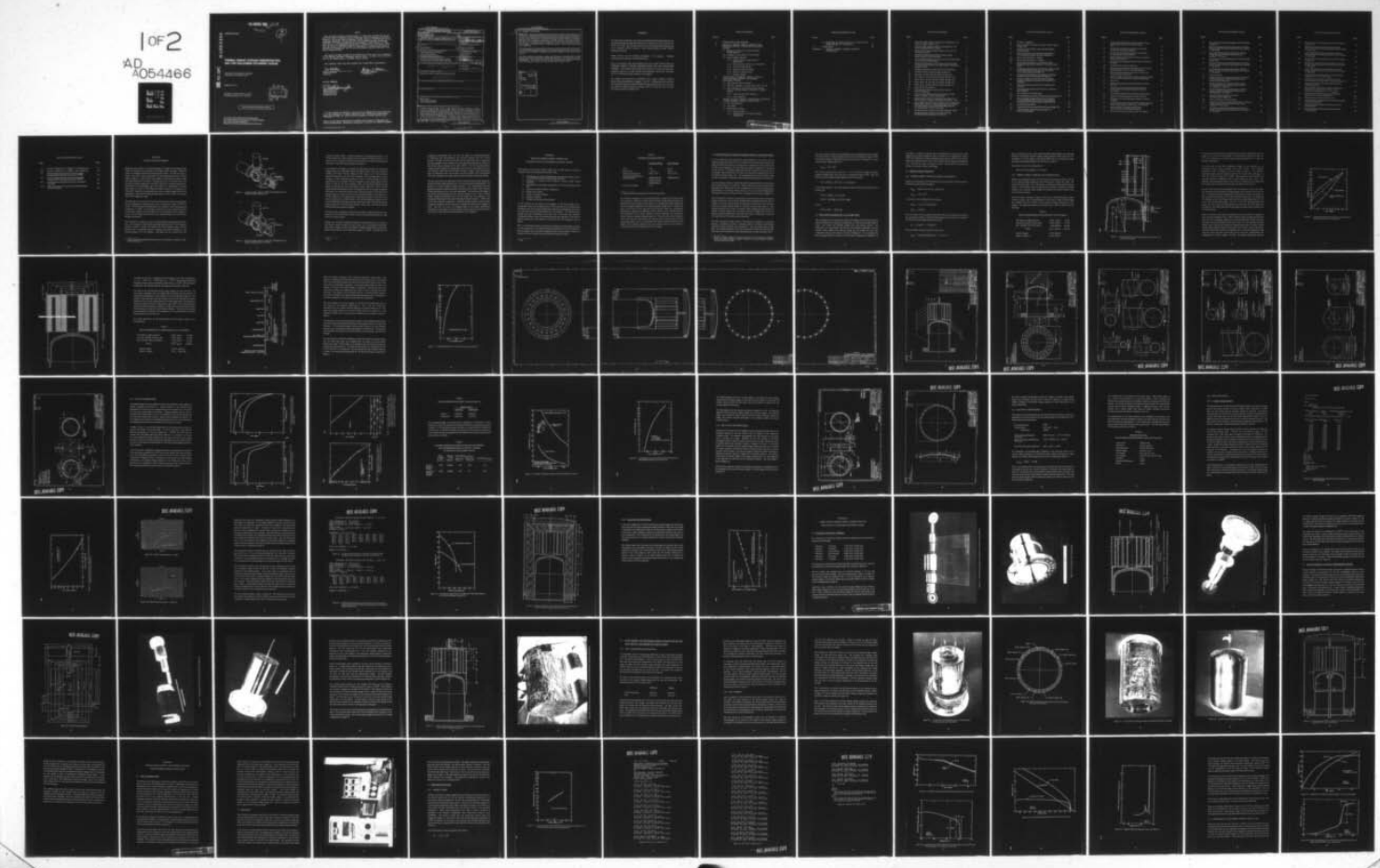

FOR FURTHER TRAN

A040895

2

AD A054466

DDC FILE COPY

AFAPL-TR-77-65

THERMAL ENERGY STORAGE DEMONSTRATION UNIT FOR VUILLEUMIER CRYOGENIC COOLER

XEROX ELECTRO-OPTICAL SYSTEMS
PASADENA, CALIFORNIA 91107

FEBRUARY 1978

DDC
RECEIVED
JUN 1 1978
E

TECHNICAL REPORT AFAPL-TR-77-65
Final Report October 1976 – July 1977

Approved for public release; distribution unlimited.

AIR FORCE AERO PROPULSION LABORATORY
AIR FORCE WRIGHT AERONAUTICAL LABORATORIES
AIR FORCE SYSTEMS COMMAND
WRIGHT-PATTERSON AIR FORCE BASE, OHIO 45433

NOTICE

When Government drawings, specifications, or other data are used for any purpose other than in connection with a definitely related Government procurement operation, the United States Government thereby incurs no responsibility nor any obligation whatsoever; and the fact that the government may have formulated, furnished, or in any way supplied the said drawings, specifications, or other data, is not to be regarded by implication or otherwise as in any manner licensing the holder or any other person or corporation, or conveying any rights or permission to manufacture, use, or sell any patented invention that may in any way be related thereto.

This report has been reviewed by the Information Office (OI) and is releasable to the National Technical Information Service (NTIS). At NTIS, it will be available to the general public, including foreign nations.

This technical report has been reviewed and is approved for publication.

Tom Mahefkey
PROJECT ENGINEER
AFAPL/POE

Jerry E. Beam
PROJECT ENGINEER
AFAPL/POE-2

FOR THE COMMANDER

R. Barthelemy for
JOSEPH F. WISE, TECH MGR
Solar Energy Conversion
Energy Conversion Branch
Aerospace Power Division

"If your address has changed, if you wish to be removed from our mailing list, or if the addressee is no longer employed by your organization please notify AFAPL/POE-2 *,W-PAFB, OH 45433 to help us maintain a current mailing list".*

Copies of this report should not be returned unless return is required by security considerations, contractual obligations, or notice on a specific document.

AIR FORCE/56780/17 April 1978 — 150

UNCLASSIFIED

SECURITY CLASSIFICATION OF THIS PAGE *(When Data Entered)*

REPORT DOCUMENTATION PAGE

READ INSTRUCTIONS BEFORE COMPLETING FORM

1. REPORT NUMBER: AFAPL-TR-77-65	2. GOVT ACCESSION NO.
3. RECIPIENT'S CATALOG NUMBER	
4. TITLE *(and Subtitle)*: THERMAL ENERGY STORAGE DEMONSTRATION UNIT FOR VUILLEUMIER CRYOGENIC COOLER	5. TYPE OF REPORT & PERIOD COVERED: Final Report 15 Oct 1976 – 31 July 1977
	6. PERFORMING ORG. REPORT NUMBER: 2340-Final
7. AUTHOR(s): Robert Richter	8. CONTRACT OR GRANT NUMBER(s): F33615-75-C-2045
9. PERFORMING ORGANIZATION NAME AND ADDRESS: Xerox Electro-Optical Systems, 300 N. Halstead Street, Pasadena, California 91107	10. PROGRAM ELEMENT, PROJECT, TASK AREA & WORK UNIT NUMBERS: Project No. 2126, Task No. 03, Work Unit No. 10
11. CONTROLLING OFFICE NAME AND ADDRESS: Air Force Aero Propulsion Laboratory/POE, Wright Patterson Air Force Base, Ohio 45433	12. REPORT DATE: October 1977
	13. NUMBER OF PAGES: 139
14. MONITORING AGENCY NAME & ADDRESS *(if different from Controlling Office)*: 16 2126 17 03	15. SECURITY CLASS. *(of this report)*: Unclassified
	15a. DECLASSIFICATION DOWNGRADING SCHEDULE

16. DISTRIBUTION STATEMENT *(of this Report)*

Approved for public release; distribution unlimited.

14 2340-F

17. DISTRIBUTION STATEMENT *(of the abstract entered in Block 20, if different from Report)*

18. SUPPLEMENTARY NOTES

19. KEY WORDS *(Continue on reverse side if necessary and identify by block number)*

Space Power
Thermal Energy Storage
Phase Change Material

20. ABSTRACT *(Continue on reverse side if necessary and identify by block number)*

A thermal energy storage unit for a High Capacity (Hi-Cap) Vuilleumier Cryogenic Cooler was designed, built and performance tested. The unit was specified to have a sufficient thermal energy storage capacity for supplying one hot cylinder of the Hi-Cap Cryogenic cooler for 18 minutes with 650W of power at a maximum power loss of 5 percent through the insulation. The discharge of the unit was to take place at a nominal temperature of 1250°F ±25°F. A thermal energy storage (TES) unit with the hot cylinder of the Vuilleumier cooler was designed with a total thermal capacity of

DD FORM 1 JAN 73 1473 EDITION OF 1 NOV 65 IS OBSOLETE

UNCLASSIFIED

SECURITY CLASSIFICATION OF THIS PAGE *(When Data Entered)*

+ or - B → 124650

JDB

737100

20. ABSTRACT (Continued)

~~7.371 x 10^5~~ J. The thermal energy is stored in the form of latent heat of fusion in the eutectic salt composed of lithium fluoride, magnesium fluoride and potassium fluoride. The unit was insulated with a multiple radiation shield super-insulation consisting of alternate layers of 0.020-inch thick Fiberfrax paper without binder and 0.001-inch Nickel foil. The insulation is maintained in a vacuum inside of an insulation container. The TES unit is instrumented for temperature control with two chromel alumel thermocouples. The single resistance temperature detector (RTD) failed during testing and is inoperative.

All specified goals for the operation of the TES unit were achieved except for the maximum thermal loss through the insulation which exceeded the goal by 8W. This deviation could easily be corrected by interposing a conduction insulation at the thermal ring of the unit.

The report presents all pertinent design and fabrication information. It includes detailed reduced test data that were generated with the unit in the performance test configuration. The Hi-Cap TES unit is fully compatible for replacing a directly electrically heated hot cylinder of a Hi-Cap Vuilleumier cryogenic cooler.

ACCESSION for
NTIS White Section X
DDC Buff Section ☐
UNANNOUNCED ☐
JUSTIFICATION
BY
DISTRIBUTION/AVAILABILITY CODES
Dist. AVAIL. and/or SPECIAL
A

FOREWORD

The information presented in this report was generated during the performance of the Thermal Energy Storage Demonstration Unit contract, Air Force Contract No. F33615-75-C-2045. The work was carried out in the Advanced Systems Department of the Radiation Systems Division of Xerox Electro-Optical Systems, (XEOS), Pasadena, California.

Robert Richter was the principal investigator of the program. Individual contributors were members of the XEOS Division.

This is a final report which was preceded by the interim report AFAPL-TR-76-110 "THERMAL ENERGY STORAGE DEMONSTRATION UNIT FOR VUILLEUMIER COOLER." The technical results which were presented in the interim report are frequently referred to as they furnished the background material for the design which was undertaken during this phase of the program.

The program was sponsored by SAMSO/SZ under Project 21260310, "Thermal Energy Storage Demonstration Program," with Mr. T. Mahefkey of the Air Force Aero Propulsion Laboratory (AFAPL/POE-2) acting as technical monitor. The work was performed during the period 15 October 1976 to 31 July 1977 with the draft final report submitted in August 1977.

TABLE OF CONTENTS

PRECEDING PAGE BLANK-NOT FILMED

TABLE OF CONTENTS (Contd)

LIST OF ILLUSTRATIONS

LIST OF ILLUSTRATIONS (Contd)

LIST OF ILLUSTRATIONS (Contd)

LIST OF ILLUSTRATIONS (Contd)

LIST OF ILLUSTRATIONS (Contd)

LIST OF ILLUSTRATIONS (Contd)

SECTION I

INTRODUCTION AND SUMMARY

During this second phase of a two-phase program,[1] a single thermal energy storage (TES) unit including the hot cylinder for the High Capacity Cryogenic Vuilleumier Cooler was designed, fabricated and performance tested. The TES unit shown in Figure 1 was to be a direct replacement for the electrically heated hot cylinder shown in Figure 2. The TES unit was to supply the Vuilleumier cryogenic cooler with 650W of power for 18 minutes. The goal was to limit the thermal losses from the thermal energy storage unit to less than 5 percent of the design output power. Furthermore, the stored energy was to be released at a temperature that would permit the hot cylinder of the Vuilleumier cooler to operate at a temperature of 1250 $\pm 25^{\circ}$F. Based on the stated goals, the thermal energy storage unit had to be designed for a total thermal energy storage capacity of 7.371×10^5 J to be released over a 50°F temperature range.

The performance test results of the unit indicated that the thermal energy storage unit was supplying the specified power over a temperature range of 1279°F to 1227°F. The total losses were determined to be 154 watt at the nominal operating temperature of 1250°F. Of these losses, a total of 113.4 watt could be attributed to conduction through the hot cylinder wall to the crankcase of the Vuilleumier cooler. The remaining 40.6 watt has to be considered losses from the TES unit through the insulation.

This insulation loss is about 8.1 watt or 25 percent above the specified goal of 32.5 watt. The temperature distribution along the outside surface of the insulation container, however, seemed to indicate that the insulation losses occurred primarily due to conduction along the radiation heat shield insulation to the mounting flange of the hot cylidner. Only about 11W are removed from the

---

1 Thermal Energy Storage Demonstration Unit for Vuilleumier Cryogenic Cooler AFAPL-TR-76-100.

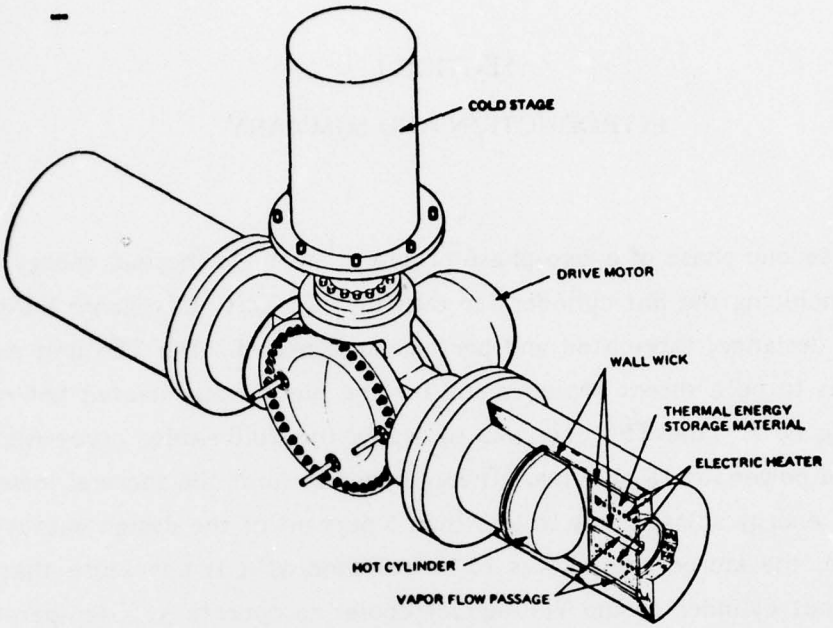

Figure 1. Long Life, High Capacity Vuilleumier Refrigerator with Thermal Energy Storage Units

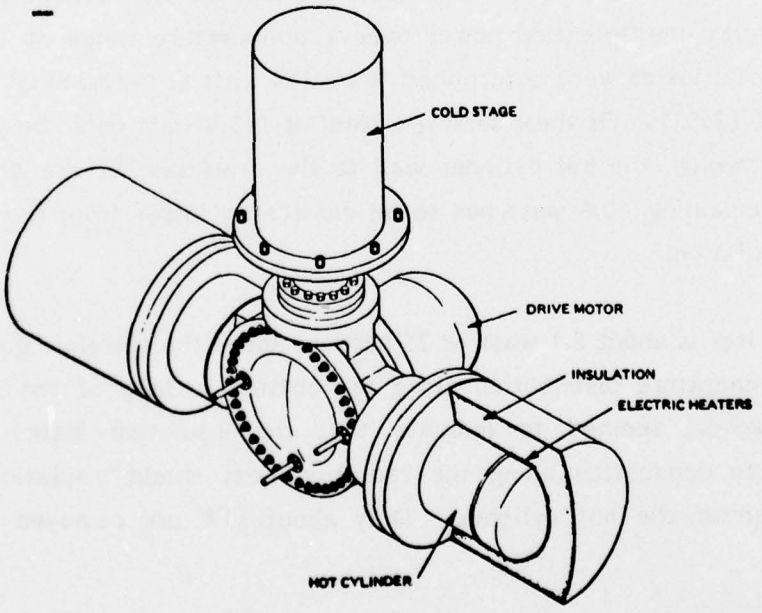

Figure 2. Long Life, High Capacity Vuilleumier Refrigerator with Battery Energized Electric Heaters

insulation container itself. It should be possible by replacing approximately 1 inch of the radiation heat shield insulation with a conduction insulation material at the flange of the hot cylinder to reduce the thermal losses and achieve the design goal with respect to thermal losses through the insulation.

In this phase of the program, the design and fabrication procedures for the thermal energy storage unit of the High Capacity Cryogenic Cooler were fully established. Changes in the basic TES unit design from the design of the 1 kW-hr Thermal Energy Demonstration Unit that was developed in the preceding phase[1] became necessary. Check calculations pointed out that the stated storage and power requirements for the Hi-Cap TES unit demanded a much larger energy transfer surface in order for the unit to operate within the specified temperature range during the discharge of the stored thermal energy. While the 1 kW-hr Thermal Energy Storage Demonstration Unit was designed for 60 watt-minutes storage per watt power, i.e., 1,000 W-hr capacity with 1 kW power output, the Hi-Cap thermal energy storage unit called for only 18 watt-minutes storage per watt power, i.e., 650 watt capacity for 18 minutes with a constant power output of 650 watt, similar to that invisioned for the SIRE mission. The thermal loading per energy transfer area would therefore have been more than three times larger in the Hi-Cap thermal energy storage unit if the same basic design as that of the 1 kW Thermal Energy Demonstration Unit had been employed.

The heat transfer calculations indicated that a different design approach had to be taken for the Hi-Cap TES unit in order to satisfy the operating temperature range of 50°F at the hot cylinder.

Initially, two resistance temperature detectors were specified for the control of the thermal energy storage unit input power and its operating temperature. Performance testing of some commercially available RTD's indicated the unreliability of such devices in the temperature regime on 1300°F. The final TES unit

---

1 Ibid

configuration incorporated only one RTD and added two ungrounded sheathed K calibration type thermocouples, one 1/16-inch diameter and one 1/8-inch diameter. Though the RTD unit had been tested extensively prior to installation and had undergone several temperature cycles, it failed during the first heat-up of the thermal energy storage unit at about 1200°F. The two remaining thermocouples controlled reliably the temperature of the TES unit. The output of the 1/8-inch diameter ungrounded thermocouple indicated a slightly lower temperature than the temperature that was incidated by bare grounded 1/16" thermocouples which were installed on the inside surface of the hot cylinder during final testing.

The test results that were generated with the Hi-Cap thermal energy storage unit verified the basic design approach which was based on good understanding of the behavior of thermal energy storage material. This understanding had been generated during the design, fabrication and testing of the 1 kW-hr Thermal Energy Storage Demonstration Unit in the preceding phase. The deviation of the design of the Hi-Cap thermal energy unit from the basic design of the 1 kW-hr Thermal Energy Storage Demonstration Unit and the design that was presented in the Conceptual Flight Device Parameter Development Study (Section V - AFPAL-TR-76-110) was completely unexpected. A general standard optimum thermal energy storage unit design for the hot cylinder of a Vuilleumier cooler does not appear to exist. Each unit will have to be designed based on the specific performance requirements with respect to thermal energy storage capacity and power demand from the unit if optimum energy storage density is to be obtained.

SECTION II

DESIGN OF THERMAL ENERGY STORAGE UNIT

FOR HIGH CAPACITY VUILLEUMIER CRYOGENIC COOLER

The design of the thermal energy storage unit for high capacity Vuilleumier cryogenic cooler encompassed several distinct tasks.

1) Development of correct thermodynamic and transport property data of the contemplated thermal energy storage material
2) Evaluation of eutectic and non-eutectic thermal energy storage materials
3) Development of the proper configuration of the thermal energy storage unit
4) Selection of electrical heater configuration
5) Design of hot cylinder
6) Design of insulation container
7) Design of insulation
8) Evaluation of suitable instrumentation

At the initiation of this phase of the program, it had been thought that a considerable amount of the design work for the Hi-Cap TES unit had already been completed under the Conceptual Flight Device Parameter Development task, which was undertaken during the preceding phase of this program.[1] The thermal energy storage and power requirements that were used in that task were, however, considerably different from the requirements that were specified for the Hi-Cap thermal energy unit of this phase as can be seen from the comparison made in Table 1.

When the temperature history of the thermal storage unit whose design was based on the configuration of the Thermal Energy Demonstration Unit was checked, it became apparent that a modified configuration had to be developed to assure the operation of the hot cylinder within the specified temperature range.

---

1 Ibid

TABLE 1

REFRIGERATOR REQUIREMENTS

	Conceptual Design	Present Design
Orbit	12 hr	72 min.
Eclipse Time	1 $\pm$ 0.1 hr	18 min.
Operating Temperature	1250° $\pm$ 25°F	1250° $\pm$ 25°F
Total Power Requirement/ Storage Capacity	1000W/1000 Whr*	1300W/400 Whr*
	1500W/1500 Whr	
	2000W/2000 Whr	
No. of Hot Cylinders	1 or 2	2

* Single hot cylinder demonstration hardware design points.

The modified configuration that evolved demanded a change in the heater design and its location. While the 1 kW-hr Thermal Energy Storage Demonstration Unit contained the heater elements which operate at a considerably higher temperature than the average temperature of the thermal energy storage unit, in a heater well close to the center of the unit, the Hi-Cap thermal energy unit configuration demanded the placement of additional heater elements at the outside surfaces. This distribution of the heater elements modified drastically the temperature profile across the thermal energy storage unit. Thus, the outer surface temperature of the TES unit which affects the thermal losses from the unit was to be considerably higher. This in turn demanded that greater attention be given to the design of the insulation, especially since the maximum loss was to be limited to only 5 percent of the nominal power of the hot cylinder.

2.1 BACKGROUND EVALUATION OF THERMAL ENERGY STORAGE MATERIAL

From the experience that was gained in the development of the 1 kW-hr Thermal Energy Storage Demonstration Unit, the behavior of the eutectic TES material LiF-MgF_2-KF during the release of its energy which is stored in the form of latent heat of fusion was recognized as the most important design consideration for sizing the Hi-Cap TES unit. The phase change energy and the temperature range over which the energy is being released are the two major parameters influencing the size of the thermal energy storage unit. The understanding of the fusion energy release process was therefore considered a major background requirement for the program.

Since the literature does not furnish any detailed experimental data concerning the phase change behavior of eutectics, a distinct effort had to be directed towards generating some design data for the contemplated TES materials, and gaining an understanding of the energy release process of the eutectic 64LiF-30MgF_2-6KF. The approach and the test results of that investigation are compiled in Appendix A.

Three independent methods for measuring the thermal energy release during phase change are reported. Two methods, the Differential Scanning Calorimeter and the testing of an actual thermal energy storage device, produced the most consistent values for the phase change energy of a thermal energy storage material. Both methods indicated that at least two distinct phase changes take place during the release of thermal energy from the ternary eutectic LiF-MgF_2-KF and that the energy was being released over a relatively wide range of temperature rather than at a single "eutectic" transformation temperature.

The drop calorimeter method used for determining the enthalpy of a specimen requires a considerable number of individual tests for producing a well defined correlation between enthalpy and temperature. Still, the second phase change below the melting temperature that was obvious from the DSC and the TES unit tests, could not be detected from the data produced by the drop calorimeter test.[2]

---

2 Bimonthly Progress Report for Period Ending 8-15-76: "Evaluation of Inorganic Oxides for Thermal Energy Storage," University of Dayton Research Institute Contrat F33615-76-C-2096.

The most important result of the investigation was the establishment of the amount of latent heat that is being released over the specified temperature range of $50^{o}F$. The Thermal Energy Storage Demonstration Unit has been designed for a total thermal energy storage capacity of

$$C_{TES} = 4.37 \times 10^{6} J$$

The test data indicate that a total of $E = 2.77 \times 10^{6} J$ of the energy was relased during the solidification of the salt over a temperature range of $50^{o}F$. Thus, the effective thermal energy storage capacity of the unit was only

$$(2.77 \times 10^{6}/4.32 \times 10^{6}) \times 100 = 64.12 \text{ percent}$$

of the design capacity. This means that the effective latent heat of fusion of the eutectic salt

30 LiF - 64 MgF_3 - 6 KF by mole

42.8 LiF - 48.2 MgF_2 - 9.0 KF by weight

is only

$$0.6412 \times 788.4 = 505.52 \text{ J/g}$$

2.2 EVALUATION OF NON-EUTECTIC SALT MIXTURES

The investigation of the eutectic salt made of LiF, MgF_2 and KF indicate that the effective latent heat of fusion was considerably less than the ideal latent heat of fusion. The eutectic salt actually behaved like a non-eutectic mixture. The employment of a non-eutectic salt mixture was therefore considered if such a mixture should release more thermal energy per unit weight over the same temperature range as the eutectic mixture LiF-MgF_2-KF. As an example the thermal energy release of mixtures, of LiF and NaF is presented in Appendix A of

this report. It seems to indicate that no combination of these two salts would release as much thermal energy per gram of mixture over the temperature range of 50°F at the required hot cylinder operating temperature of 1250°F as the eutectic mixture that had been used in the 1 kW-hr Thermal Energy Storage Demonstration Unit. The idea of using a non-eutectic mixture was therefore not pursued any further, as it seemed to have no advantage.

2.3 GENERAL DESIGN APPROACH

2.3.1 THERMAL ENERGY STORAGE MATERIAL REQUIREMENT

Based on the evaluation of the TES material, the total amount of TES material for storing the required thermal energy of

$$E_{TES} = 650W \times 1.05 \times 18 \text{ min.} \times 60 \text{ sec/min.}$$

$$E_{TES} = 7.371 \times 10^5 J$$

in the eutectic salt LiF-MgF_2-KF was therefore

$$W_{TES} = 7.371 \times 10^5 \text{ J}/505.52 \text{ J/g}$$

$$W_{TES} = 1458.03 \text{ g}$$

The total volume that is occupied by the TES material was calculated by assuming the same specific weight of the liquid TES material that was used in the design of the Thermal Energy Storage Demonstration Unit.

$$\rho_L = 2.13 \text{ g/cm}^3 = 31.324 \text{ g/in.}^3$$

Thus, the volume of the Hi-Cap TES unit has to be

$$V_{TES} = 1458.1025 \text{ g}/34.904 \text{ g/in.}^3 = 41.775 \text{ in.}^3$$

Since no distortion of the 1 kW-hr Thermal Energy Demonstration Unit had been observed, the effective thermal energy storage material volume was also to be increased in the final design of the Hi-Cap TEST unit by 5 percent by simply increasing the calculated length of the TES unit by 5 percent.

The eutectic salt was to be prepared from

624.2 g LiF, 703.0 g MgF_2 and 131.0 g KF

2.3.2 THERMAL ENERGY STORAGE UNIT CONFIGURATION

Based on the established amount of TES material and its volume, the first lay-out of the thermal energy storage unit for the Hi-Cap hot cylinder was made. The layout restricted itself to the incorporation of standard available Inconel 600 pipe material. The difficulty that was experienced in finding a qualified and willing vendor to form thermal energy storage unit cylinders out of plate material made this restriction necessary.

The first iteration indicated a length of 4.107 inch for the thermal energy storage material container and an outside diameter of 5.373 inch in a basic TES unit design that evolved from the 1 kW-hr Thermal Energy Storage Demonstration Unit program. The weight distribution for this design which is shown in Figure 3 was the following:

TABLE 2

WEIGHT DISTRIBUTION OF TWO-ANNULAR TES UNIT DESIGN

TES Material (MgF_2-LiF-KF)	1,458.1 grams	31.2%
Structural Material (Inconel 600)	2,674.6 grams	57.2%
Wick (Bolting cloth and sodium)	540.3 grams	11.6%
TOTAL	4,673.0 grams	100.0%
Specific Weight	52.78 lb/kW-hr	
Specific Capacity	18.94 W-hr/lb	

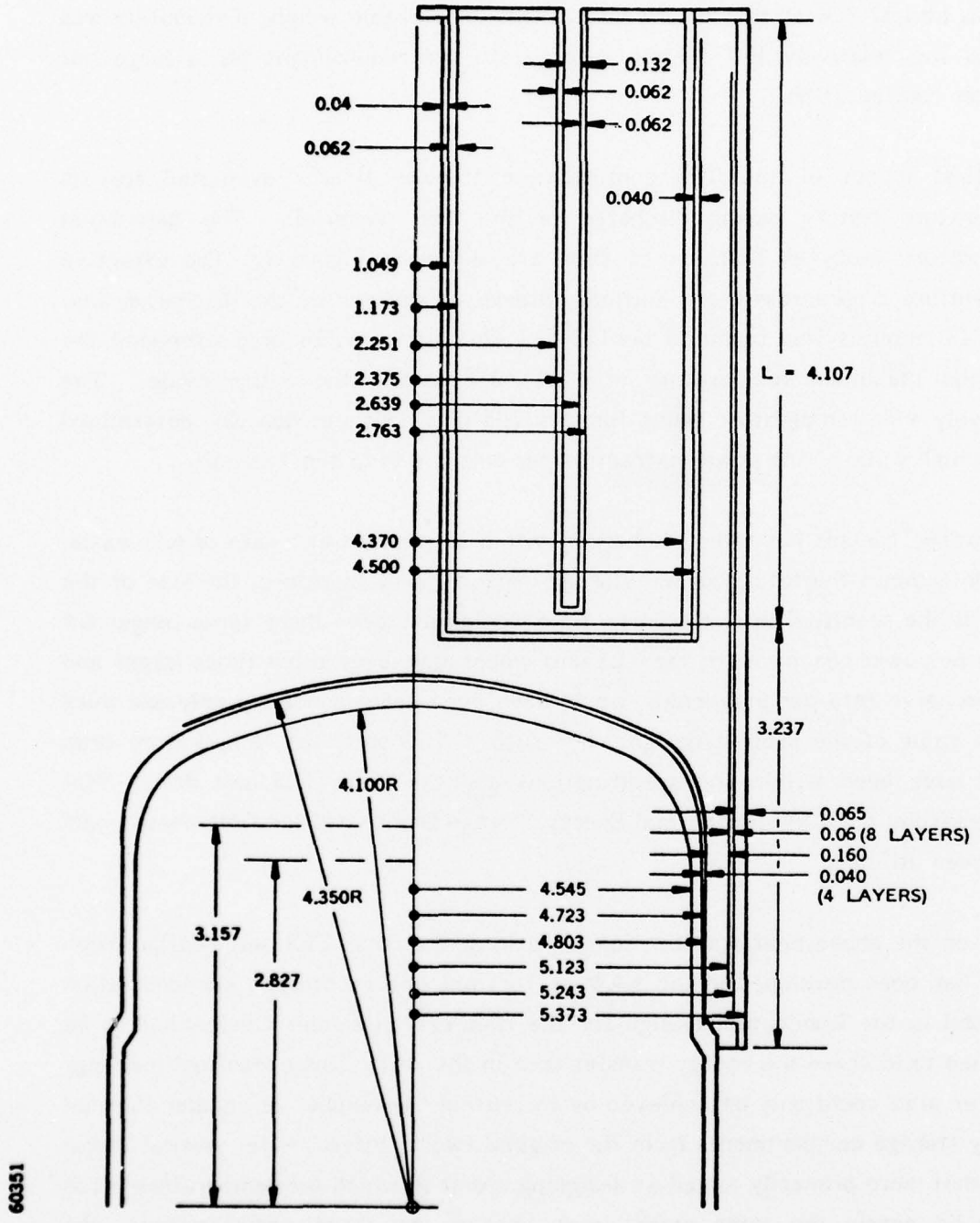

Figure 3. Initial Hi-Cap Thermal Energy Storage Unit Layout with Hi-Cap Hot Cylinder

It was obvious that the structural material was demanding a considerable amount of weight, i.e., 57.2 % of the total weight. This unfavorable weight distribution was due to the relatively low thermal energy storage requirement for a large hot cylinder configuration.

The first layout of the TES configuration (Figure 3) was evaluated for its temperature history during discharge of the TES material. The calculated temperature drops as function of time are shown in Figure 4. The effective temperature drop across the solidified material at the end of the discharge, i.e., after 18 minutes was found to be $122^{o}F$. This temperature drop exceeded the specified maximum temperature drop of $50^{o}F$ during the entire cycle. The relatively wide temperature swing for this TES unit configuration was determined by the high value of the power extraction per unit length of the TES unit.

The entire TES unit has to be discharged within 18 minutes at a rate of 650 watts. This determines the total thermal storage capacity and, therefore, the size of the unit. If the specified total discharge time would have been three times longer for the same power requirement, the TES unit would have been three times larger and the discharge rate per unit length would have been correspondingly only one third of the value of the present design. For such a TES unit, the temperature drop would have been within the specifications and the basic TES unit design that evolved from the 1 kW-hr Thermal Energy Storage Demonstration Unit phase could have been utilized.

Based on the above heat transfer considerations, the basic TES unit configuration which had been developed in the 1 kW-hr Thermal Energy Storage Demonstration Unit and in the Conceptual Design for the Hi-Cap Vuilleumier Cooler, had to be modified to increase the energy transfer area in the unit. This expansion in energy transfer area could only be achieved by increasing the number of annular thermal energy storage compartments from the original two to three. After several iterations that were primarily aimed at designing a unit in which the temperature drops would be nearly the same across each one of the three compartments, the configuration as shown in Figure 5 evolved. The highest temperature drop was

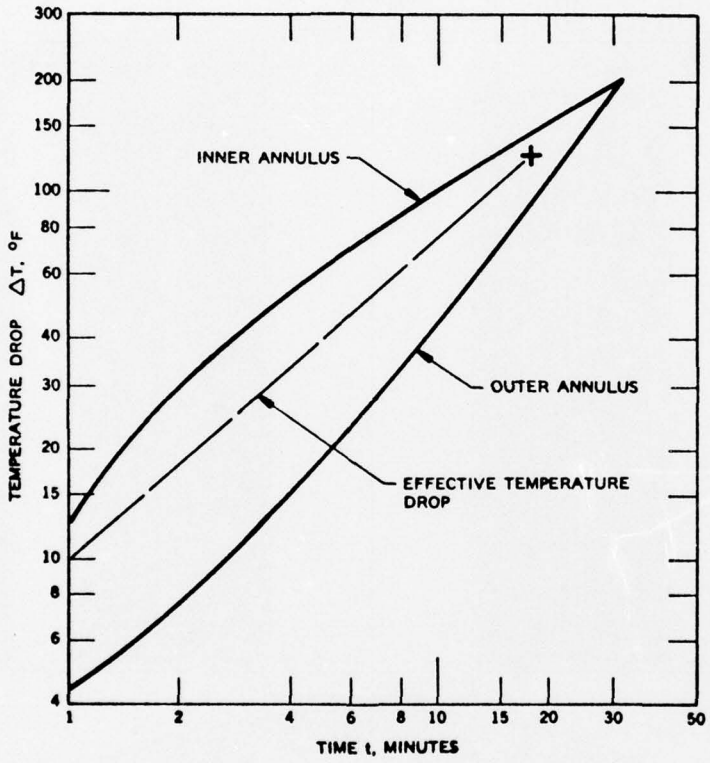

Figure 4. Temperature Drop Across Thermal Energy Storage Material During Time of Discharge

60320

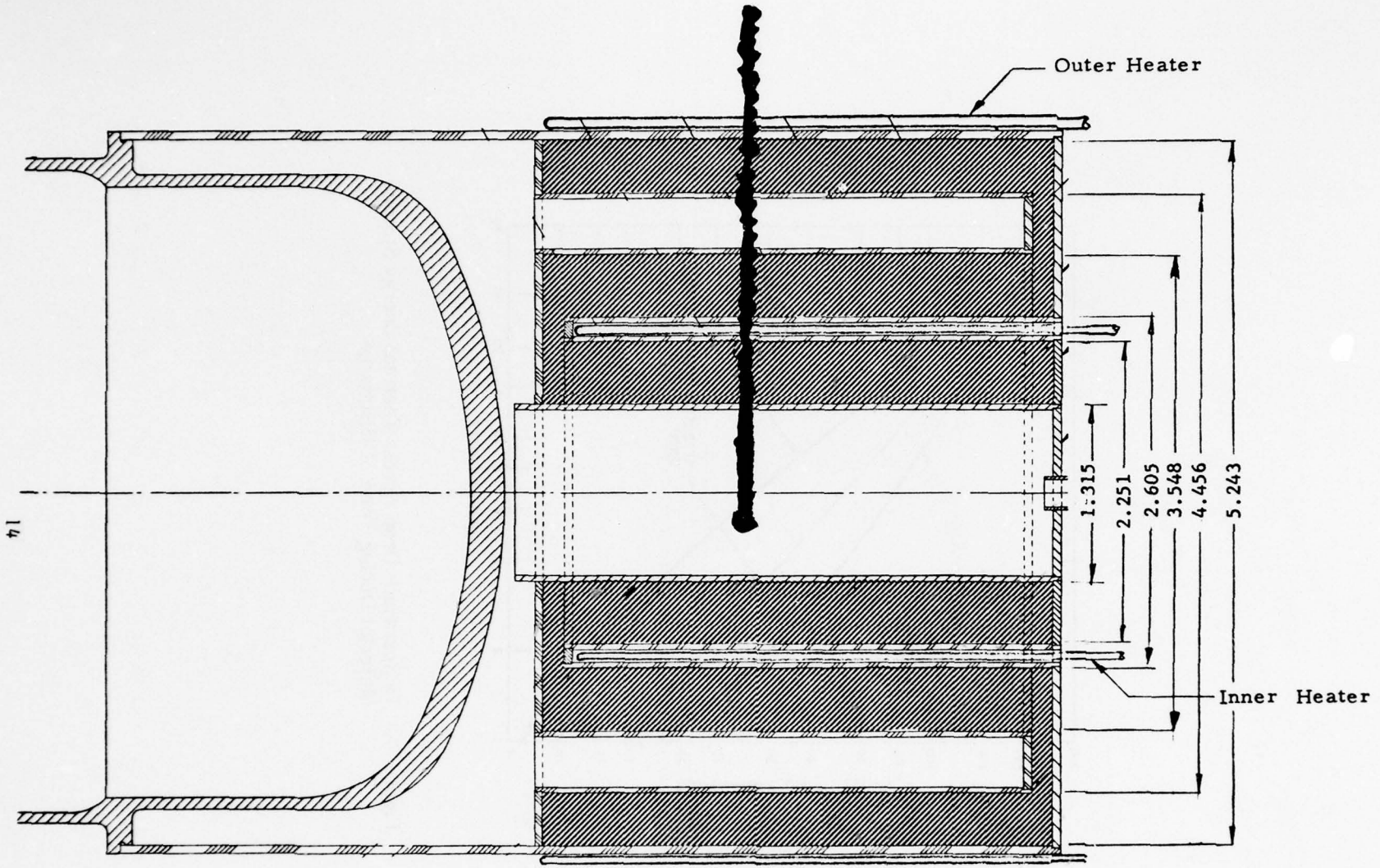

Figure 5. Thermal Energy Storage Unit Lay-Out for Hi-Cap Vuilleumier Cooler (Three-Annular Design)

calculated for the inner compartment and the lowest for the outer compartment, i.e., ΔT_I = 40.3°F, ΔT_C = 38.8°F, and ΔT_O = 27.5°F. The anticipated effective temperature drop was to be the highest of the three, i.e., 40.3°F. The temperature distribution in the TES unit based on this design was that shown in Figure 6.

The length of the three-annular thermal energy storage unit was 3.710 inch. The most drastic divergence from the original TES unit design was the need for an additional heating element on the outside of the thermal energy storage unit. But because of the relatively large heat transfer area and the relatively low power requirement for the outer heater element, the heater temperature was expected to exceed the average TES unit temperature by only 144°F. This increased surface temperature was anticipated to contribute to higher thermal losses than would have been experienced without the outside heater element. The total thermal losses were estimated to be 34.4W for this configuration. This compared with a maximum allowable thermal loss of 32.5 watt.

The weight distribution for the three-annular TES unit design is shown in the following table.

TABLE 3

WEIGHT DISTRIBUTION OF THREE-ANNULAR TES UNIT DESIGN

TES Material (MgF_2-LiF-KF)	1,458.1 grams	35.26%
Structural Material (Inconel 600)	2,338.5 grams	56.56%
Wick (Bolting Cloth and Sodium)	338.1 grams	8.18%
TOTAL	4,134.7 grams	100.00%
Specific Weight	46.704 lb/kW-hr	
Specific Capacity	21.41 watt-hr/lb	

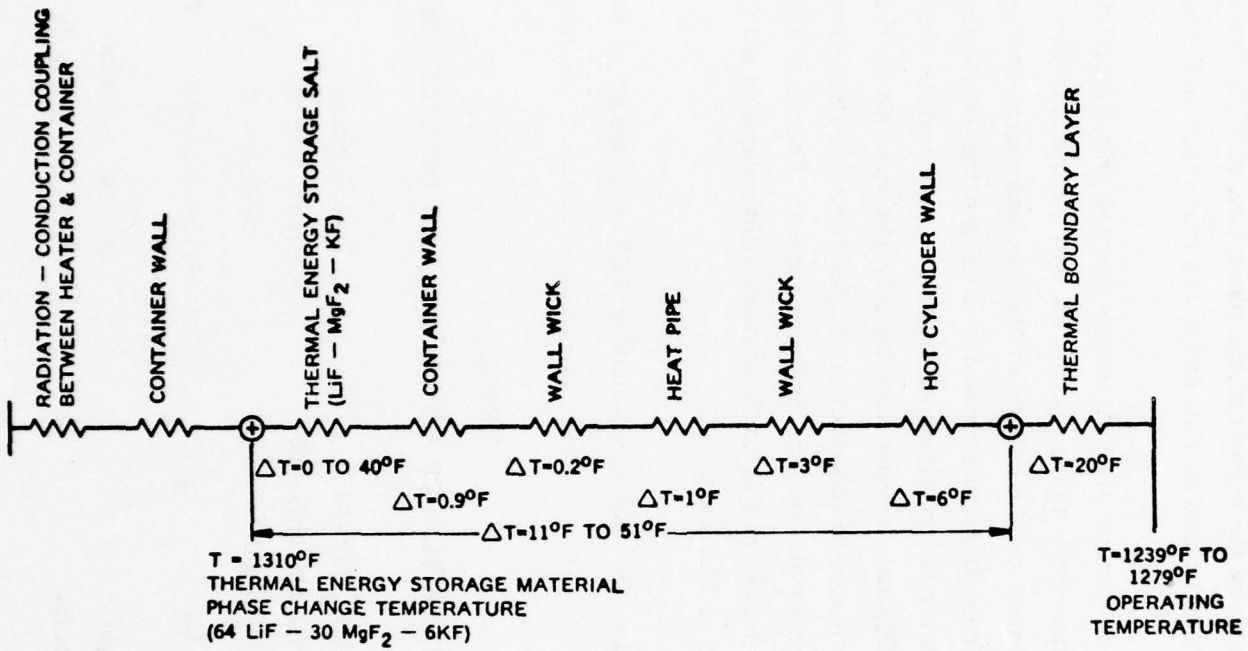

Figure 6. Temperature Distribution in the Thermal Energy Storage Unit and the Hot Cylinder of the High Capacity Vuilleumier Cryogenic Cooler

When the original two-annular TES material compartment design (Table 2 and Figure 3) is compared with the three-annular TES unit design, it has to be realized that in the three-annular design, the wick structure has been reduced in size, as the outer wick was decreased in thickness. In the three-annular design the outer wick became a structure across which energy is transferred. The thickness had to be minimized to reduce the temperature drop across it and to maximize the vapor flow pass. The weight of the structural material in the three-annular design is lower than the weight of the original design approach because the wall thickness of the inner components of the TES unit were decreased to 0.040 inch.

The wall thickness of the outer cylinder of the TES unit remained 0.062 inch, as was required by the pressure differential of 1 atm. The very conservative assumption, that the cylinder would be exposed to a pressure difference of 1 atm when the cylinder material is hot, and a safety factor of 4 called for a wall thickness of 0.060 inch to assure structural stability of the cylinder, as shown in Figure 7.

The adequacy of the wick design had been verified in the Conceptual Design Study which was conducted during the initial phase of the program and did not need to be repeated. The dominating pressure drop had been found to be the elevation pressure which is associated with the large diameter of the TES unit. The diameter was dictated by the diameter of the hot cylinder of the V/M cooler, which had not changed.

The hot cylinder of the Hi-Cap Vuilleumier cooler with the thermal energy storage unit was 12.04 inches long. This compared with the length of the electrically heated hot cylinder of 7.44 inches, i.e., the length of the hot cylinder structure has increased by only 62 percent. The total outside surface was increased from 259 $inch^2$ to 383 $inch^2$, i.e., 48 percent. The hot cylinder with the insulation container is shown in the assembly drawing (Figure 8). The detail drawings are presented in Figure 9.

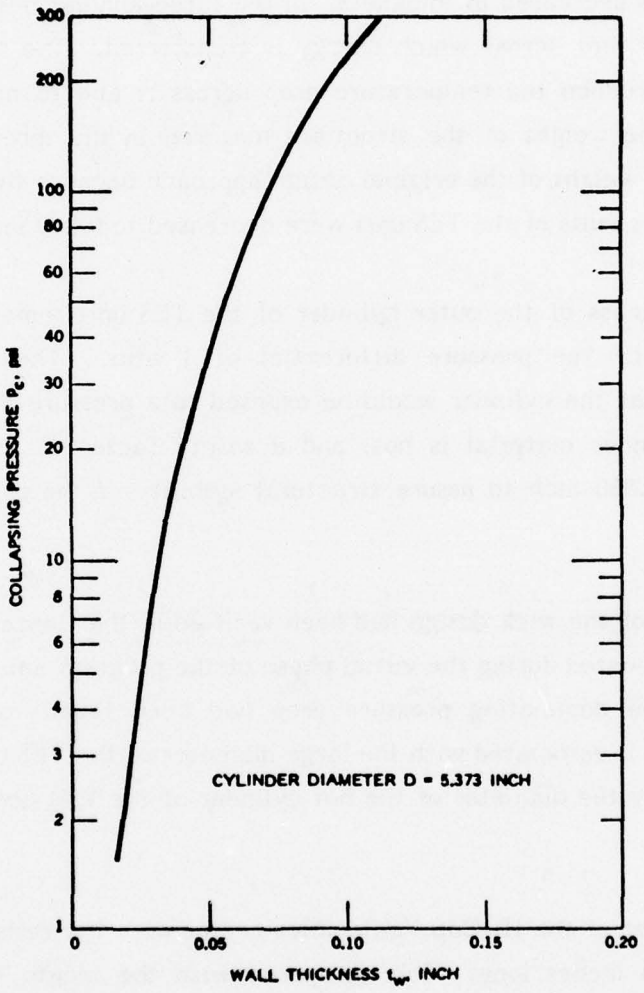

Figure 7. Collapsing Pressure for Outer Tube of Hi-Cap TES Unit

60319

SECURITY CLASSIFICATION

NOTES: UNLESS OTHERWISE SPECIFIED

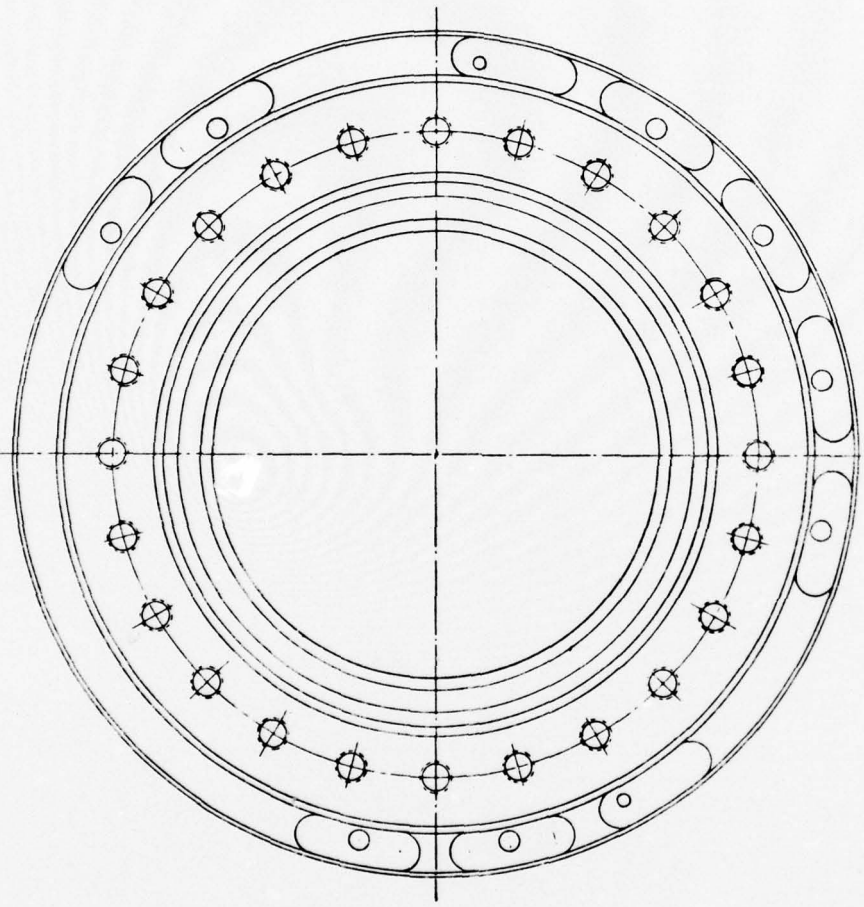

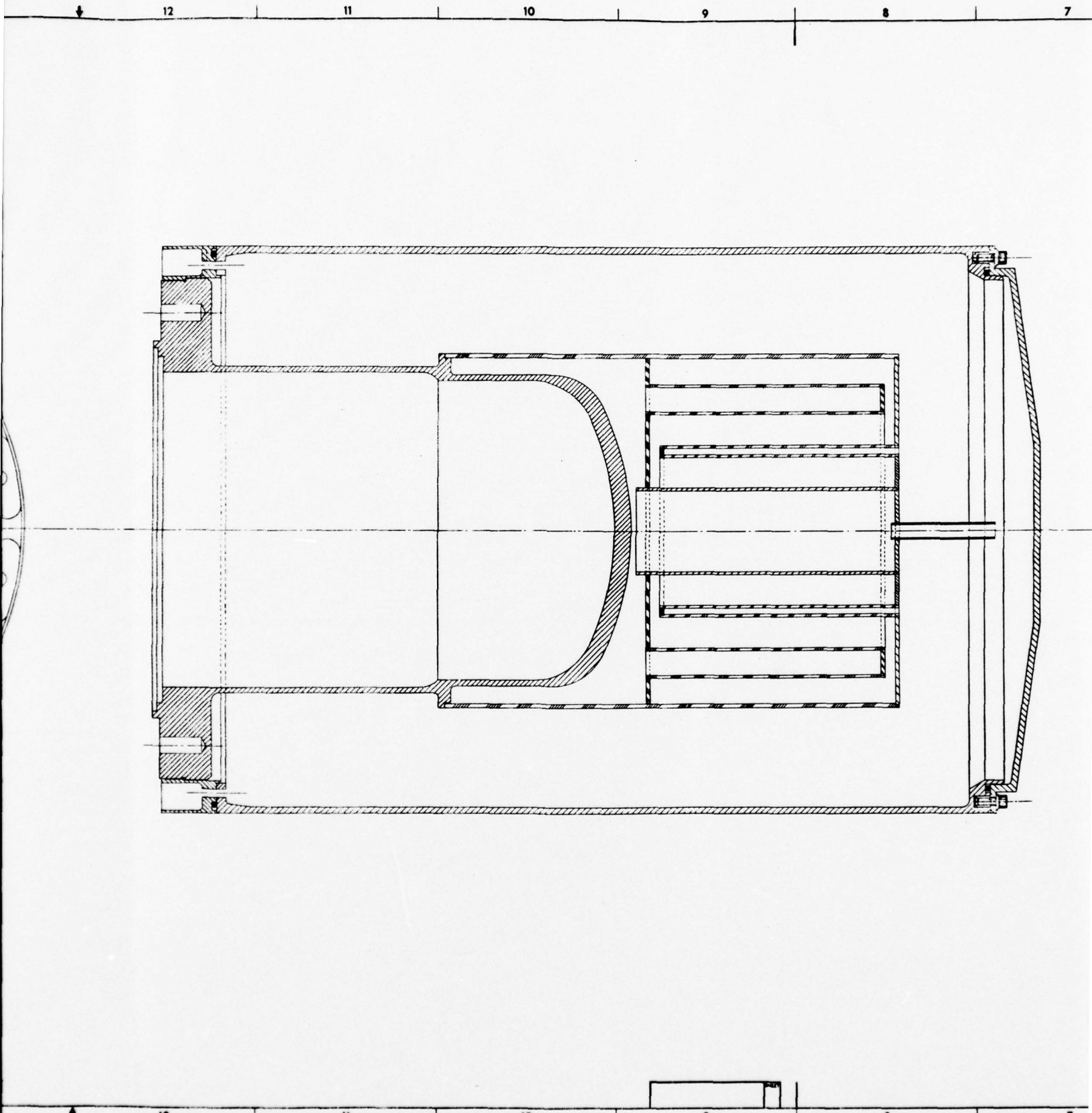
12
11
10
9
8
7
12
11
10
9
8
7

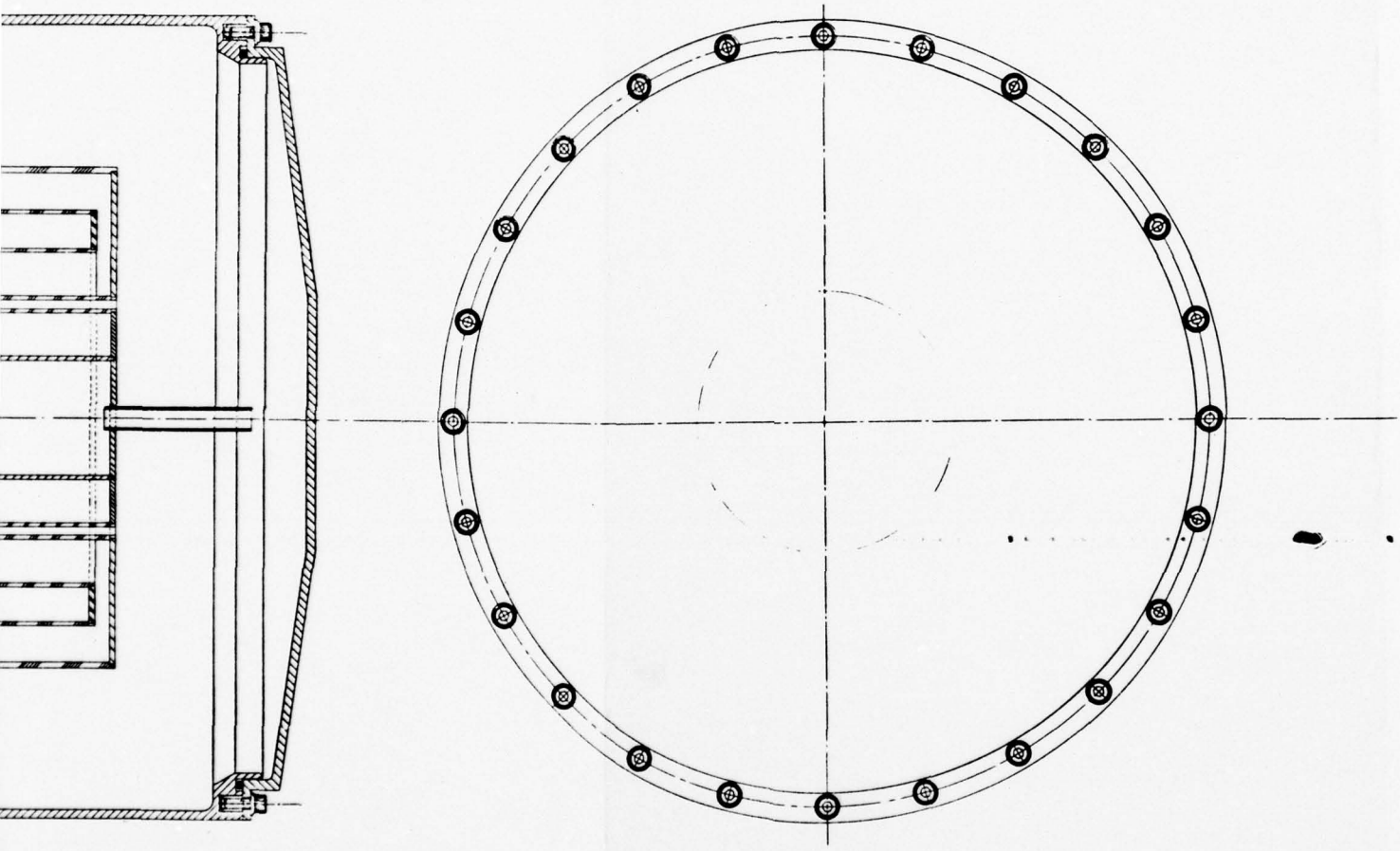

QTY REQD					
UNLESS OTHERWISE SPECIFIED LINEAR DIMS. IN TOLERANCES DECIMAL .XX ± .03 .XXX ± .010 DO NOT SCALE					
MATERIAL					
TREATMENT FINISH					
SIMILAR TO					
ON	THRU	PART/ASSY NO.	NEXT/FINAL QTY REQD PER ASSY	NEXT ASSY	USED ON
EFFECTIVE SERIAL NO.				APPLICATION	
USAGE DATA				DRAWING LEVEL	

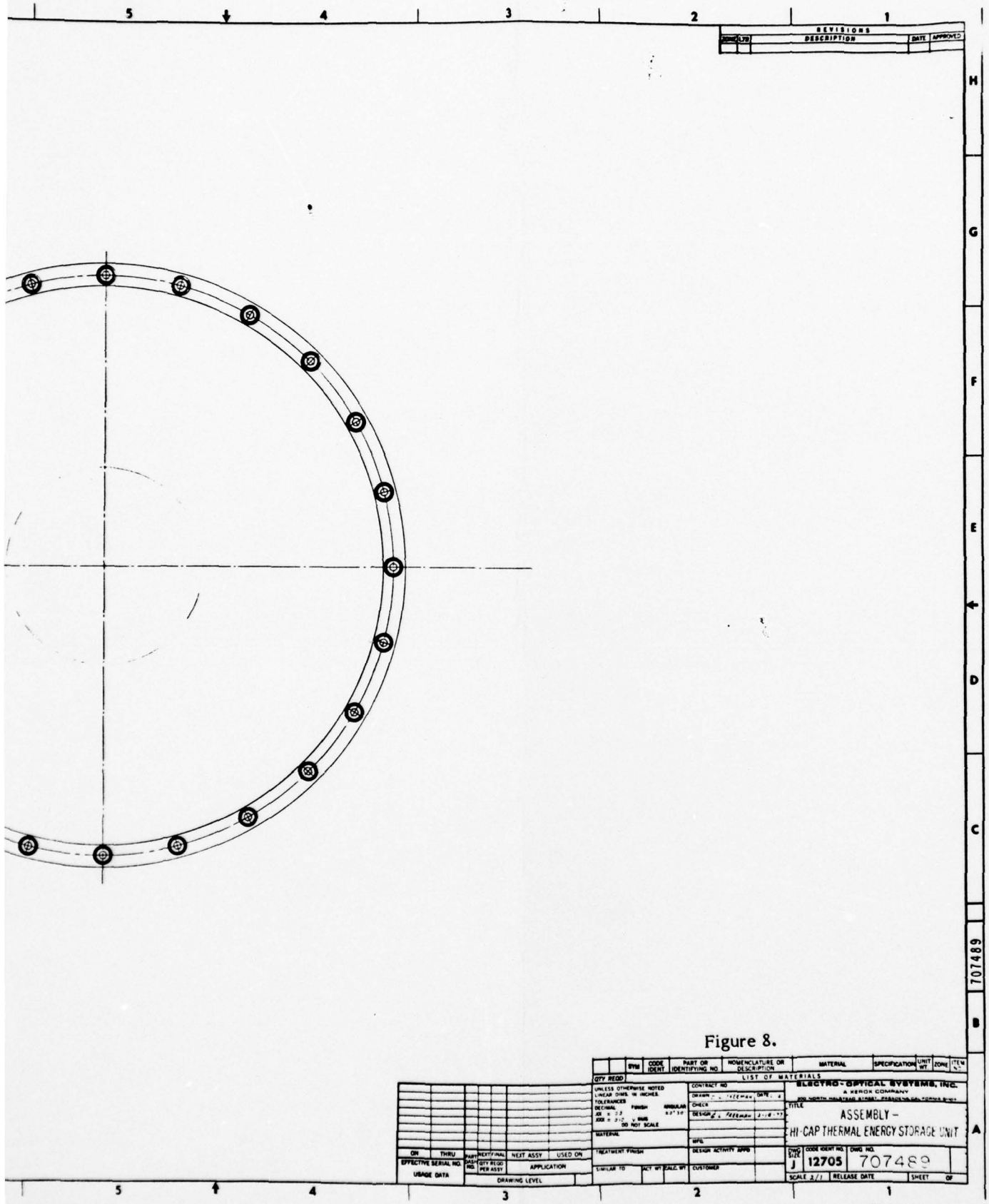
REVISIONS
DESCRIPTION
DATE
APPROVED
707489
ELECTRO-OPTICAL SYSTEMS, INC.
A XEROX COMPANY
TITLE
ASSEMBLY -
HI-CAP THERMAL ENERGY STORAGE UNIT
DWG SIZE
J
12705
707489
SCALE 2/1
RELEASE DATE
SHEET
LIST OF MATERIALS
QTY REQD
PART OR IDENTIFYING NO.
NOMENCLATURE OR DESCRIPTION
MATERIAL
SPECIFICATION
UNIT WT
ZONE
ITEM
UNLESS OTHERWISE NOTED
LINEAR DIMS. IN INCHES
TOLERANCES
DECIMAL
DO NOT SCALE
CONTRACT NO
CHECK
MATERIAL
MFG.
TREATMENT FINISH
DESIGN ACTIVITY APPD
SIMILAR TO
ACT WT
CALC WT
CUSTOMER
NEXT ASSY
USED ON
APPLICATION
DRAWING LEVEL
EFFECTIVE SERIAL NO.
USAGE DATA

Figure 8.

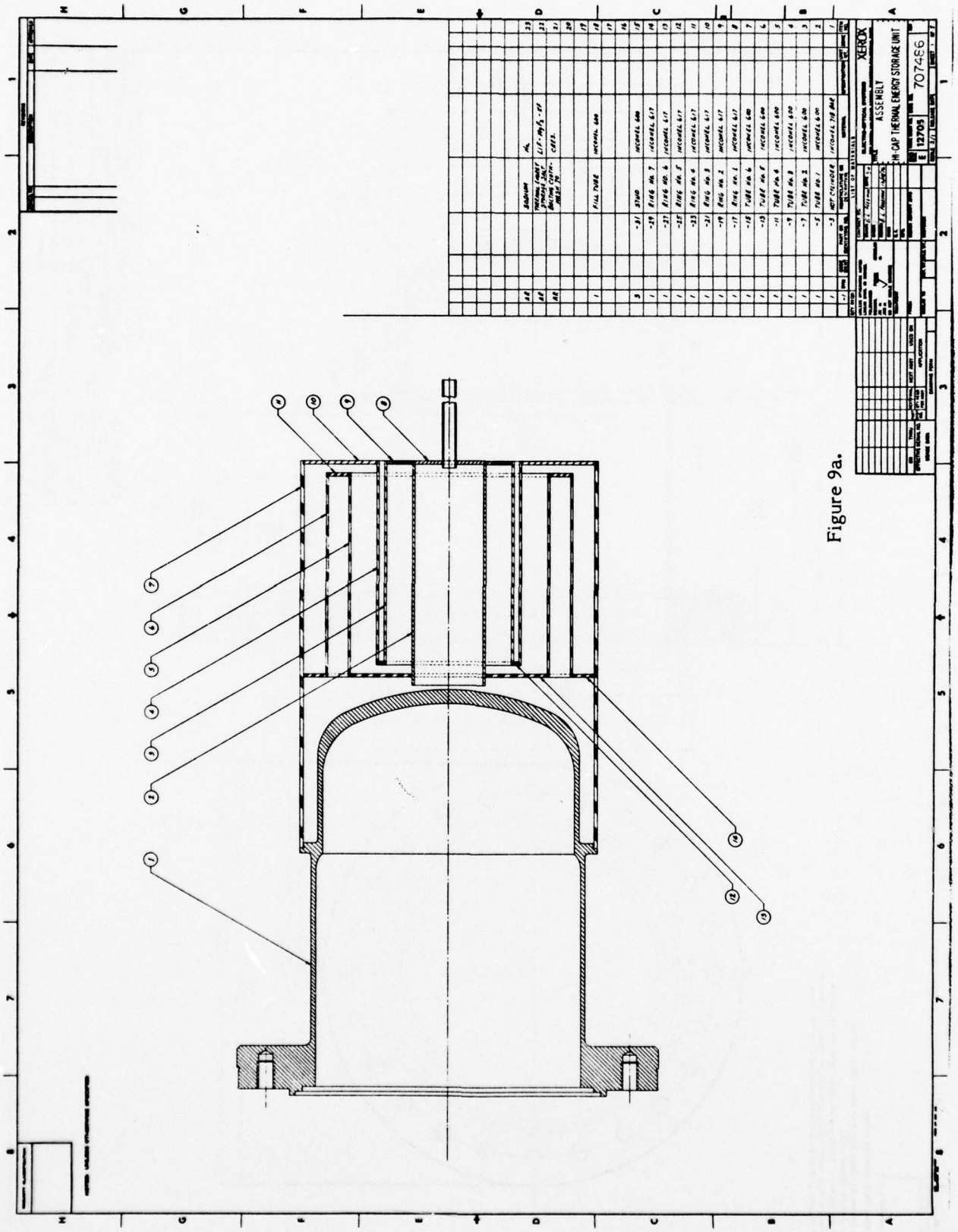

Figure 9a.

BEST AVAILABLE COPY

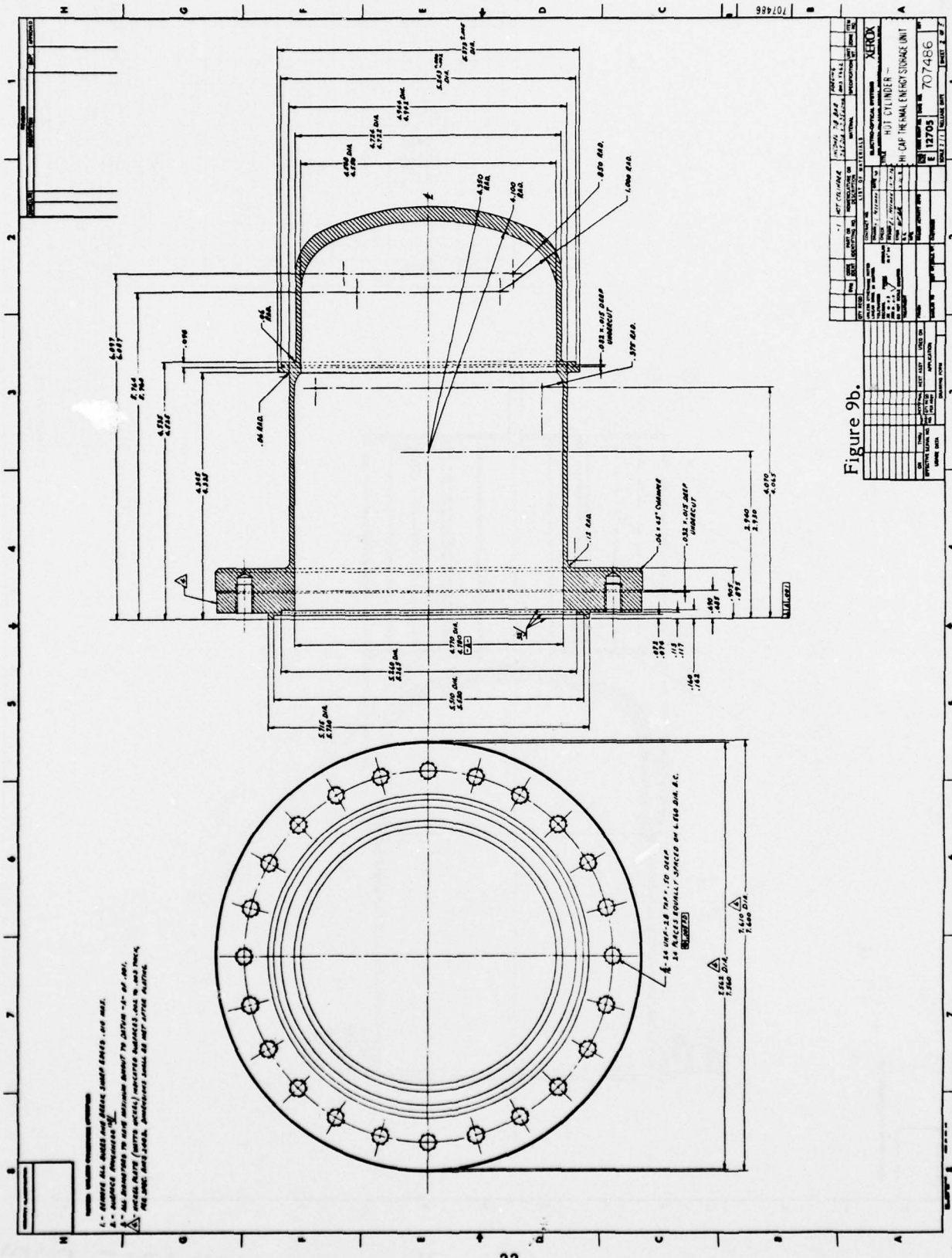

Figure 9b.

BEST AVAILABLE COPY

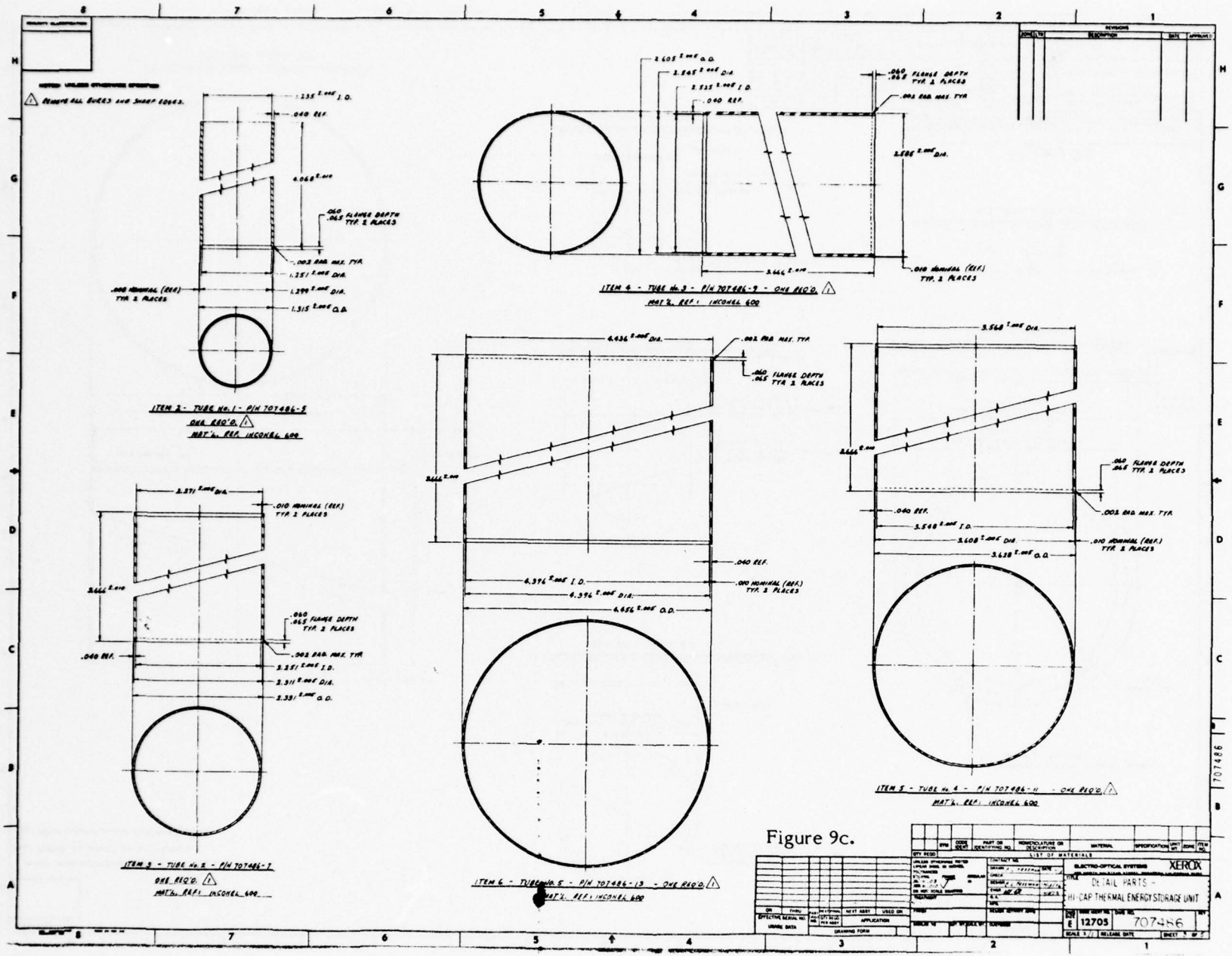

Figure 9c.

BEST AVAILABLE COPY

BEST AVAILABLE COPY

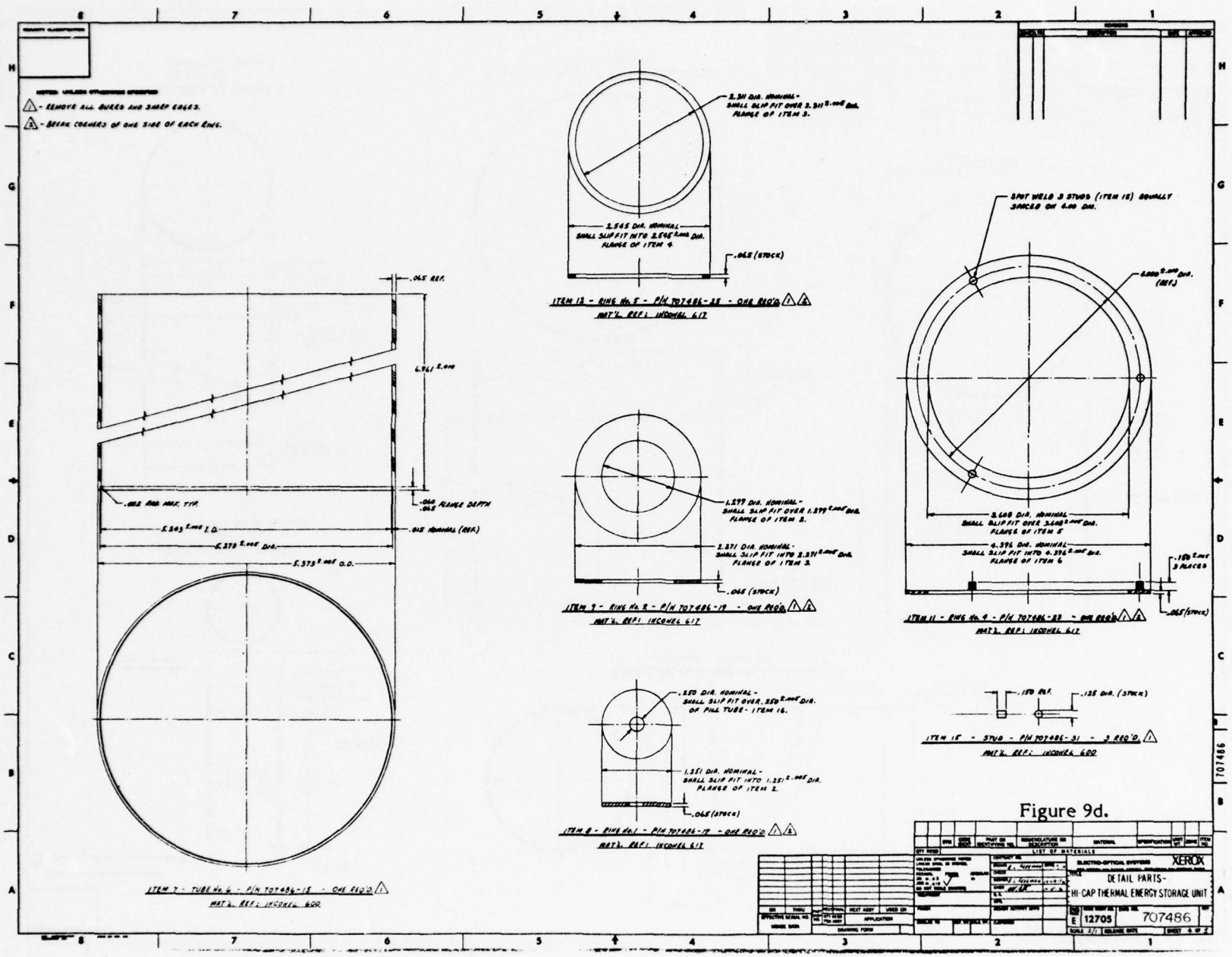

Figure 9d.

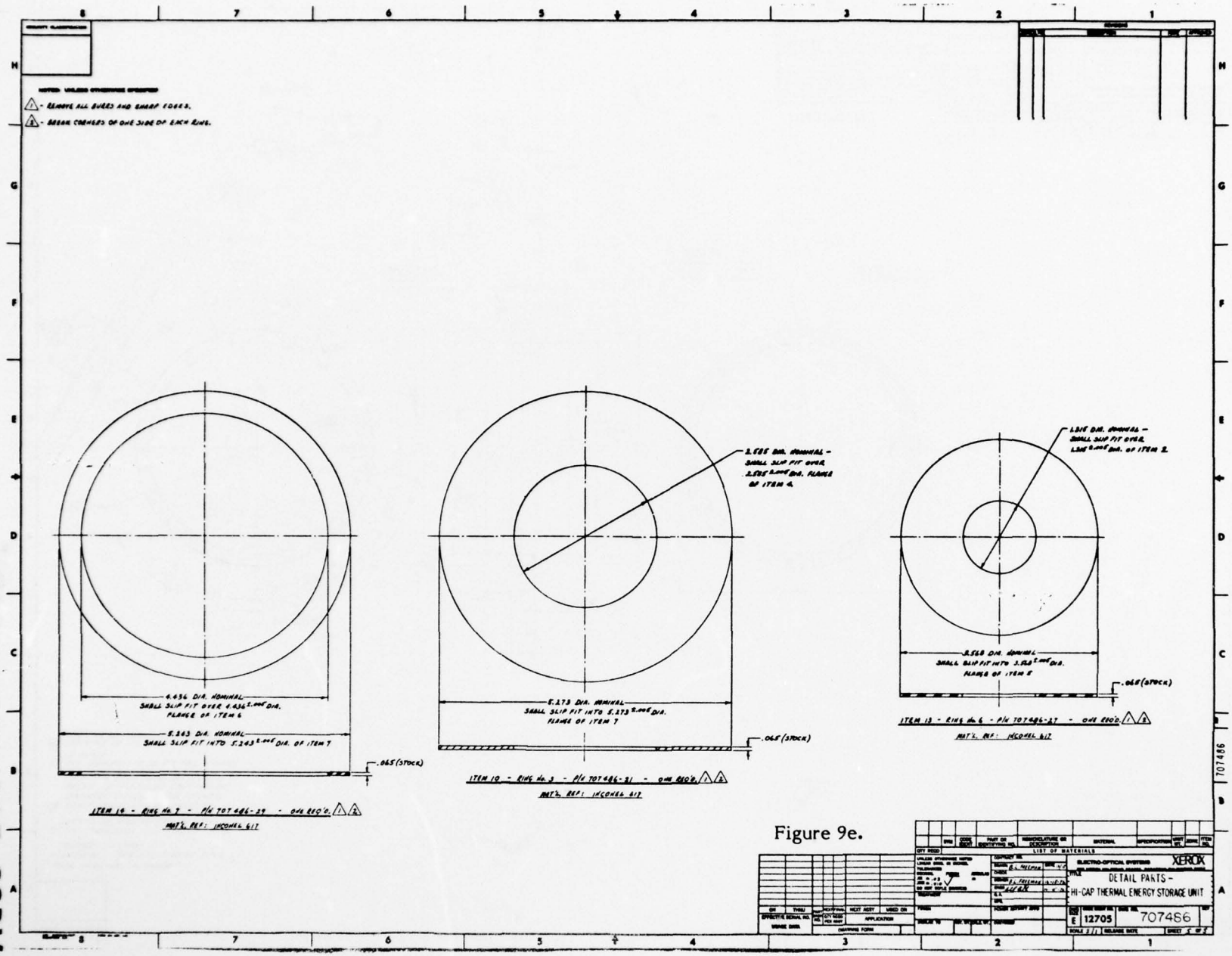

Figure 9e.

BEST AVAILABLE COPY

BEST AVAILABLE COPY

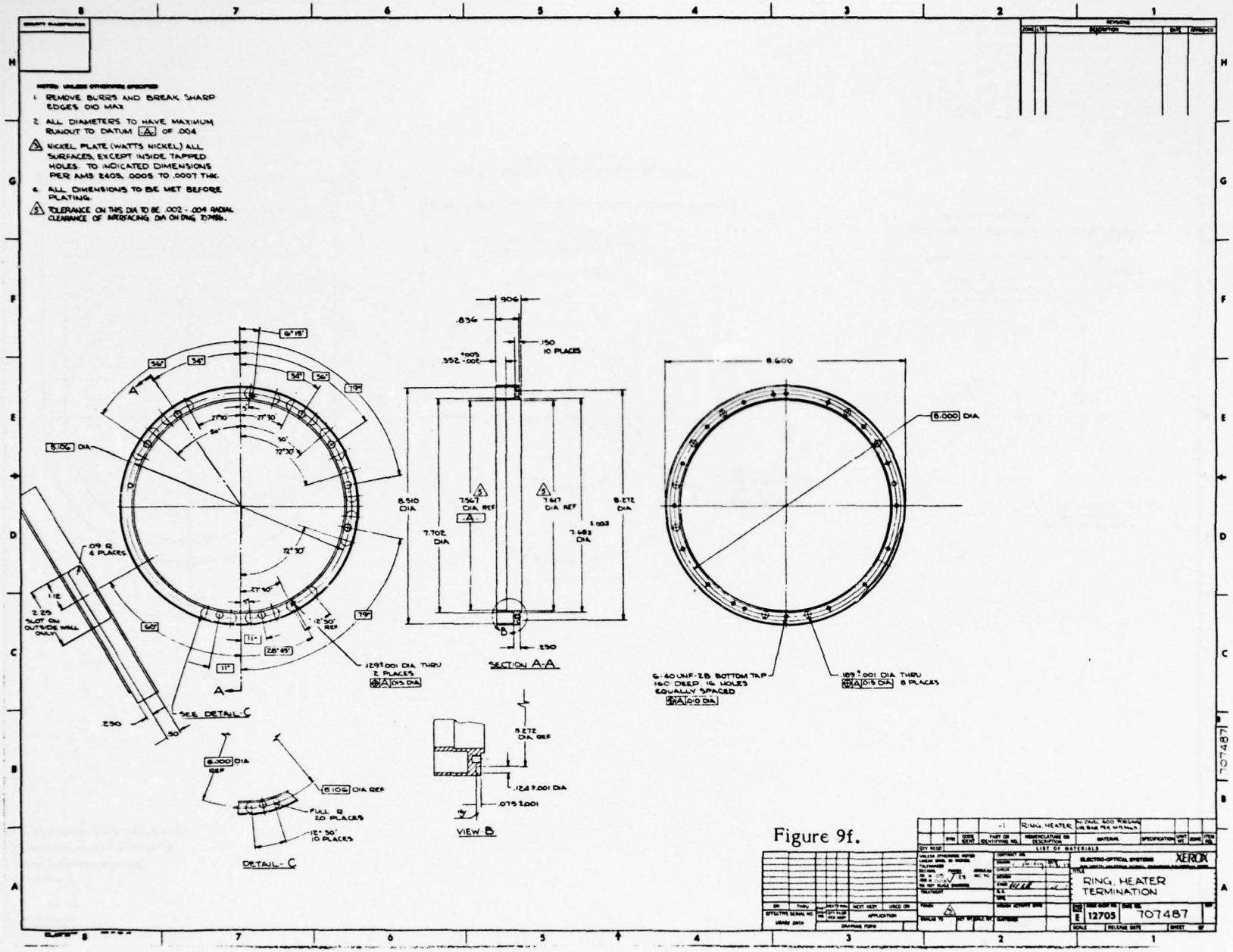

Figure 9f.

2.3.3 HI-CAP CYLINDER DESIGN

The original design of the hot cylinder of the Hi-Cap Vuilleumier cooler called for a cylinder machined from Rene' 41. Several vendors of this material were approached for the delivery of an approximately 8-inch diameter bar. No vendor was found who could supply the material. Forging companies did not want to undertake the forging of Rene' 41 as it is too abrasive to dyes. Only a special mill run could have produced the material. Because the unavailability of Rene' 41 for this program which could not have supported a special mill run or the replacement of forging dyes, Inconel 718 was selected as the hot cylinder material.

In Figure 10 and 11, the ultimate stresses and the 0.2% off-set yield stresses for Rene' 41 and Inconel 718 are presented. It can be seen that at the effective operating temperature of the hot cylinder (T_o = 1275^{o}F), the yield stress of Inconel 718 is only slightly lower than that of Rene' 41, i.e., 123 kpsi vs. 112 kpsi. Since the properties of these materials are very much a function of the forging processes and the heat treatment, substantial divergence from the quoted stresses can occur. The relatively small difference in the yield stresses appeared therefore rather academic.

If the hot cylinder is designed for operation under a continuous pressure of 800 psi at the operating temperature of 1275^{o}F, the rupture stresses have to be calculated from the Larson-Miller parameters, which are shown for the materials under consideration in Figures 12 and 13. Naturally, the hot cylinder will not be exposed continuously to the highest internal pressure of the Vuilleumier cooler, as the operation of the Vuilleumier cooler is based on cycling of the internal pressure. Nevertheless, all pertinent rupture stresses are presented in Table 4.

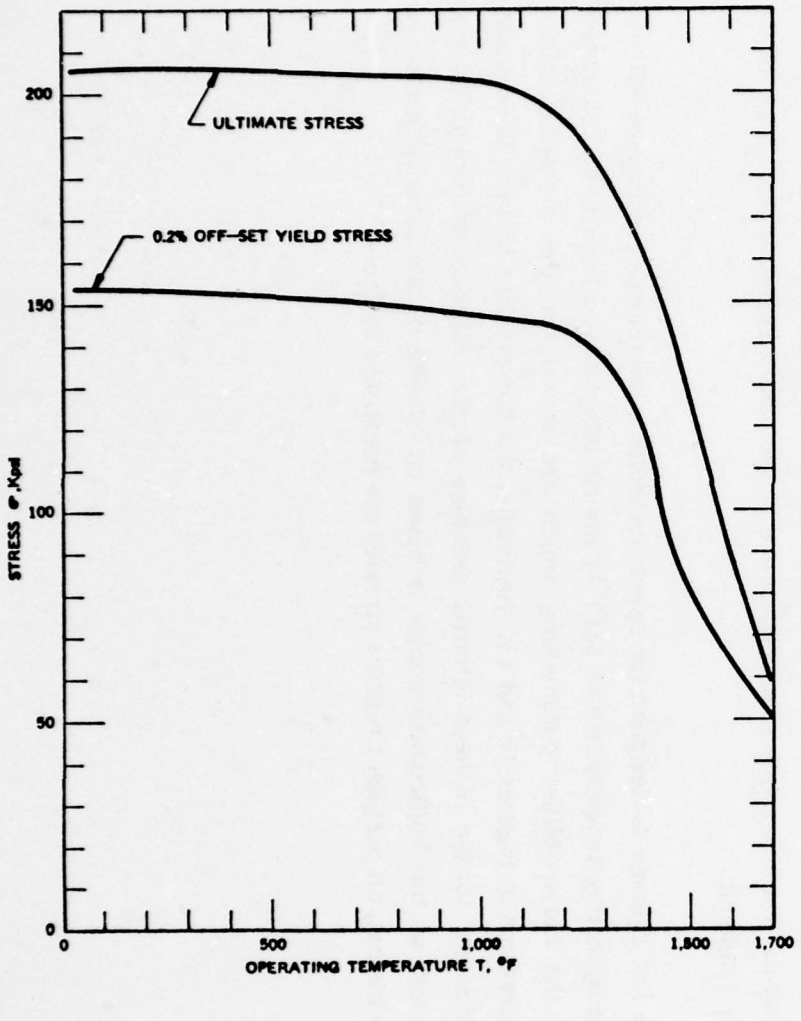

Figure 10. Ultimate and 0.2 Percent Off-Set Yield Stress of Rene' 41 Forged Bar

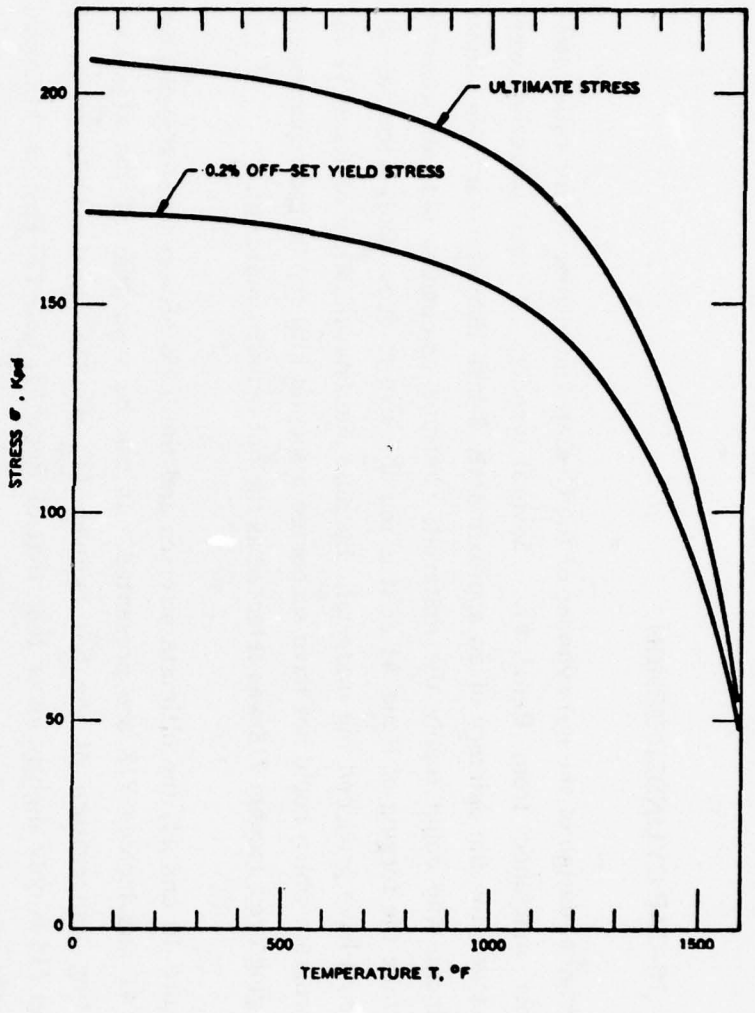

Figure 11. Ultimate Tensile Stress and 0.2 Percent Off-set Yield Stress of Inconel 718 Bar Stock Forged

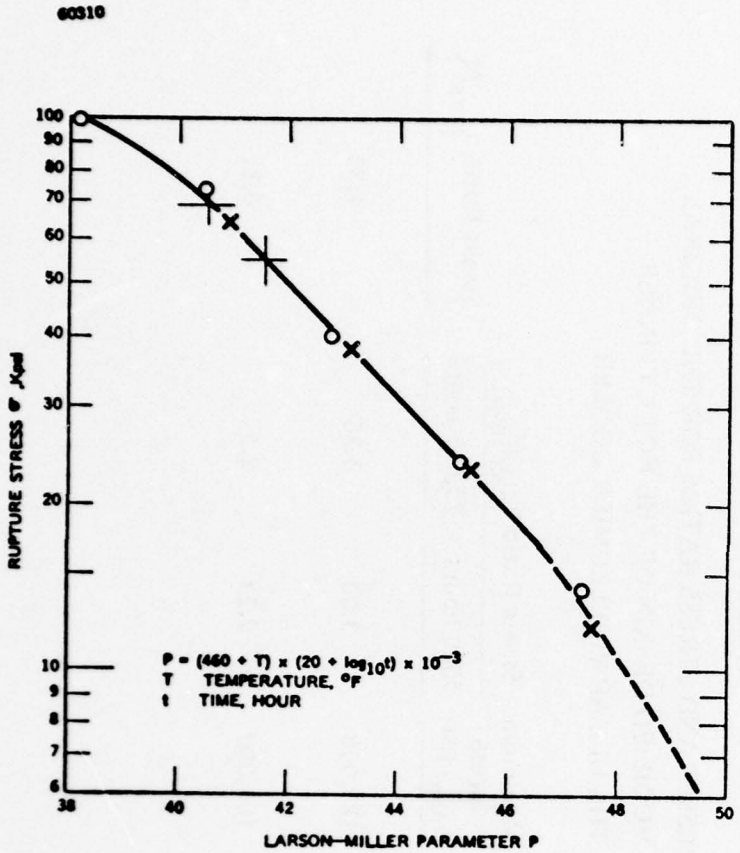

Figure 12. Rupture Stress of Rene' 41 (Carpenter Vacumeltrol 41) (Technical Data, Carpenter Technology Corporation 6/70)

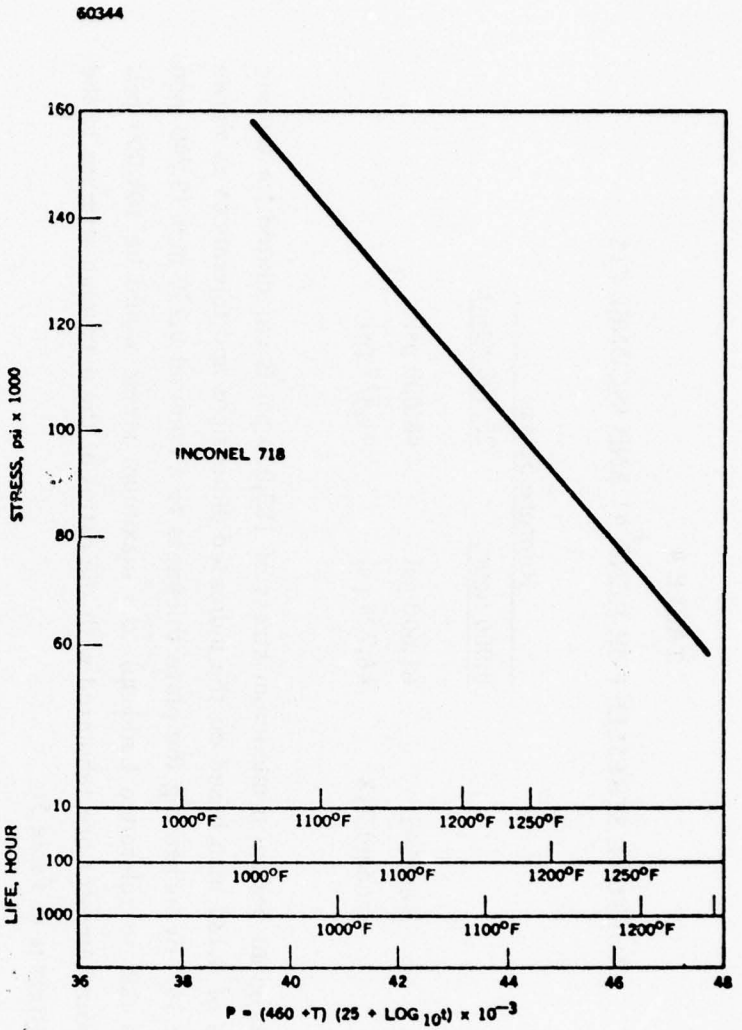

Figure 13. Larson-Miller Parameter Plot of Rupture Life of Cold-rolled Sheet, 0.025 - 0.250 in. (Annealed and aged in accordance with AMS 5596B). In the Larson-Miller Parameter, P, T is Temperature, °F, and t is time hour

TABLE 4

RUPTURE STRESSES FOR RENE' 41 AND INCONEL 718

	Rupture Stress	
	5,000 hours	20,000 hours
Rene' 41	61,000 psi	48,000 psi
Inconel 718	46,724 psi	41,477 psi

For the original design, a maximum stress of 183,000 psi is calculated for a plate thickness of 0.180 inch based on the indicated dimensions and tolerances as shown in Figure 14. By increasing the plate thickness to a nominal 0.250 inch (0.240 inch minimum due to tolerance build-up), the maximum stress would be 104,000 psi. These quoted stresses are tabulated with the ratios of the maximum stresses to the rupture stresses in Table 5.

TABLE 5

MAXIMUM STRESSES AND STRESS RATIOS FOR THE ORIGINAL AND THE MODIFIED DESIGN OF THE HOT CYLINDER OF THE HI-CAP VUILLEUMIER COOLER

	Plate Thickness t_p, inch	Maximum Stress σ_{max}, psi	Stress Ratio $\sigma_{max}/\sigma_{rupt.}$		Stress Ratio σ_{max}/σ_y
			5000 hours	20,000 hours	
Rene' 41 (Original Design)	0.180	183,000	3.00	3.80	1.33
Inconel 718 Modified Design)	0.240	104,000	2.23	2.5	0.81

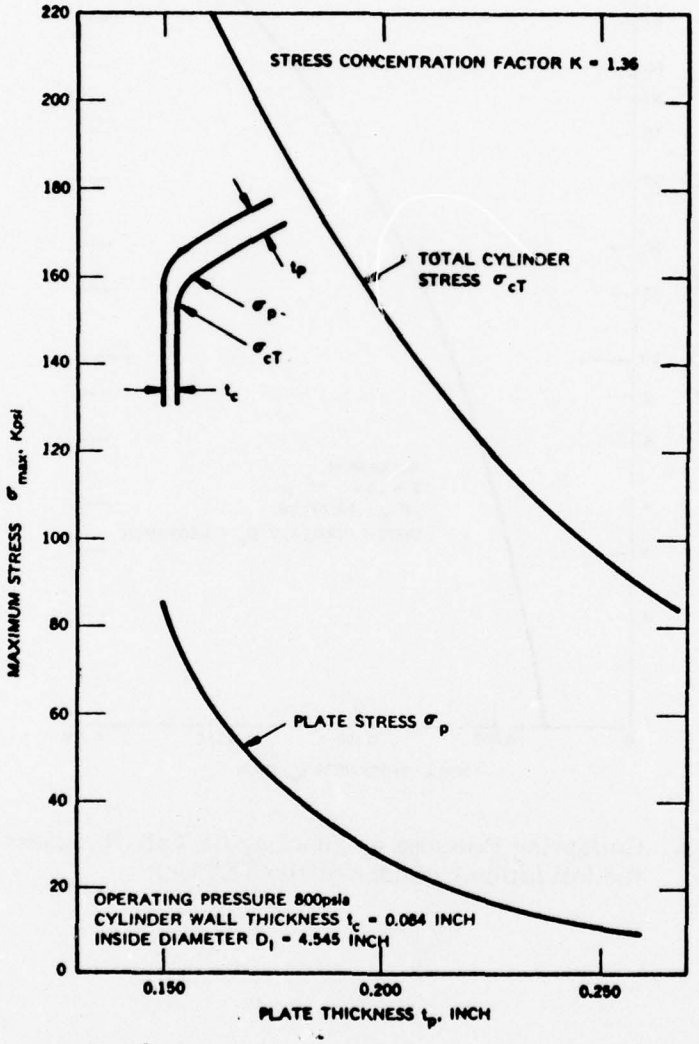

Figure 14. Stresses in the Hot Cylinder of Hi-Cap Vuilleumier Cooler

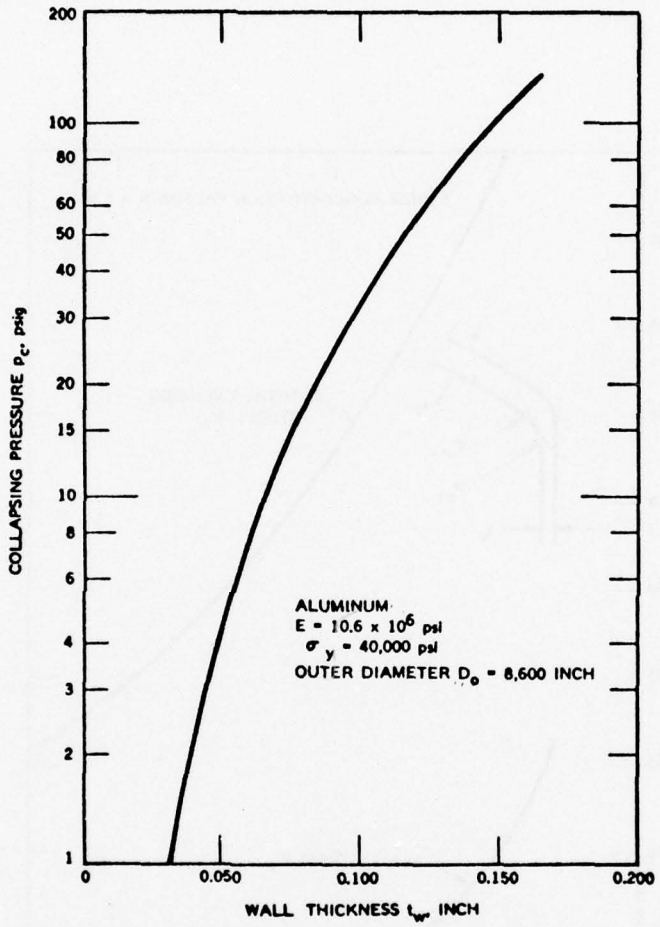

Figure 15. Collapsing Pressure as Function of Wall Thickness for the Insulation Cylinder of the TES Unit

The modified design of the hot cylinder appears to be exposed to lower relative stresses than the original design, i.e., all stress ratios are lower for the Inconel 718 cylinder with the 0.240 inch thick plate than for the Rene' 41 cylinder with the nominal 0.200 inch thick plate.

The final design of the hot cylinder was shown in Figures 9a to 9f. A flange was added to which the thermal energy storage unit was to be welded. The mounting flange was modified to permit insertion of bolts without breaking through the flange. Thus vacuum could be maintained in the insulation without the sealing of 24 bolt holes.

2.3.4 INSULATION CONTAINER DESIGN

Drawings were received from the Hughes Aircraft Company including those for the insulation container of the heat shield of the hot cylinder of the Vuilleumier cryogenic cooler. The container was designed with a wall thickness of only 0.035 inch to minimize its weight. However, for the thin cylinder to withstand atmospheric pressure when the inside is evacuated, the cylinder would have had to be packed densely with insulation material in support of its wall. In the XEOS design, the hot cylinder and the thermal energy storage unit were to be insulated with super insulation consisting of layers of Fiberfrax and metal foil to achieve minimum thermal losses. This type of insulation would have made the packing of additional insulation material in support of the container difficult. Calculations whose results are shown in Figure 15, included a safety factor of 2. They suggested a wall thickness of 0.100 inch for the insulation container. The final design is shown in Figure 16.

The lid of the insulation container was modified to decrease the machining cost for this component and increase its safety margin. The final design of the lid is shown in Figure 17.

BEST AVAILABLE COPY

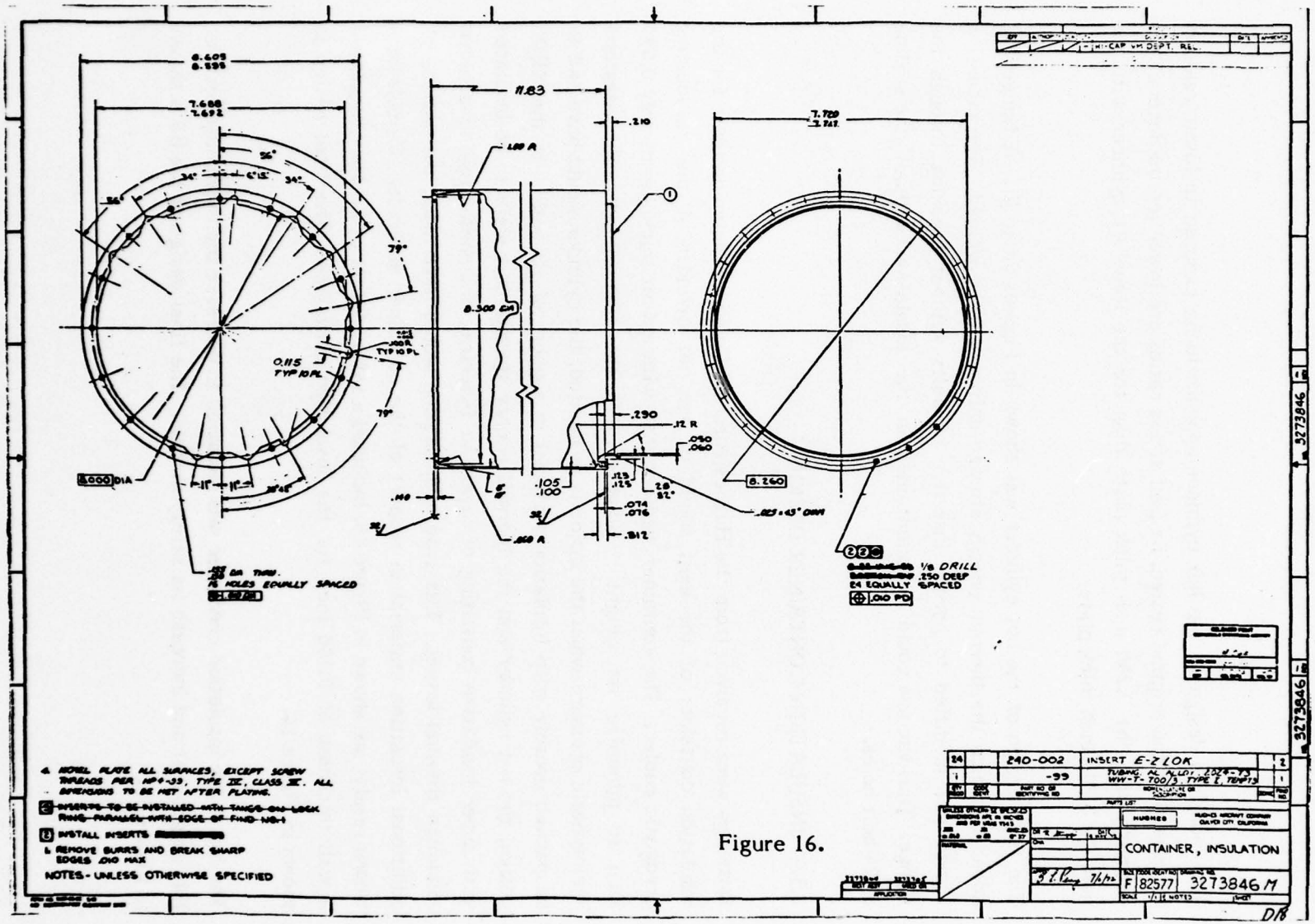

Figure 16.

BEST AVAILABLE COPY

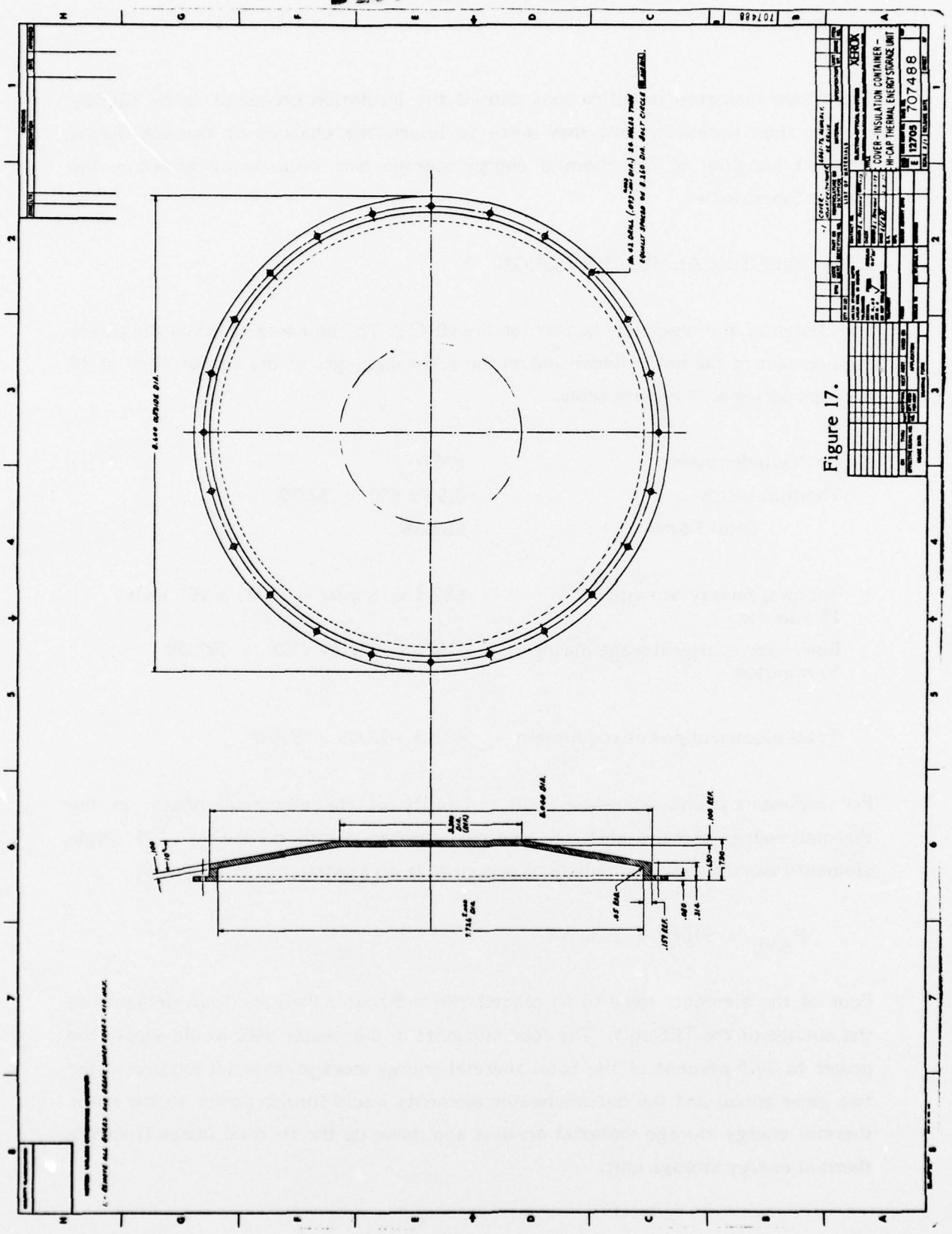

Figure 17.

The above indicated modifications caused the insulation container to be slightly heavier than necessary, but they were to lessen the chances of damage during frequent handling of the thermal energy storage unit while being tested in the various laboratories.

2.3.5 ELECTRICAL HEATER DESIGN

The design of the electrical heater for the Hi-Cap TES unit was based on the power requirement of the hot cylinder and on the assumed length of the eclipse time of 18 minutes during a 72 minute orbit.

Hot cylinder power	650W
Thermal losses	$0.05 \times 650 = 32.5W$
Total Power	682.5W
Thermal Energy Storage for 18 minutes	$682.5 \times 18 \times 60 = 7.371 \times 10^5$ joules
Power for energy storage during 54 minutes	$7.371 \times 10^5/(54 \times 60) = 227.5W$
Total electrical power requirment	$682.5 + 227.5 = 910W$

For redundancy and achieving high reliability of the electrical heater in the thermal energy storage unit, an electrical heater design consisting of 8 single elements was chosen. Each element was to have an average power output of

$$P_{AVE} = 910/8 = 113.75W$$

Four of the elements were to be placed into the heater well and four elements on the outside of the TES unit. The four elements in the heater well would supply the power to 54.5 percent of the total thermal energy storage material located in the two inner annuli and the outside heater elements would furnish power to the outer thermal energy storage material annulus and make up the thermal losses from the thermal energy storage unit.

For covering half of the surface of the heater well, a total heater length of L_H = 218 inch was indicated, i.e., 54 inch per element. After consulting with several heater manufacturers, it was decided to specify a resistance of 40 ohms per element. A resistance of 88 ohms per element would have been more desirable for a better match with the available voltage. It appeared, however, that a heater element with a thinner heater wire, which the higher resistance would have required, would have lowered the reliability of the unit.

The specifications for the heater elements were established in consultation with the manufacturer and were designed to procure the least expensive elements that would still fulfill all requirements. It was realized that a considerable amount of money could be saved by relatively loose specifications. The final specifications for the elements are shown in Table 6.

TABLE 6

SPECIFICATIONS FOR
DOUBLE ENDED HEATER ELEMENTS FOR HI-CAP TES UNIT

Construction	Double ended
Resistance	40 ohms $\pm$8 ohms
Sheath Diameter	0.050 to 0.060 inch
Heated Length	48 inch $\pm$1 inch
Cold Length	2-1/2 inch $\pm$1/4 inch
Terminations	3/16 inch dia. x 3/4 inch long
Lead Wire	2 inch
Operating Temperature	1450^{o}F
Sheath	Inconel

2.3.6 INSULATION DESIGN

2.3.6.1 Radiation Shield Insulation

The specifications for the Hi-Cap Thermal Energy Storage Unit called for thermal losses of less than 5 percent of the hot cylinder power requirement of 650W. Thus, less than 32.5W could be conducted through the insulation. Calculations indicated that even with the best standard insulation consisting of Flexible Min-K material the losses could not be kept below approximately 180W as shown in Figures 18 and 19, this being more than five times the allowable heat loss. The requirements could, therefore, only be fulfilled by applying superinsulation to the TES unit consisting of multiple radiation heat shields in a vacuum.

The original insulation design called for 0.001-inch thick Tantalum foil separated by 0.01-inch Fiberfrax paper. The 0.01 inch thick Fiberfrax paper was only available with a filler which gave the paper the strength for handling it. The presence of the filler, however, was not advisable because of its outgassing at the operating temperature and the possible contamination of the radiation shield foil. A 0.02-inch Fiberfrax paper was therefore selected that could be handled without a filler. Though the original design had called out Tantalum foil as the radiation shield material, it could not be located in the size and amount required for the insulation of the TES unit. A special mill run for the program could not be justified. The next best available material was nickel. In Figures 20 and 20a the normal total emittance of nickel and tantalum are presented. The data confirms that tantalum would be a better material due to its lower emittance in the regime of interest, i.e., 1050^{o}K.

Tests indicated that in the insulation construction, each layer consisting of one layer of 0.02 inch thick Fiberfrax paper and one layer of 0.001 inch thick nickel foil, would have an effective thickness of 0.032 inch. The thermal energy storage unit could therefore be insulated with 34 layers and the hot cylinder barrel with 43 layers.

BEST AVAILABLE COPY

```
 SET F:105/DCON

!SET F:106 ME

!RUN
     LINKING $
'P1' ASSOCIATED.
          CONDUCTIVE HEAT TRANSFER CALCULATIONS

 INNER DIAMETER D  LENGTH L    TEMPERATURE DIFFERENCE DELT
      INCH           INCH                 DEGREE F
    5.373            7.117                 1178.00
 HEAT TRANSFER COEFFICIENT,B-INCH/FT2-HR-DEG.F     .500

 OUTER DIAMETER   THICKNESS TI       POWER LOSS
      INCH             INCH             KW

      5.873            .250            .623
      6.373            .500            .335
      6.873            .750            .239
      7.373           1.000            .191
      7.873           1.250            .162
      8.373           1.500            .143
      8.873           1.750            .129
      9.373           2.000            .119
      9.873           2.250            .111
     10.373           2.500            .104
     10.873           2.750            .099
     11.373           3.000            .095
     11.873           3.250            .091
     12.373           3.500            .088
     12.873           3.750            .085
 *STOP* 0

!EDIT
EDIT HERE
*EDIT CON
*EDIT DCON
*T1-3
-C1: UNKN CMND
*TY1-3
   1.000 5.373,7.117,1178.,
   2.000 0.25,15,
   3.000 0.5,
*END

!
```

Figure 18. Conductive Heat Transfer Losses Through Flexible Min-K Insulation

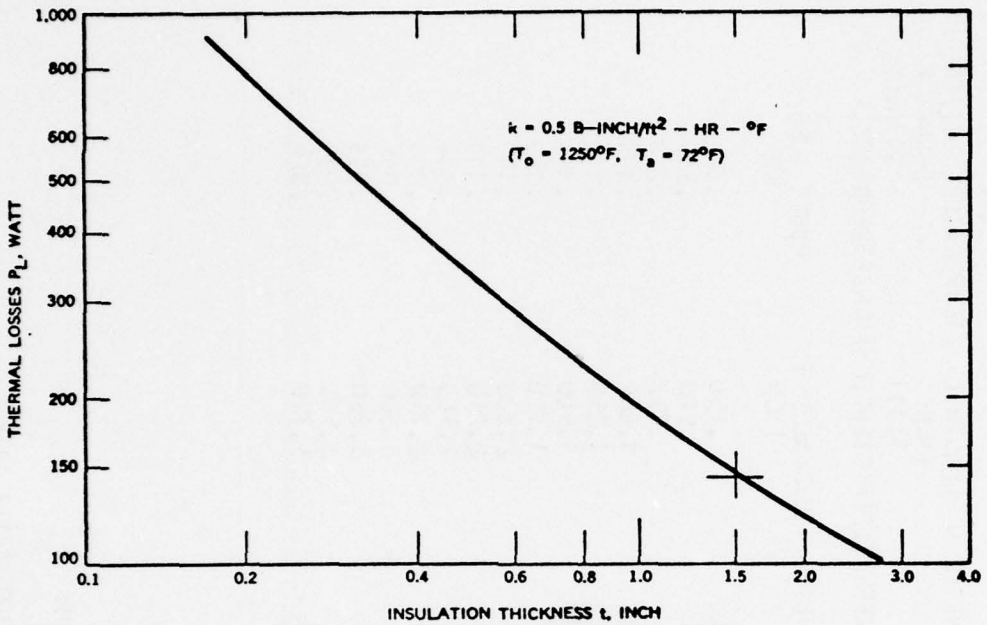

Figure 19. Thermal Losses from Hi-Cap Thermal Storage Unit in Its Initial Performance Testing Configuration

BEST AVAILABLE COPY

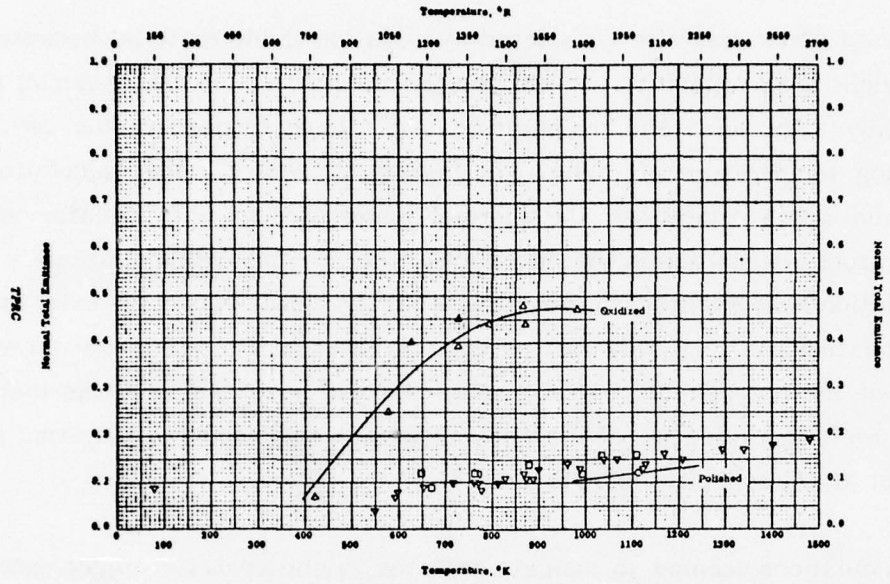

Figure 20. Normal Total Emittance -- Nickel

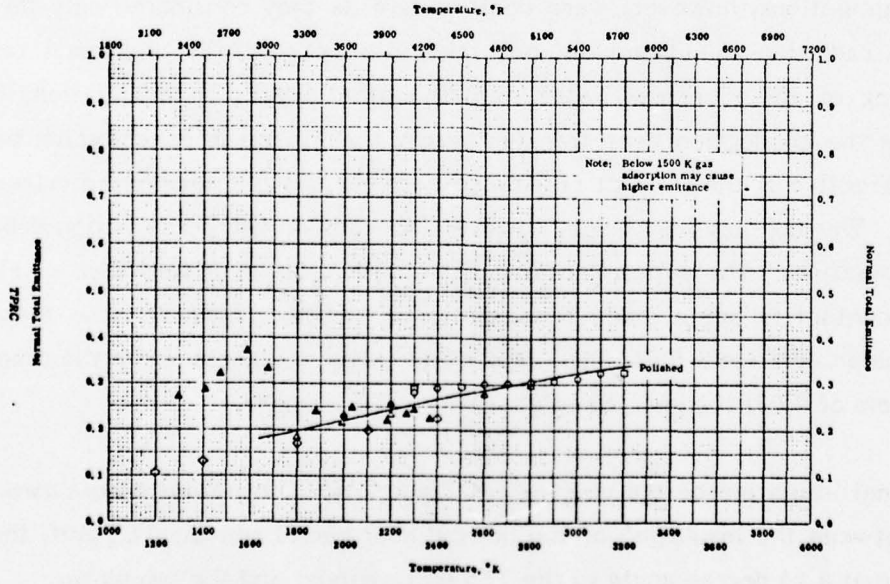

Figure 20a. Normal Total Emittance -- Tantalum

Metallized mylar was also considered as radiation shield material because of its lightweight and availability. It was thought possible to use this material for the outer layers in which the temperature would have dropped to the permissible operating temperature of mylar. In Figures 21 and 22, the calculations are presented which established the thermal losses through the insulation and the temperature distribution in the insulation. Since the insulation is primarily based on radiation heat transfer, the temperature drops slowly across the inner layers of the insulation and relatively fast across the outer layers. Only the three outer layers of the hot cylinder barrel insulation could have employed the metallized mylar, while the insulation of the TES unit itself would not have permitted the use of mylar at all, as indicated by Figure 23.

The calculations seemed to indicate that the insulation losses might exceed the goal of 32.5 watt. The total calculated losses were 2.27 watt from the barrel, 27.55 watt from the cylindrical wall of the TES unit and 4.5 watt from the top of the TES unit. Some additional losses were anticipated to occur through the seams of the insulation and the breakthroughs for the instrumentation and the heaters.

The calculations, however, were conservative as they considered only the metal foil as radiation shield and did not take into account the additional radiation shielding of the Fiberfrax paper. On the other hand, the calculations did not include the conduction heat transfer across the Fiberfrax paper which becomes only effective if the contact resistance between the foil and the Fiberfrax paper is low. This contact resistance, however, depends on the construction process of the insulation. The experimental construction tests indicated that a relatively loose contact is being made between the Fiberfrax paper and the metal foil, because an additional 0.011 inch in effective layer thickness above the theoretical thickness of 0.021 inch per complete layer was measured.

The final insulation design is shown in Figure 24. The insulation has two seams, one between the insulation of the hot cylinder barrel and the TES unit, the other running at a 45 degree angle to the TES unit cylinder and the top plate.

BEST AVAILABLE COPY

```
      CYLINDRICAL RADIATION SHIELDING HEAT TRANSFER  11 JULY 1977

UPPER TEMPERATURE TO = 727.00 DEG.K
LOWER TEMPERATURE TA = 310.60 DEG.K
NUMBER OF LAYERS N=43, LAYER THICKNESS T = .0813CM
THETA = .150
INNER DIAMETER D = 12.555 CM, LENGTH L = 8.738 CM
ESTIMATE = 2.7004E 11

TEMPERATURE TI THRU T43, DEG.K
   721.8   716.6   711.4   706.0   700.7   695.2   689.8   684.2
   678.6   672.9   667.1   661.2   655.3   649.2   643.0   636.8
   630.4   623.8   617.2   610.3   603.4   596.2   588.8   581.3
   573.5   565.5   557.2   548.5   539.6   530.3   520.5   510.3
   499.5   488.0   475.9   462.8   448.6   433.1   415.9   396.5
   373.8   346.4   319.6

TOTAL HEAT TRANSFER Q̇ = 2.27 WATT

NUMBER OF ITERATIONS = 7
```

Figure 21. Temperature Distribution in and Thermal Losses through the Multi-Layer Insulation of the Hot Cylinder Barrel

```
      CYLINDRICAL RADIATION SHIELDING HEAT TRANSFER  11 JULY 1977

UPPER TEMPERATURE TO = 1059.00 DEG.K
LOWER TEMPERATURE TA = 310.60 DEG.K
NUMBER OF LAYERS N = 34, LAYER THICKNESS T =.0813 CM
THETA = .150
INNER DIAMETER D = 13.609 CM,   LENGTH L = 17.915 CM
ESTIMATE = 1.2062E 12

TEMPERATURE T1 THRU T34, DEG.K
  1040.8  1031.5  1022.1  1012.4  1002.6   992.7   982.5   972.1
   961.5   950.7   939.6   928.1   916.4   904.4   801.8   897.1
   865.8   852.8   837.6   822.7   807.0   790.4   773.0   754.5
   734.6   713.2   680.0   664.3   635.6   622.6   563.5   514.5
   446.0   310.6

TOTAL HEAT TRANSFER Q̇ = 27.55 WATT

NUMBER OF ITERATIONS = 7
```

Figure 22. Temperature Distribution in and Thermal Losses Through the Cylinder Portion of the Multi-Layer Insulation of the Thermal Energy Storage Unit

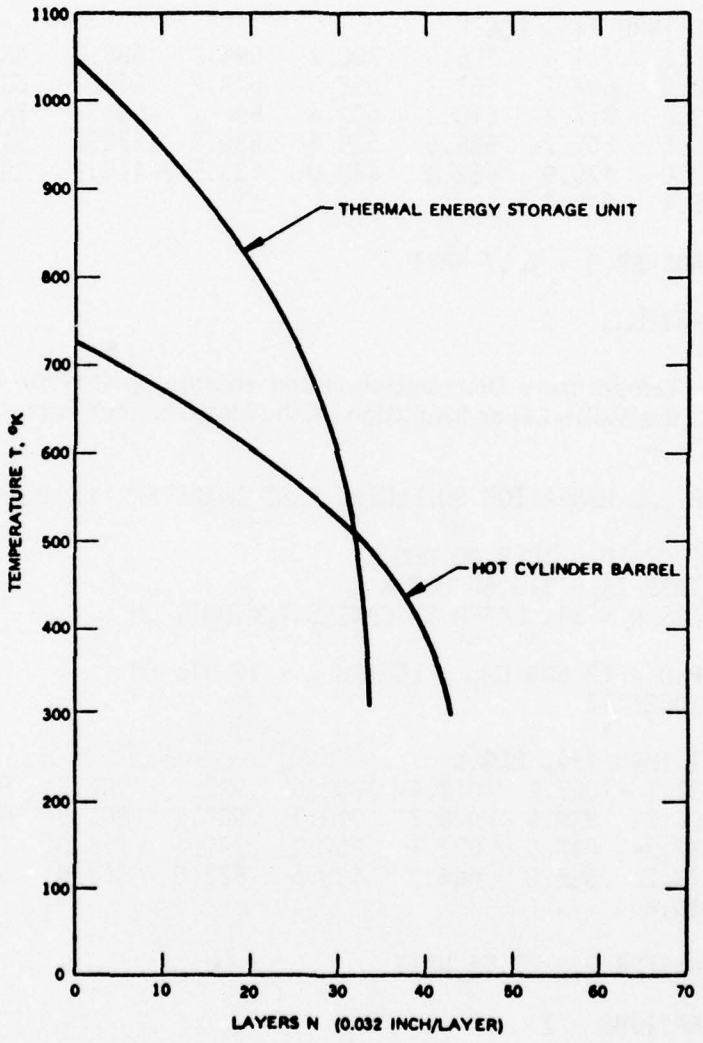

Figure 23. Temperature Distribution in the Radiation Shielding Insulation of the Thermal Energy Storage Unit

BEST AVAILABLE COPY

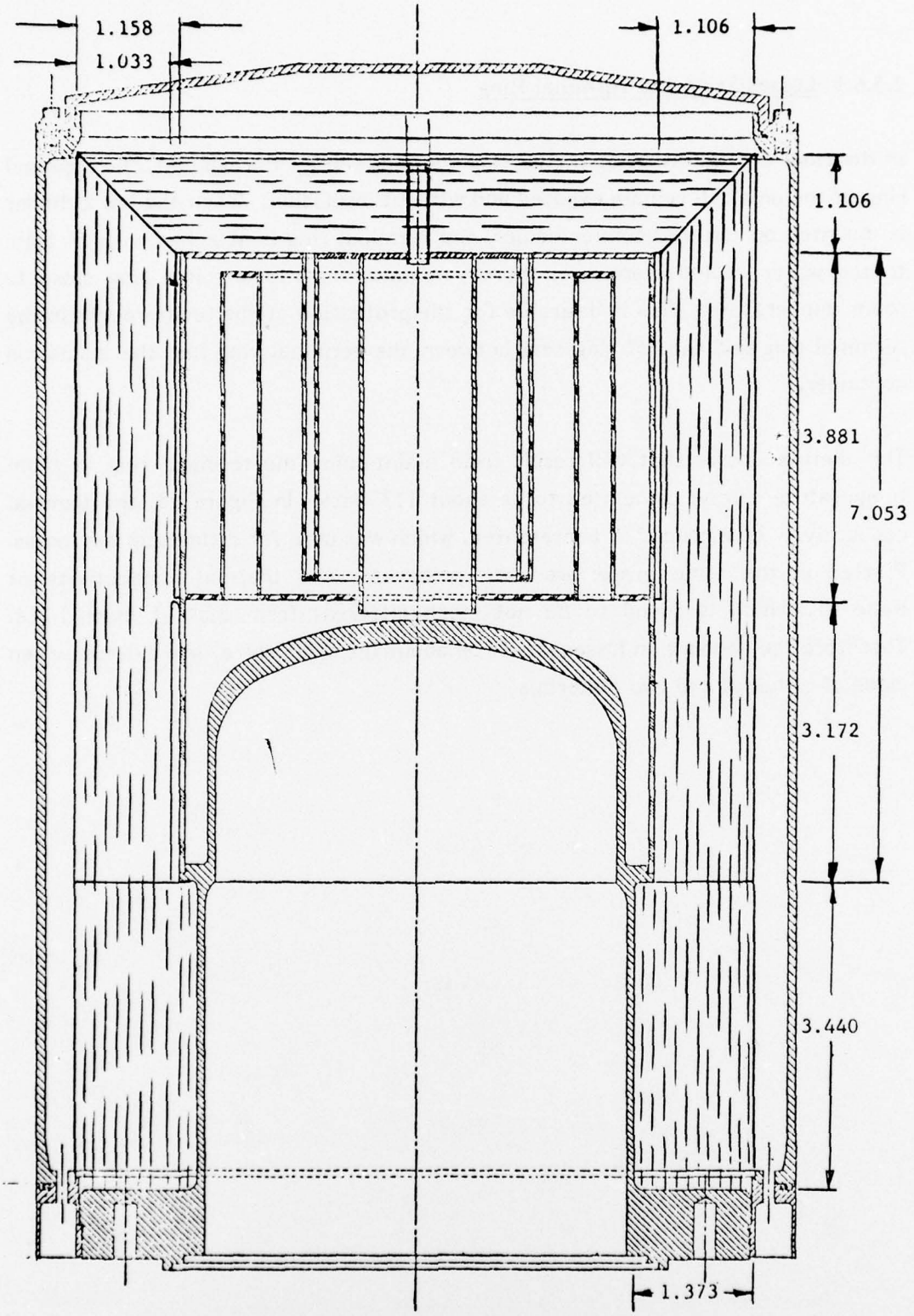

Figure 24. Insulation Design for the Hi-Cap Thermal Energy Storage Unit (0.001-inch Nickel Foil and 0.020-inch Fiberfrax)

2.3.6.2 Losses From the Terminal Ring

In the final configuration of the Hi-Cap thermal energy storage unit, the terminal ring of the unit will remain exposed and without insulation. When the hot cylinder is mounted on the Vuilleumier cooler, the terminal ring is attached with 24 bolts to the water cooled crankcase, thereby maintaining the terminal ring close to room temperature. This is desirable for the protection of the feedthroughs in the terminal ring and the "o" ring seal between the terminal ring and the insulation container.

The thermal losses that will result from maintaining the terminal ring at room temperature can be calculated to be about 113 watt. In Figure 25, the thermal conductivity of Inconel 718 is presented, which was used for estimating the losses. Plotted in the same graph are data points for the thermal conductivity of Rene' 41, which is found to be not much different from that of Inconel 718. Therefore the conduction losses should be about the same for a hot cylinder when made of either of the two materials.

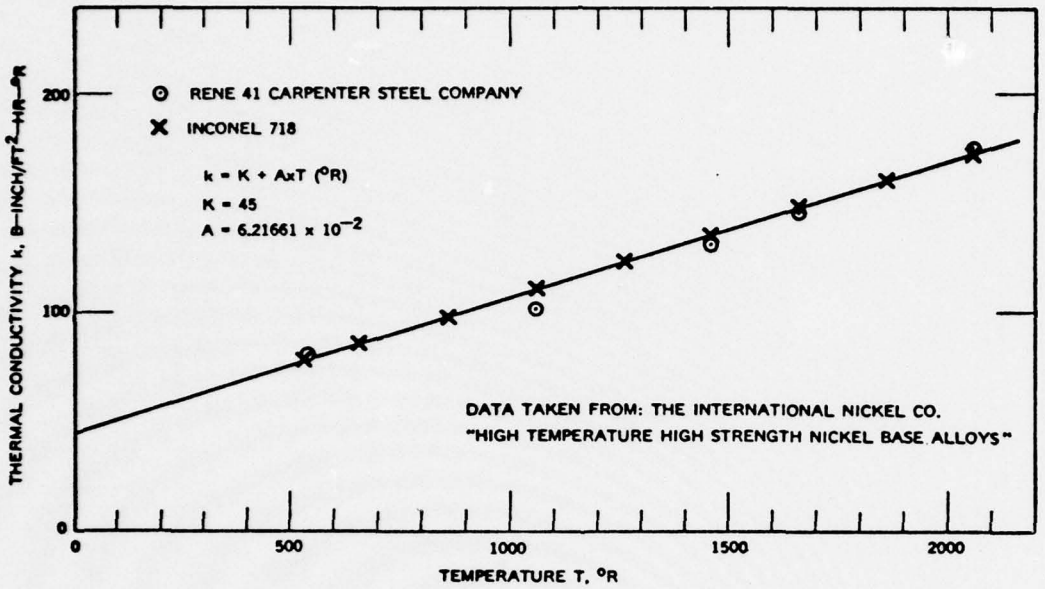

Figure 25. Thermal Conductivity of Inconel 718 Material (Hot Cylinder)

SECTION III

FABRICATION OF THERMAL ENERGY STORAGE UNIT FOR HIGH CAPACITY VUILLEUMIER CRYOGENIC COOLER

3.1 MACHINING AND INITIAL ASSEMBLY

The components of the thermal energy storage unit (Figure 9) were machined from standard Inconel 600 pipe.

Tube No. 1	1" nominal	1.315" O.D. x 0.133" wall
Tube No. 2	2" nominal	2.375" O.D. x 0.154" wall
Tube No. 3	2-1/2" nominal	2.875" O.D. x 0.023" wall
Tube No. 4	3-1/2" nominal	4.000" O.D. x 0.226" wall
Tube No. 5	4" nominal	4.500" O.D. x 0.237" wall
Tube No. 6	5" nominal	5.563" O.D. x 0.258" wall

The flanges were machined from Inconel 600 0.064 inch thick flat stock. The final machined parts of the thermal energy storage unit are shown in Figure 26.

The hot cylinder was machined from an 8-1/2-inch diameter x 7.5 inch long Inconel 718 hot finished forging. The final machined part is shown in Figure 27. The terminal flange was machined from a 9-1/4-inch diameter 1-inch long hot finished forging. The terminal flange was then furnace brazed to the hot cylinder with a nickel-gold braze material.

Tubes No. 1, No. 5 and No. 6 of the thermal energy storage unit were electron beam welded together with the interconnecting flanges, as were tubes No. 2 and No. 3. Prior to filling the thermal energy storage unit with the TES material, the internal surfaces of the heat pipe were covered with the wicking material as shown in Figures 28 and 29.

PRECEDING PAGE BLANK-NOT FILMED

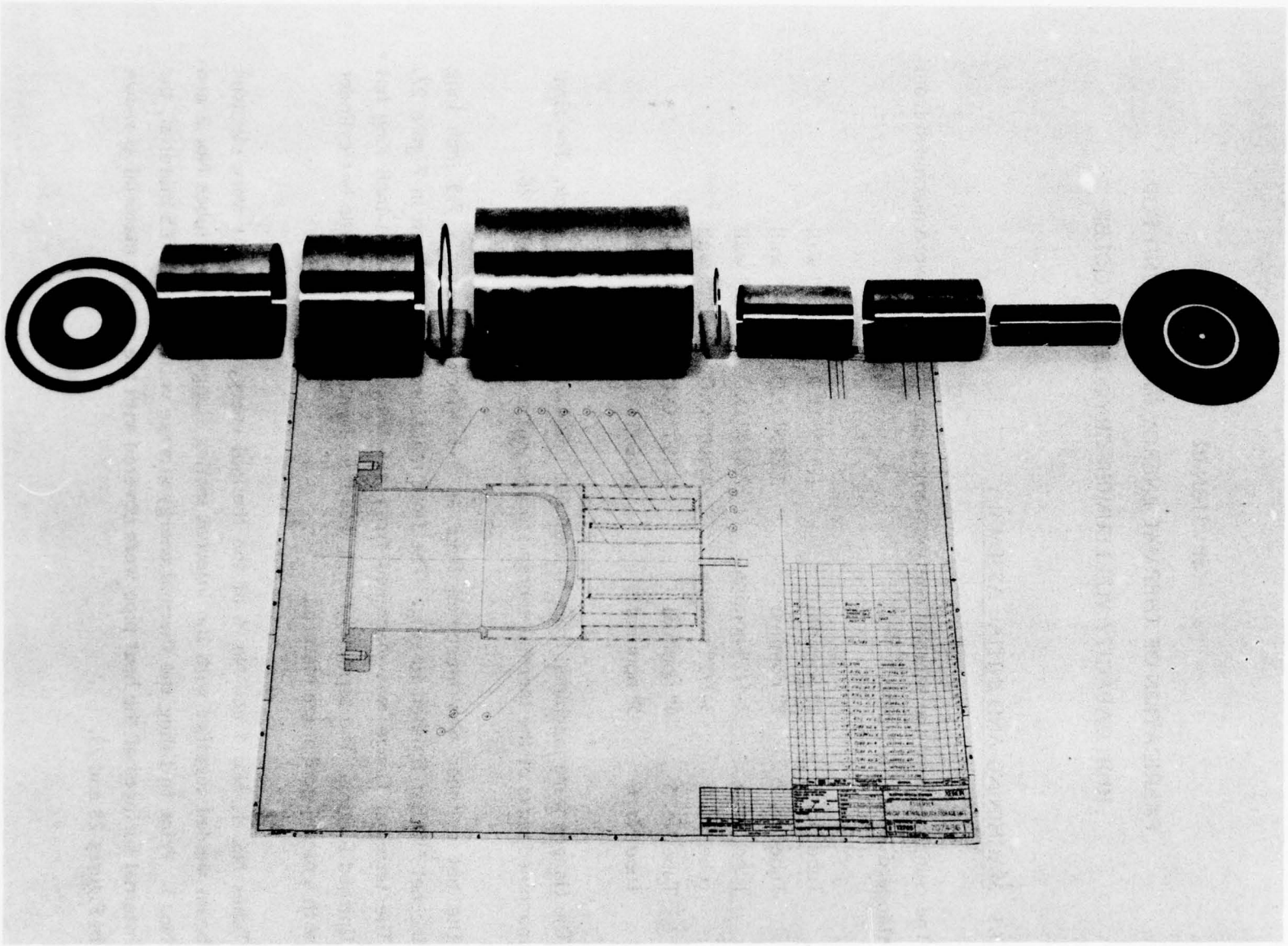

Figure 26. Thermal Energy Storage Unit Parts Prior to Electron Beam Welding

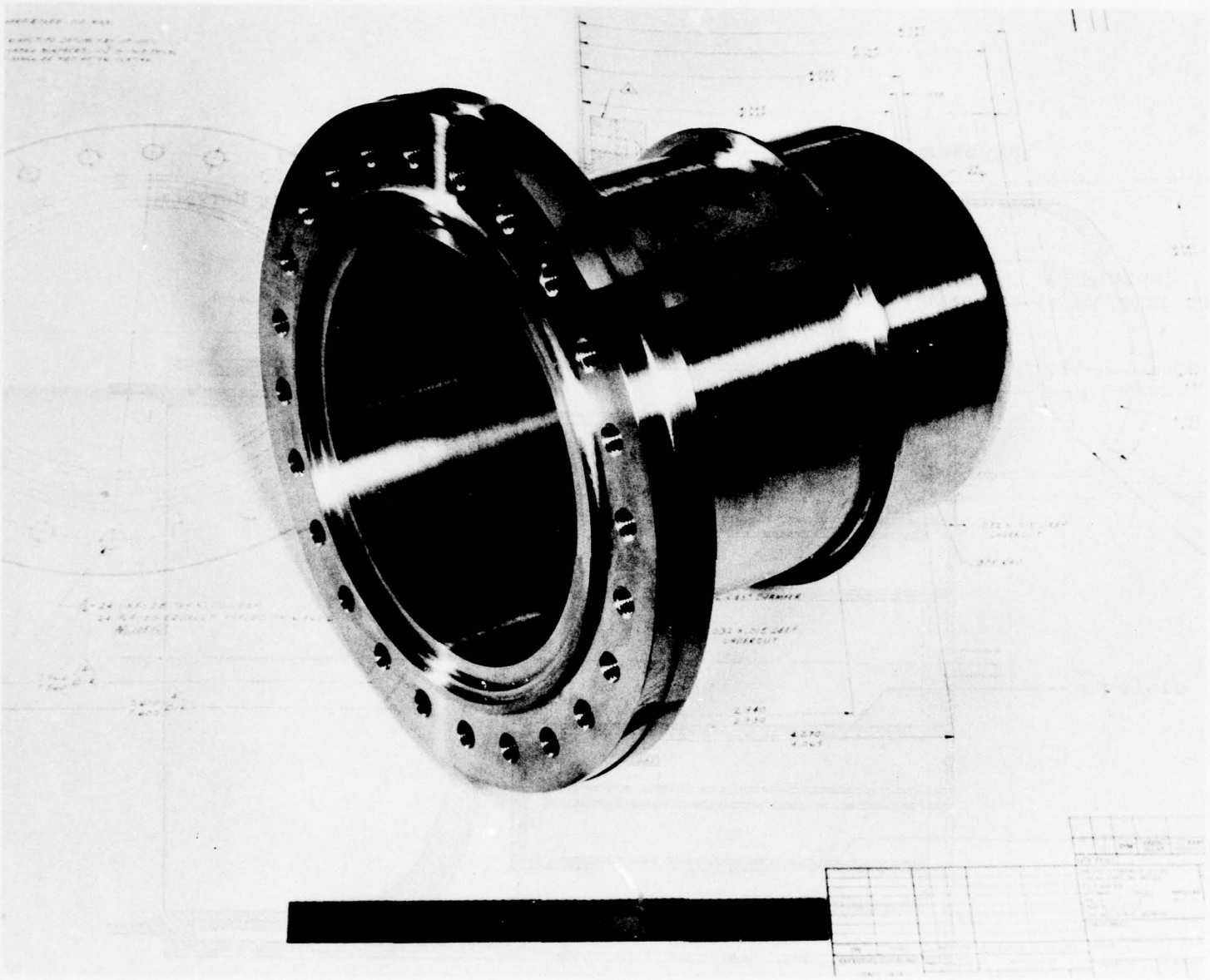

Figure 27. Hot Cylinder with Terminal Ring

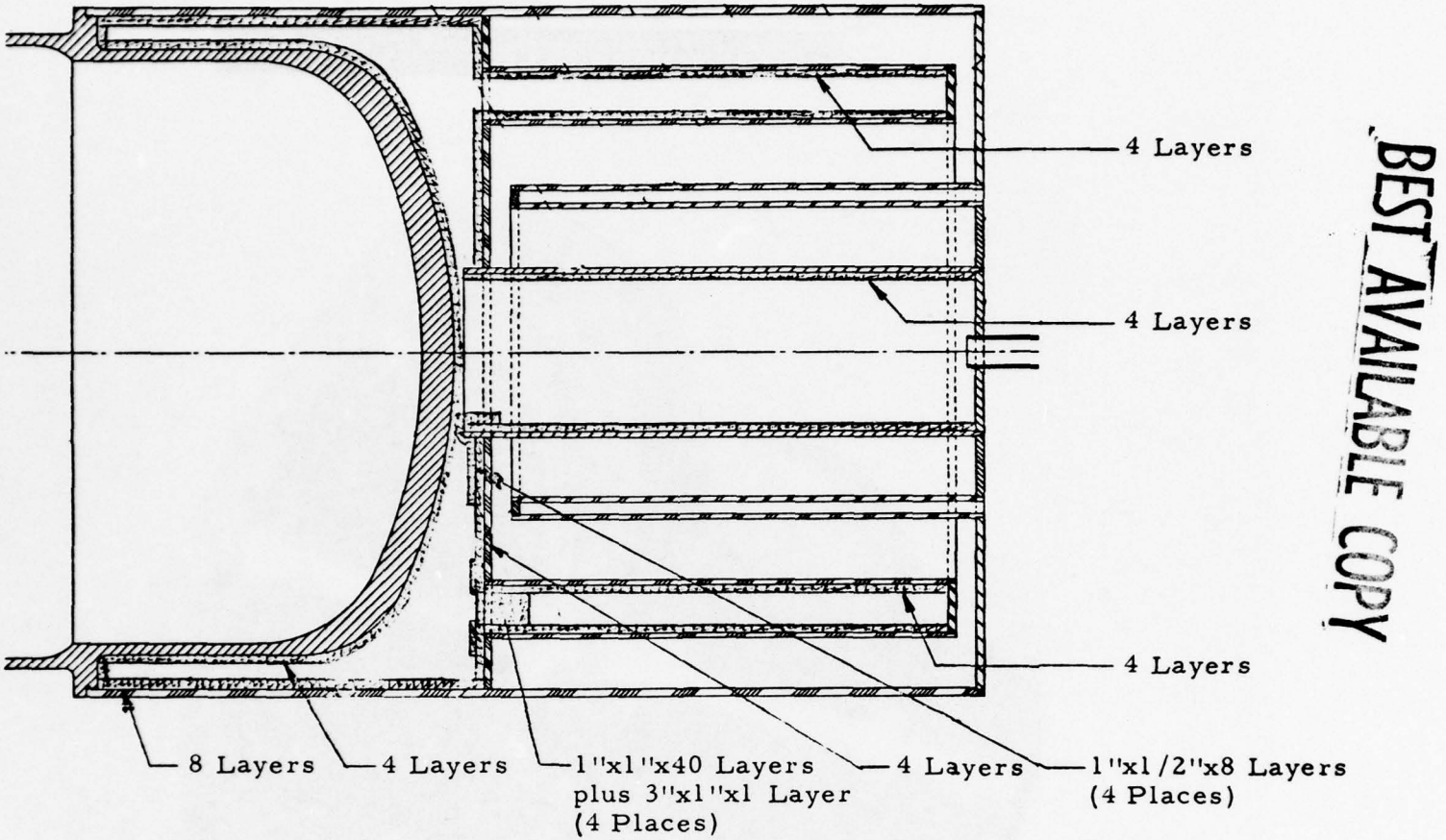

BEST AVAILABLE COPY

Wicking Material: 70 Mesh Bolting Cloth 0.00375 inch Wire Diameter

Figure 28. Wicking Design of the Hi-Cap Thermal Energy Storage Unit

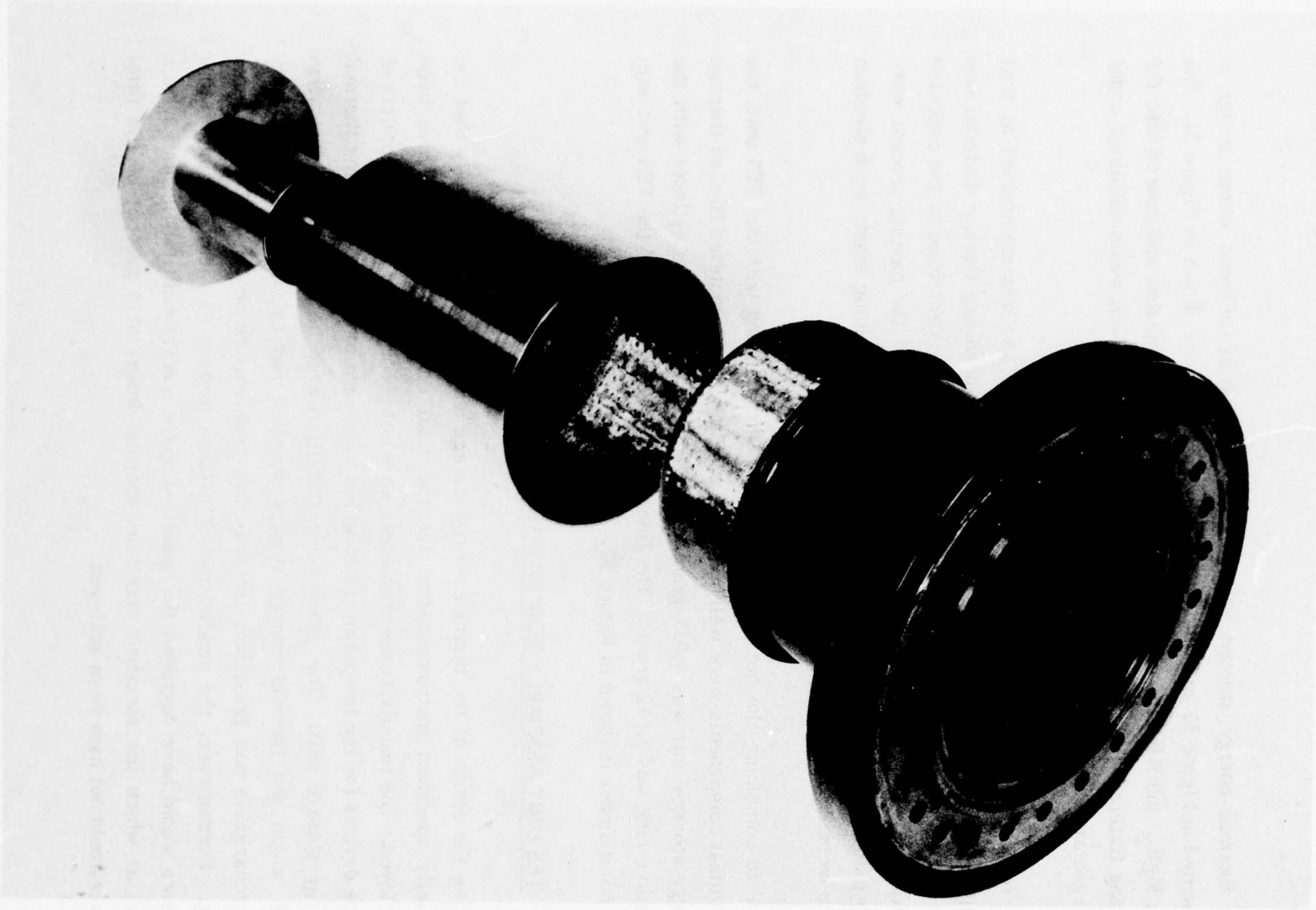

Figure 29. Thermal Energy Storage Unit with Hot Cylinder of Hi-Cap Vuilleumier Cooler Prior to Final Assembly and Loading with Thermal Energy Storage Material

The thermal energy storage salt was cast in a graphite mold whose design is presented in Figure 30 and whose finished components are shown in Figure 31. The LiF, MgF_2, and KF salts were mixed in the proper proportion and poured into the casting fixture. The fixture was placed into a retort which was maintained under an argon atmosphere during the casting process.

The retort was raised to a temperature of 1385°F and was maintained at that temperature for 2 hours. After cooling, the thermal energy storage material was found to have solidified in the fixture and its volume had decreased by the expected amount. The three TES tubes that had been formed in the casting process were then placed into the TES unit, after which the last remaining seams were electron beam welded together.

Prior to combining the hot cylinder and the terminal ring with the TES unit, the individual components were weighed. The weight of the completed Hi-Cap thermal energy storage unit was 4,039 grams and the weight of the hot cylinder with the terminal ring was 5,152 grams. The final completed assembly of the TES unit with the hot cylinder is shown in Figure 32.

3.2 TES UNIT ASSEMBLY FOR INITIAL PERFORMANCE TESTING

During the design of the thermal energy storage unit, it appeared unlikely that the initially specified instrumentation for the final configuration could have been employed. The resistivity thermometers were not recommended by the suppliers of these devices for the temperatures to which they were to be exposed in the thermal energy storage unit. The directly electrically heated hot cylinder configuration with which the thermal energy storage supplied hot cylinder was to be fully interchangable had provisions for only two temperature sensors in the terminal ring. Furthermore, the penetration of a large number of sheathed temperature sensors would have degraded the specified space quality multifoil insulation to a level at which the specified maximum thermal losses of 5 percent of the total power could not have been achieved.

BEST AVAILABLE COPY

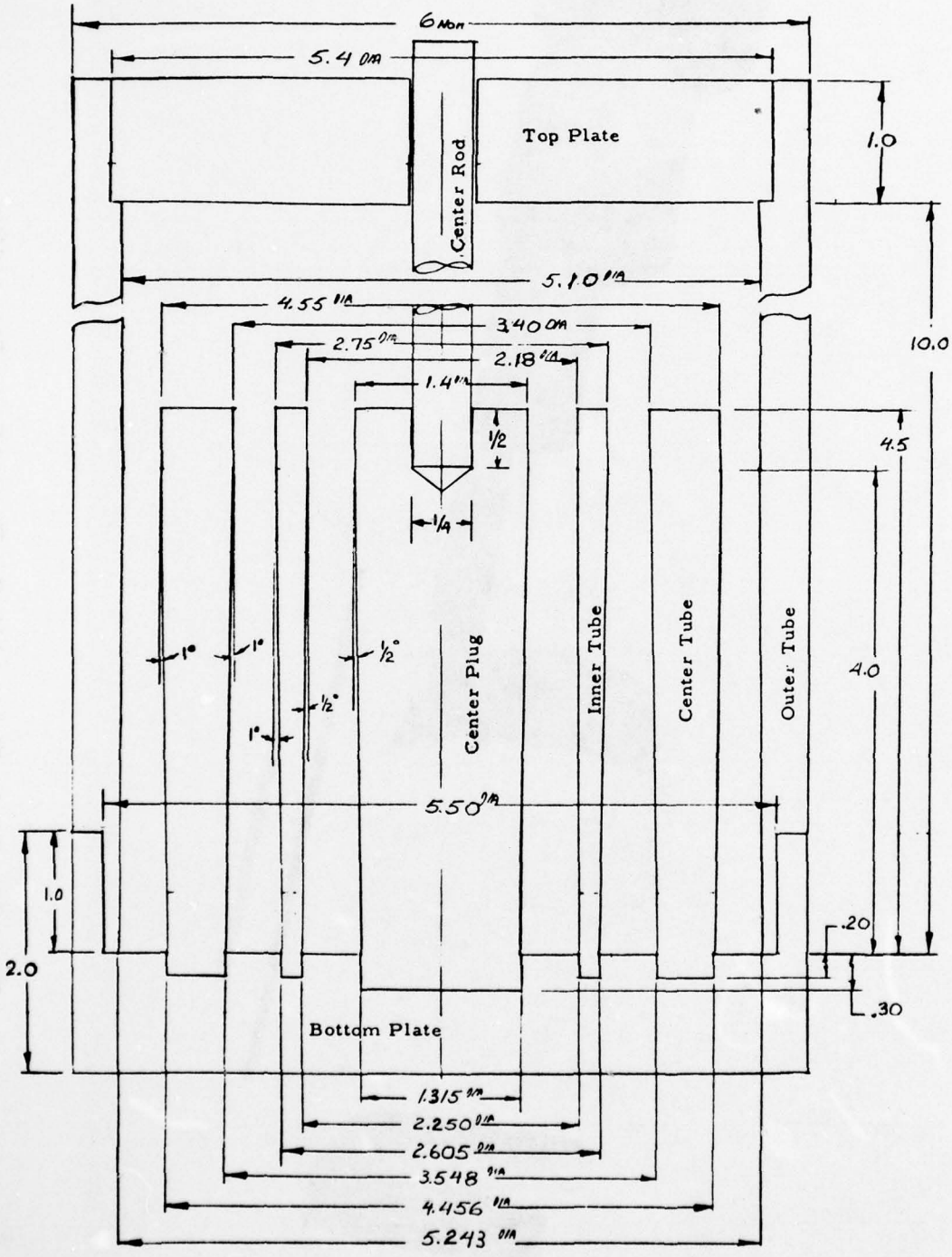

Figure 30. Graphite Casting Fixture

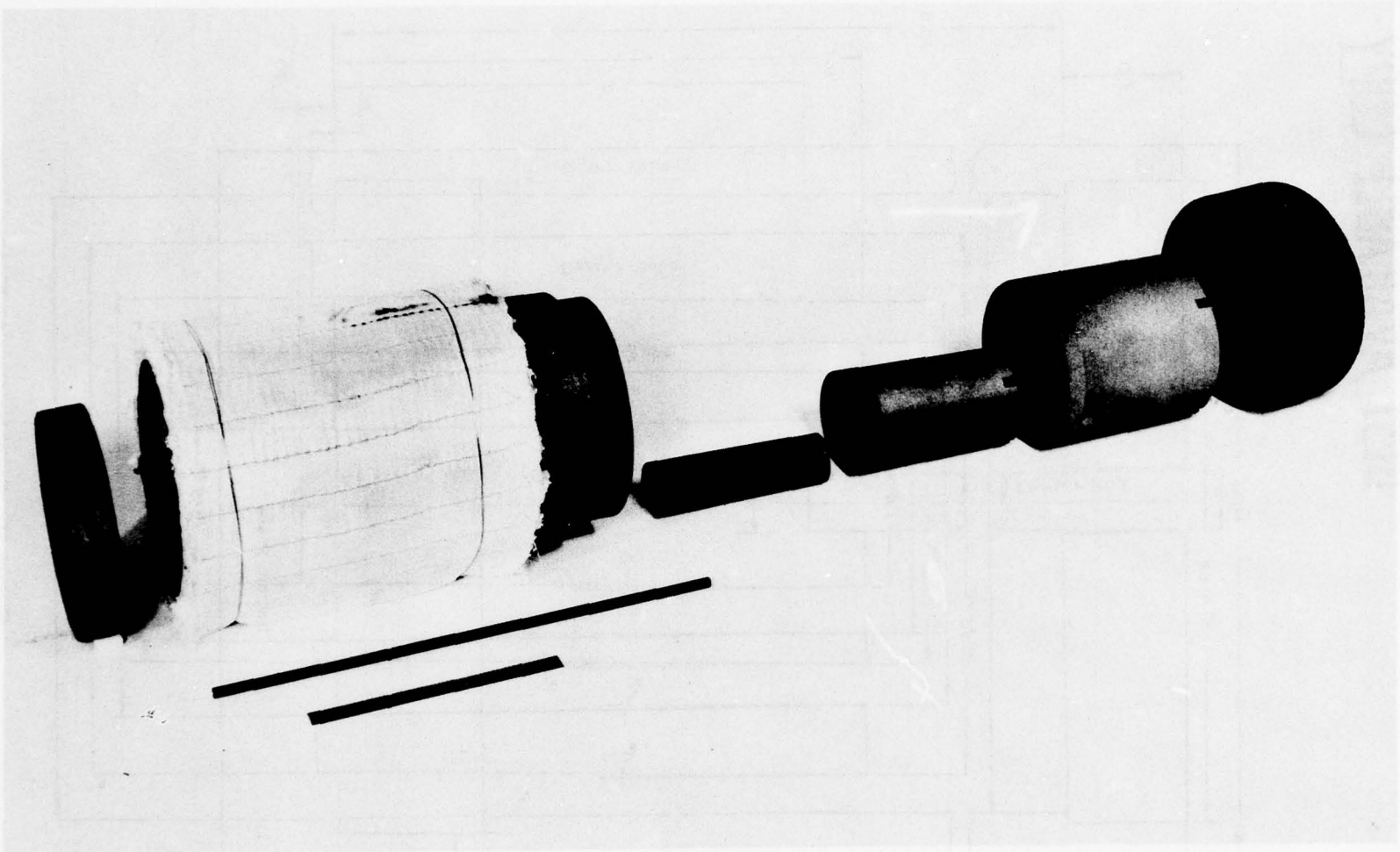

Figure 31. Casting Fixture of Hi-Cap Thermal Energy Storage Unit

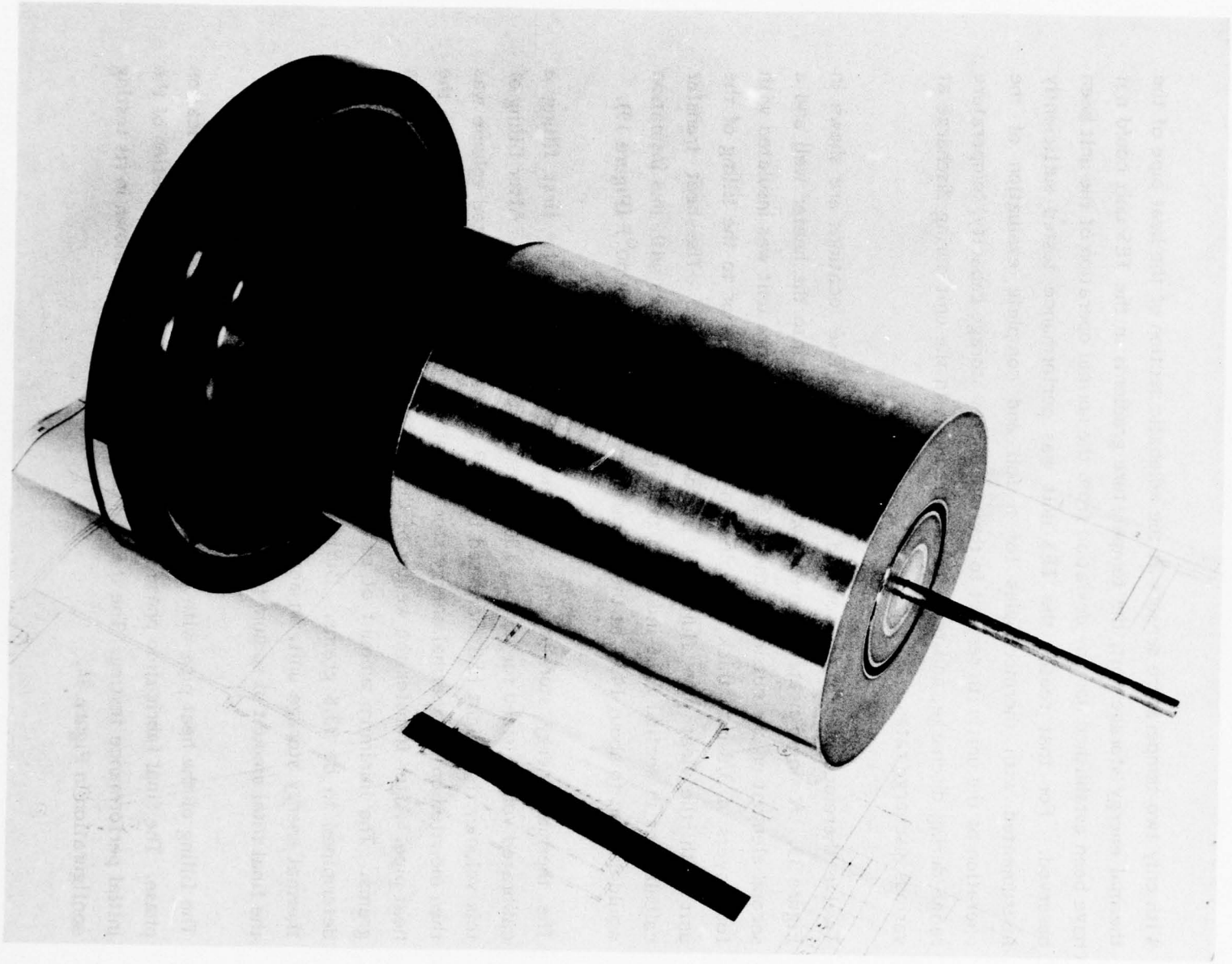

Figure 32. Fully Assembled Thermal Energy Storage Unit of Hi-Cap Vuilleumier

With only two temperature sensors at the adiabatic section of the heat pipe of the thermal energy storage unit, the temperature gradients in the TES unit could not have been established nor any deviation from the normal operation of the unit been observed. For that reason the TES unit was performance tested sufficiently instrumented with thermocouples for a full and complete evaluation of the operation of the unit with respect to thermal energy storage capacity, temperature range during discharge, and temperature gradients in the unit during discharge at various discharge rates.

Twelve thermocouples were mounted on the unit whose locations are shown in Figure 33. A single heater element was then placed into the heater well and a second element on the outside of the TES unit. The entire unit was insulated with four layers of 3/8-inch thick Flexible Min-K insulation prior to the filling of the unit with the heat pipe fluid and performance testing. The heat transfer calculations in section 2.3.6 indicated that the thermal losses with this insulation would amount to about 143W at the operating temperature of 1250^{o}F (Figure 19).

The thermal energy storage unit was charged with sodium by first filling a calibrated volume sized for holding 100 grams of sodium at 300^{o}F. After filling of this volume, its weight had increased by 99.9 grams. The calibrated volume was then mounted on the thermal energy storage unit for transfer of the sodium to the heat pipe. After transfer the weight of the calibrated volume had decreased by 94 grams. The minimum amount of sodium for the fill of the heat pipe had been determined to be 93.8 grams. During burping of the heat pipe section of the thermal energy storage unit, an additional 4 grams of sodium were added, so that the final total amount of sodium in the heat pipe was 98 grams.

The filling of the heat pipe with the working fluid completed the initial fabrication phase. The final fabrication phase was to be accomplished after completion of the initial performance testing. The thermal energy storage unit is shown in its testing configuration in Figure 34.

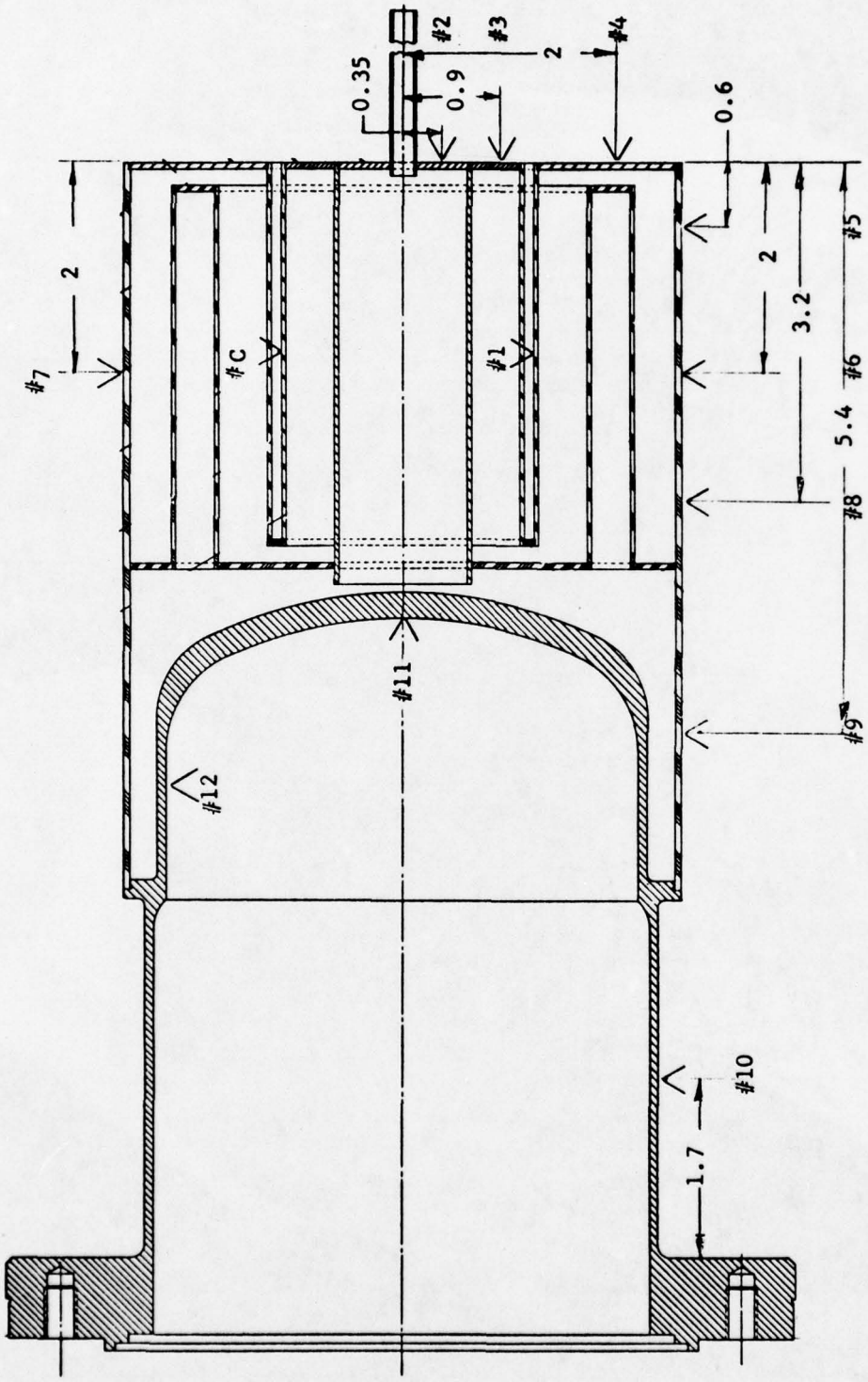

Figure 33. Thermocouple Locations for Initial Testing of Hi-Cap Vuilleumier Cooler Thermal Energy Storage Unit

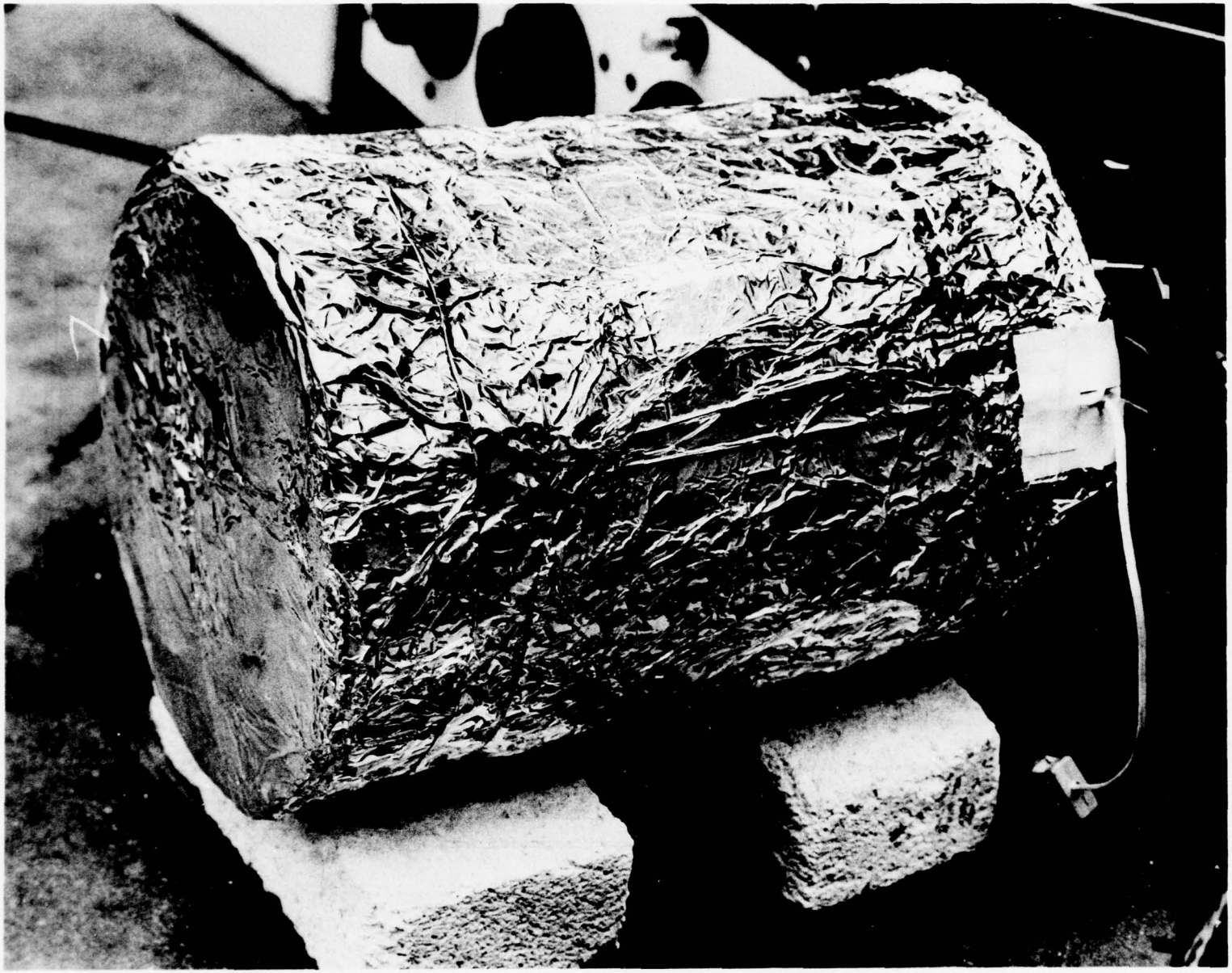

Figure 34. Hi-Cap Thermal Energy Storage Unit in Its Initial Performance Testing Configuration

3.3 FINAL ASSEMBLY OF THE THERMAL ENERGY STORAGE UNIT FOR THE HIGH CAPACITY VUILLEUMIER CRYOGENIC COOLER

3.3.1 FINAL INSTRUMENTATION SELECTION

A considerable amount of testing was performed on four commercially produced resistance temperature detectors (RTD) and on three RTD's that were assembled from commercial RTD elements. Three out of the four commercial RTD's failed when they were exposed to temperatures above 1000°F, one during the very first cycle, the other two after several cycles extending from room temperature to 1350°F. Only one of the commercial RTD's survived four temperature cycles and was therefore considered for use in the TES unit. All failures were caused by shorting of the RTD element to the sheath of the detector.

The three in-house built detectors were assembled from components which were furnished by two vendors, Omega Engineering, Inc. and RdF Corporation. The sensing elements of the two vendors were:

	Diameter	Length
Omega Engineering	0.059 inch	0.984 inch
RdF	0.100 inch	1.250 inch

These elements were placed into 7 inch long, 0.125-inch diameter, 0.010-inch wall thickness stainless steel tubing. The leads were insulated with Alumina round double bore tubing with an 0.094-inch outside diameter. The upper ends of the RTD's were closed off with Sauereisen while the two leads were secured with Epoxy. During testing of the RTD's, the RTD made up with the RdF element failed at about 1100°F due to shorting to the stainless steel sheath. The RTD's which were assembled with the Omega elements performed quite well over many cycles.

Because of the unfavorable experience with the RTD's, further investigation into their reliability was advised prior to committing the temperature control of the TES unit entirely to this type of instrumentation. Permission was asked and obtained to change the specified temperature control instrumentation from two RTD's to one RTD and two K calibration-type ungrounded sheathed thermocouples. This combination of sensors would permit the use of RTD instrumentation if so desired, while being backed up by two thermocouples.

An additional hole was drilled into the thermal ring of the hot cylinder for accepting a 1/16-inch diameter sheathed thermocouple. The temperature control and measurement instrumentation for Hi-Cap unit No. 1 consisted therefore of one 1/8-inch diameter, 7-inch long, 100 ohm platinum RTD, one 1/8-inch diameter, 7-inch long K calibration (chromel-alumel) thermocouple, and one 1/16-inch diameter, 8.5-inch long K calibration thermocouple. The most suitable instrumentation for this application would have been three 1/16-inch K calibration thermocouples, two of them 8.5-inch long and one 6.5-inch long. The two 8.5-inch long thermocouples would be used for the control of the heaters, one being a back-up for the other, and the 6.5-inch long thermocouple for the monitoring of the temperature of the hot cylinder.

3.3.2 FINAL ASSEMBLY

After completion of the performace tests, which are presented in Section 4.3 of this report, the final assembly of the thermal energy storage unit could be initiated. The temporary insulation, the thermocouples and the two test heaters which were used for the initial performance testing were removed. The fill valve of the heat pipe was eliminated by compressing the tube between the fill valve and the TES unit with a flattening tool, and cutting and welding tight the tube at the flattened section with an electron beam.

With the testing of the temperature sensors and the selection of additional thermocouples for the control of the heaters of the thermal energy storage unit completed, the installation of the final instrumentation, the eight heater elements,

and the final insulation was initiated. Figure 35 shows the eight (8) heater elements, each having a nomial resistance of 40 ohms, the 1/16-inch thermocouple, and the commercially built 1/8-inch diameter RTD installed and the insulation of the hot cylinder barrel completed.

The insulation is made up of layers of 0.020-inch thick Fiberfrax paper without binder and 0.001-inch thick nickel foil. The thickness per completed layer consisting of one thickness of Fiberfrax paper and nickel foil each was 0.032 inch. The insulation of the barrel consisted of 43 layers. The insulation of the thermal energy storage unit consisted of 34 layers on the diameter and on the end, according to the insulation design of the Hi-Cap thermal energy storage that was shown in Figures 22 and 23. After completion of the insulation, the heater elements were electrically connected. The four internal heater elements, i.e., the elements which are in the heater well of the unit, were connected in two pairs, each pair having two opposing elements in parallel. The same electrical connection was employed for the four outer elements. 1/16-inch diameter insulated nickel wire was used to make the heater connections to the terminal ring of the hot cylinder.

The connections of the heaters and the instrumentation in the terminal ring are shown in Figure 36. A picture of the TES unit with the finished insulation is shown in Figure 37. The hot cylinder with the thermal energy storage unit enclosed in its insulation container is presented in Figure 38.

Prior to the final testing of the Hi-Cap thermal energy storage unit, temporary thermocouples were installed on the outer surface of the insulation container and its cover. The location of these thermocouples with the locations of two additional thermocouples in the terminal ring of the hot cylinder and two thermocouples on the inside surface of the hot cylinder are shown in Figure 39. Instrumentation and power leads were then attached to the terminals in the terminal ring.

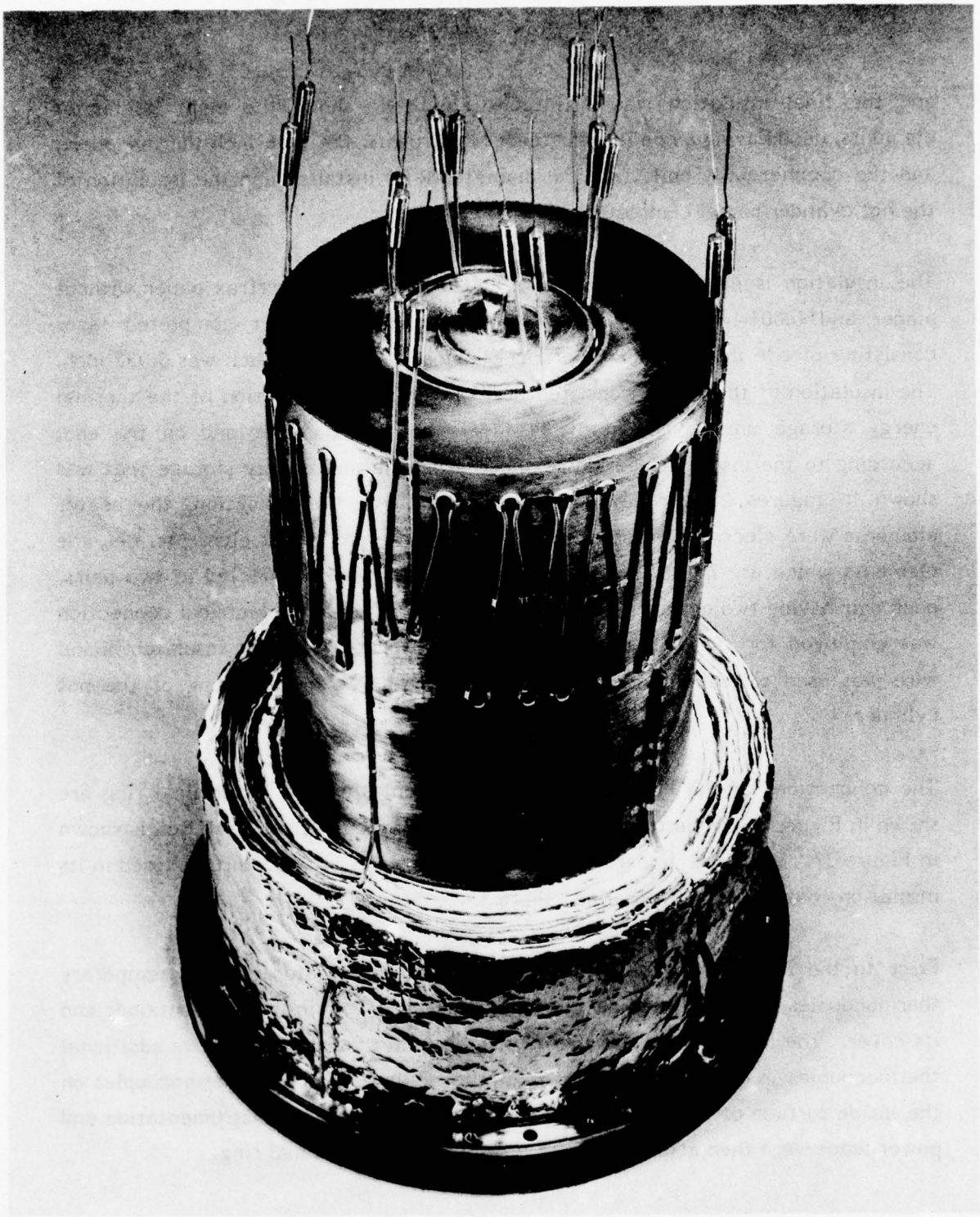

Figure 35. Hi-Cap Thermal Energy Storage Unit with Heaters and Temperature Instrumentation

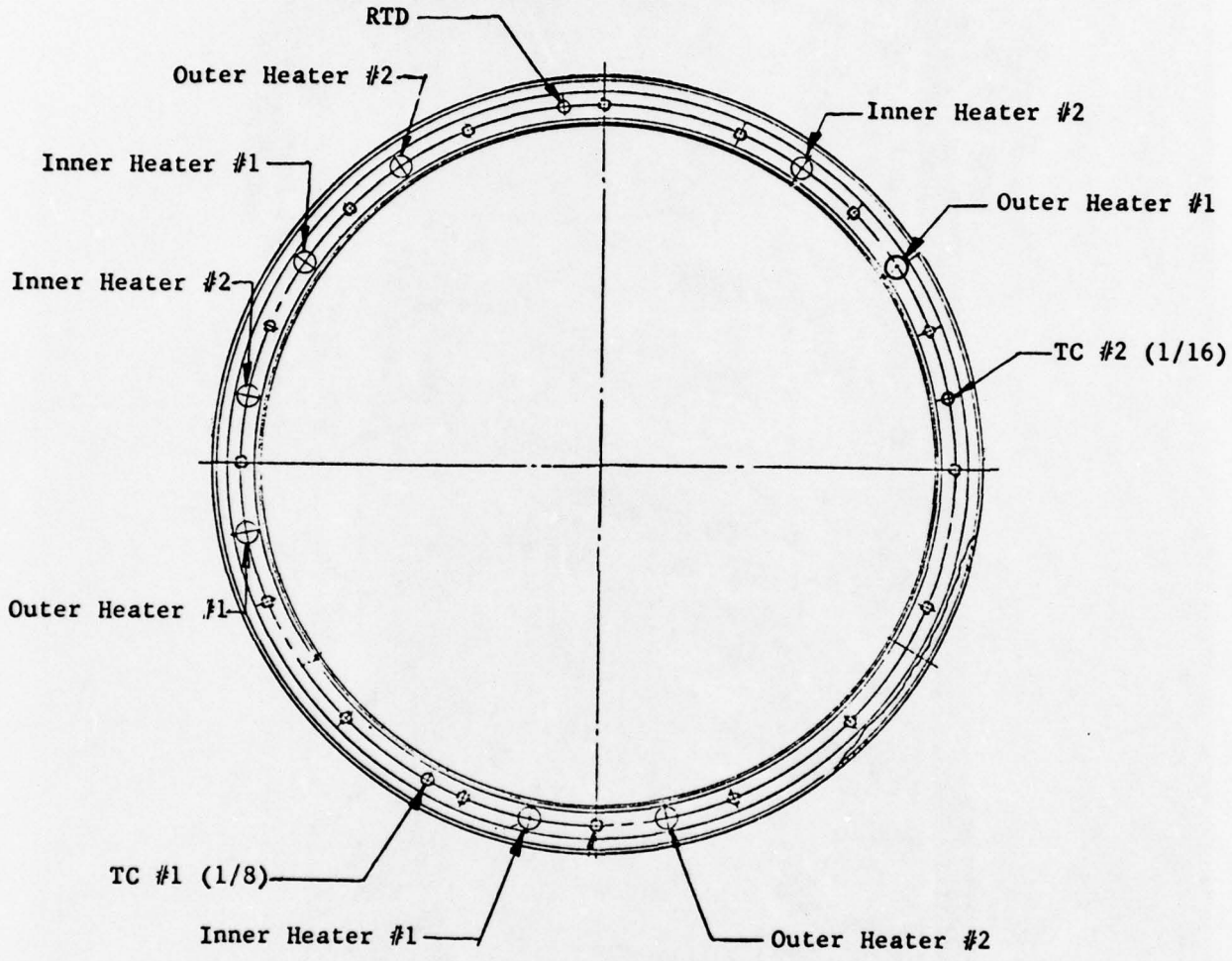

Figure 36. Heater and Temperature Sensor Connector Locations (Hi-Cap TES Unit No. 1)

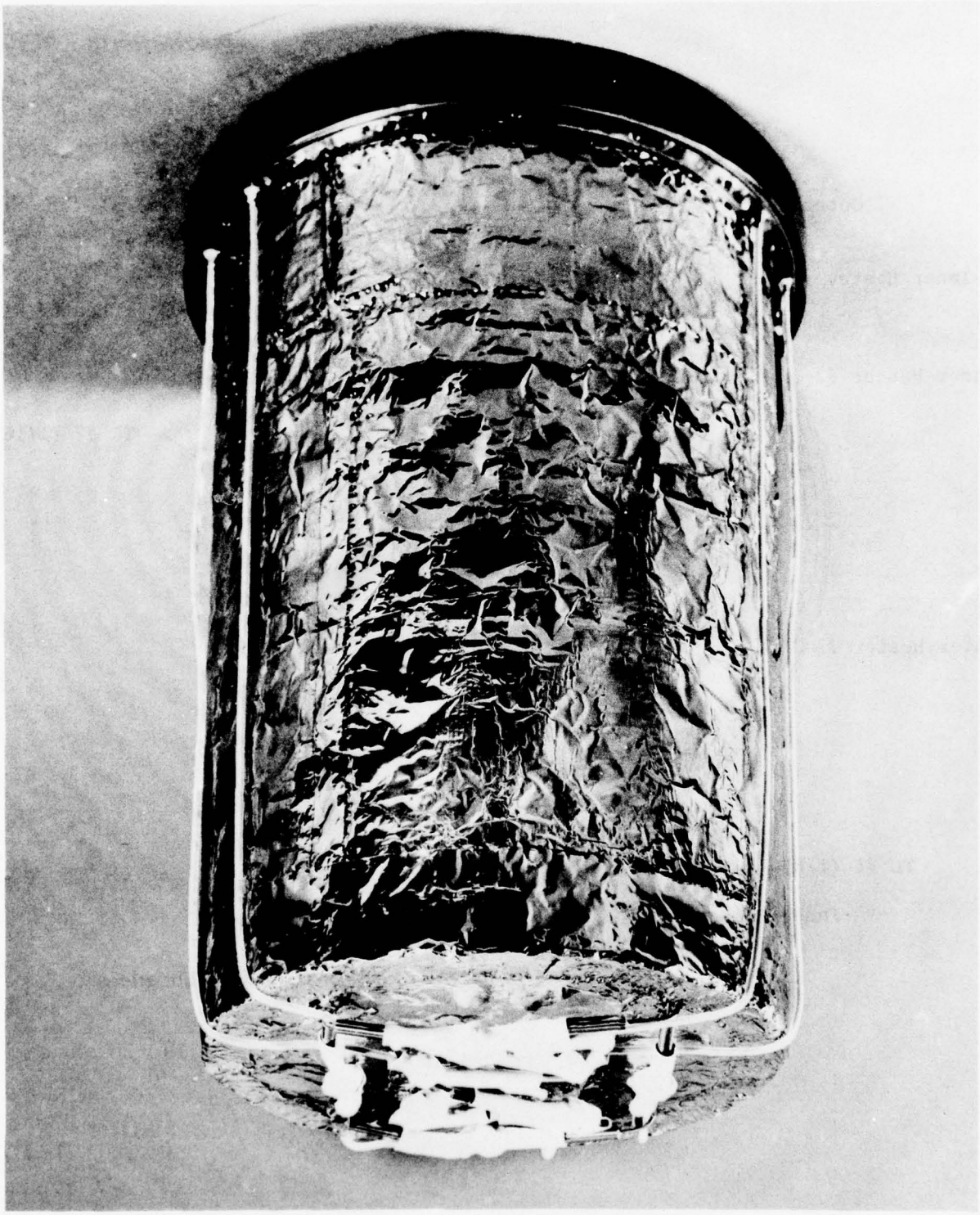

Figure 37. Hi-Cap Thermal Energy Storage Unit Without Insulation Container

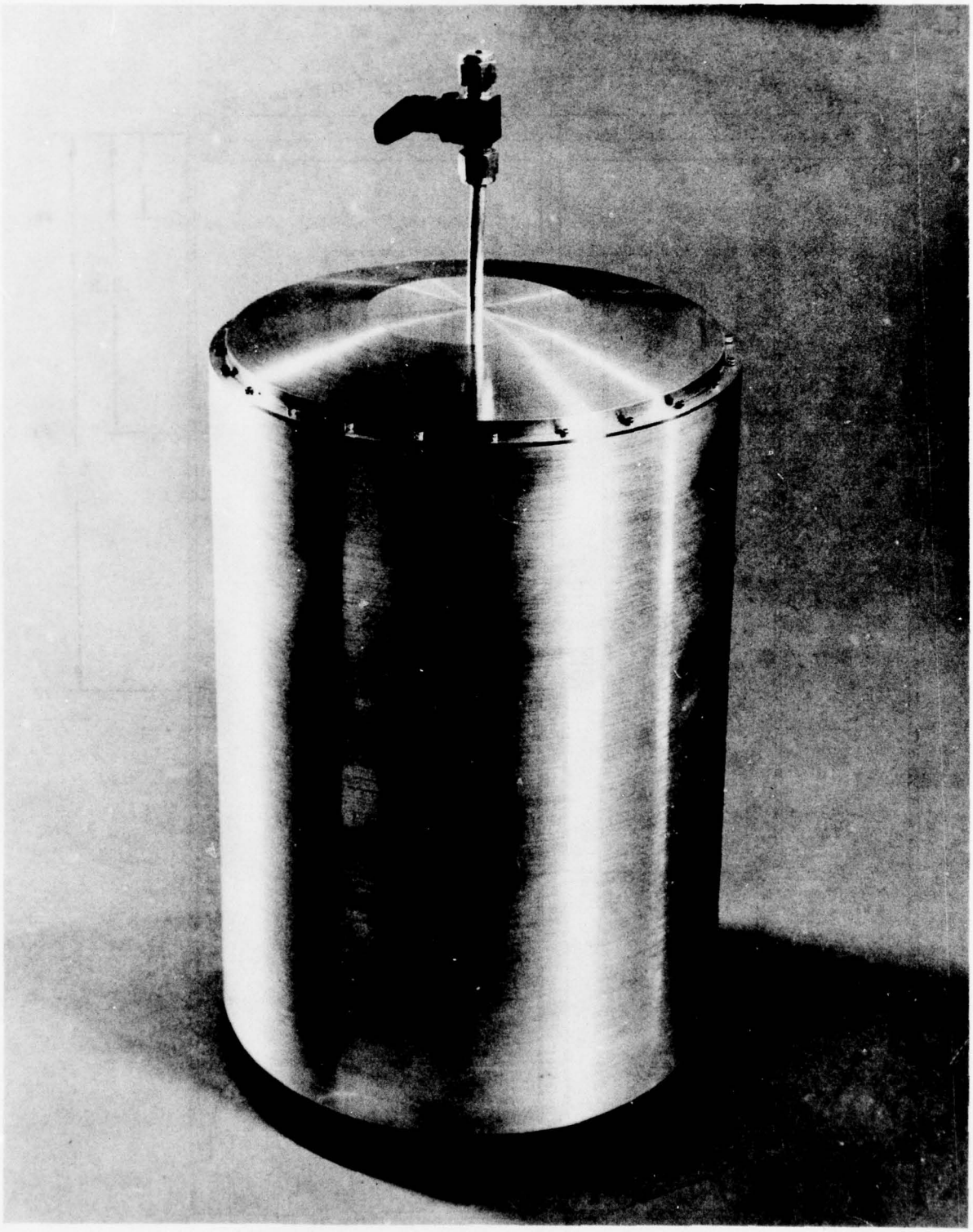

Figure 38. Hi-Cap Thermal Energy Storage Unit

BEST AVAILABLE COPY

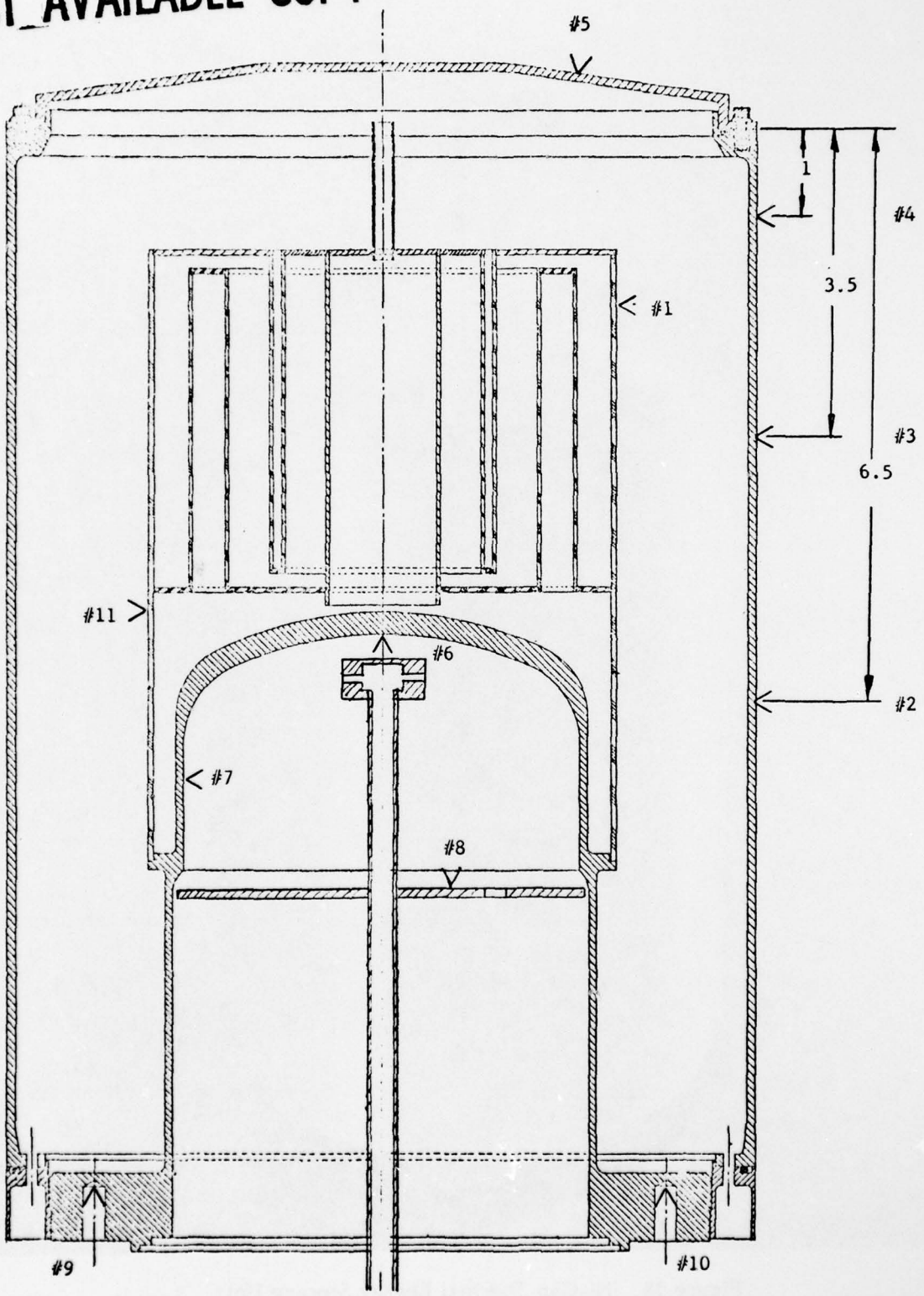

Figure 39. Thermocouple Locations for Testing of Hi-Cap Thermal Energy Storage Unit in Its Final Configuration

During the final assembly of the insulation container with the terminal ring it became apparent that it might be very difficult at a later date to disassemble the unit, due to difficulties in reaching the small screws that hold the container to the ring and compress the sealing "O" ring. A modification of the insulation container was indicated, which had been contemplated during the design phase of the program but was rejected in favor of retaining the established Hi-Cap design. A new container lid was designed and built which permitted the sealing of the container with a radial seal. This modification removed the upper ring of the container, which contained the "O" ring seat and the threads for the 24 screws that held the lid to the container.

The modified design permitted an easy access to the 24 screws that fasten the insulation container to the terminal ring and made the sealing of the lid independent of the tightness of screws. A similar modification of the seal design at the terminal ring is proposed. Since the temperature to which the "O" ring will be exposed could be considerably lower, the vacuum sealing of the unit would be more reliable, and the large number of difficult to access screws could be eliminated.

SECTION IV

TESTING OF HIGH CAPACITY VUILLEUMIER CRYOGENIC COOLER THERMAL ENERGY STORAGE UNIT

4.1 TEST CONSIDERATIONS

The testing of the high capacity Vuilleumier cryogenic cooler TES unit was undertaken in two parts, initial performance testing in a thoroughly instrumented test configuration and the determination of thermal losses in the final configuration. The limited instrumentation for the control of power and temperature of the hot cylinder consisting of two resistance temperature detectors (RTD's) that could only be accommodated in the final configuration of the TES unit, would not have permitted the full and complete characterization of the TES unit. Possible temperature gradients along the TES unit that would have indicated a malfunction of the heat pipe and would have required corrective action, could not have been detected in the final configuration, nor could the temperature ranges over which the stored thermal energy is being released as a function of the discharge rate have been measured. Thus, the design approach of the TES unit design could not have been fully verified with the TES unit in its final configuration.

It was therefore decided to performance test the TES unit in a configuration that permitted the installation of a large number of thermocouples along the outside and into the heater well of the unit. The locations of these bare grounded chromel-alumel thermocouples was shown in Figure 33.

Since these thermocouples were only to be used during the initial performance testing and had to be removed for the final configuration, the final superinsulation made up of layers of Fiberfrax paper and nickel foil could not be installed for the initial testing. Funds and time for constructing this insulation twice were not available. The insulation for the initial performance testing of the unit consisited therefore of four layers of 3/8-inch thick Flexible Min-K insulation. The thermal

PRECEDING PAGE BLANK-NOT FILMED

losses through this insulation were calculated to be 144W at the nominal operating temperature of the thermal energy storage unit. This compared with the predicted losses of 34.4W through the final superinsulation built up of Fiberfrax and nickel foil. On the other hand, no cooling of the terminal ring of the hot cylinder was necessary during initial performance testing as the "O" ring that seals the insulation container was not required in this configuration. It was indicated that the total thermal losses in the two configurations, the initial performance test configuration and the final TES unit configuration, would almost be the same. In the initial performance test configuration, the thermal losses of 144W would occur through the Flexible Min-K insulation. In the final configuration, thermal losses of 113W would result from the need of cooling the terminal ring to which energy was conducted along the barrel of the hot cylinder. The losses through the superinsulation would be only 34.4W. The total thermal losses comprised of the two components were thus expected to amount to 148W. The conduction loss along the hot cylinder barrel is peculiar to the hot cylinder design. It is suffered by the cryogenic cooler regardless of whether the hot cylinder is heated by electrical heaters or by the thermal energy storage unit. They are included in the stated power requirement for the hot cylinder.

4.2 TEST SETUP

After filling the heat pipe of the TES unit with sodium, the thermal energy storage unit was incorporated into the test setup which is shown in Figure 40. The heat pipe fill valve was not removed from the unit in case the test results should have shown some underfill or overfill of the heat pipe with working fluid or entrapment of gas which had not been removed by burping of the heat pipe during processing.

In the picture, the power panel with the variacs for the control of the heaters is shown on the right hand side. The temperature controller in the center of the panel was activated by one of the two thermocouples in the heater well. The output of the twelve additional thermocouples was recorded continuously on the 24 point chart recorder shown to the left of the power panel. The recorder had been connected to permit the output of each thermocouple to be printed twice during

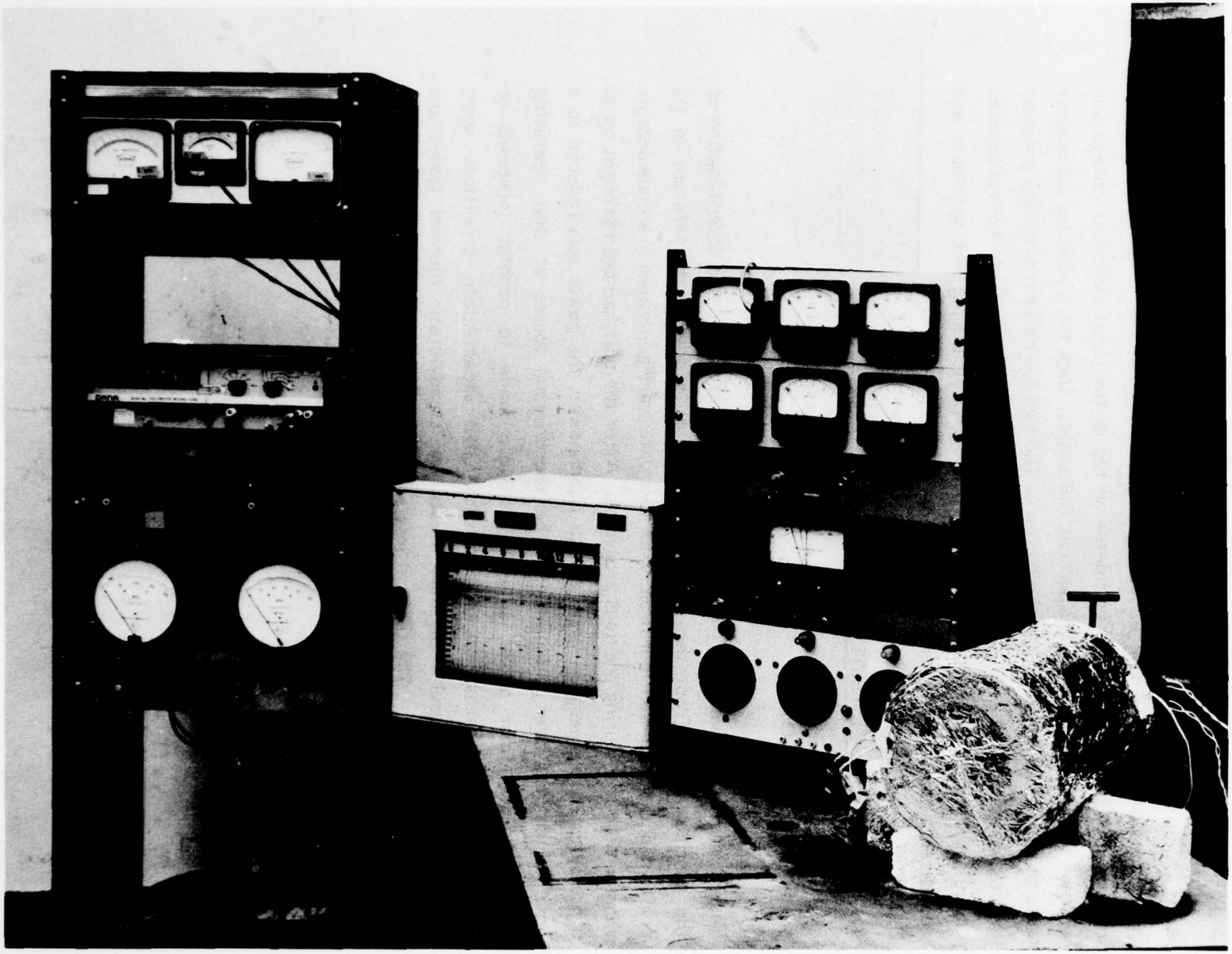

Figure 40. Test Set-up for Performance Testing of the Hi-Cap Thermal Energy Storage Unit

each cycle, each cycle lasting two minutes. The digital voltmeter in the left hand panel permitted the reading of the thermocouple outputs in millivolt. The two current meters and the single voltmeter on top of the panel indicated voltage and current with an accuracy of 1/2 percent full scale. They were used for accurately determining the power input to the heaters. The two 1/4 percent accurate pressure gauges on the bottom of the panel metered the gas flow by which the Vuilleumier cooler operation was simulated. They permitted measuring the upstream and downstream pressure of a calibrated orifice.

4.3 PERFORMANCE TESTING

4.3.1 THERMAL LOSSES

Testing of the thermal energy storage unit was initiated with the determination of the thermal losses from the unit as function of operating temperature in its performance testing configuration. The test data were generated in a considerably shorter time than during previous programs. After the unit had been brought up to a pre-selected temperature with a high input power, the power was reduced to a level which had been calculated to be the thermal losses at that operating temperature. Minor power adjustments were made to counter increases or decreases in the measured temperatures until steady-state conditions were established. The results of these tests for steady-state thermal losses are presented in Figure 41. The thermal loss at the nominal operating temperature of 1250^{o}F was found to be 155 watts. This compared with the predicted loss of 144 watts which had not considered the losses from the fill valve that remained on the TES unit.

The thermal losses could be expressed by the relation

$$P_L = A \times (T_o - T_a)^n$$

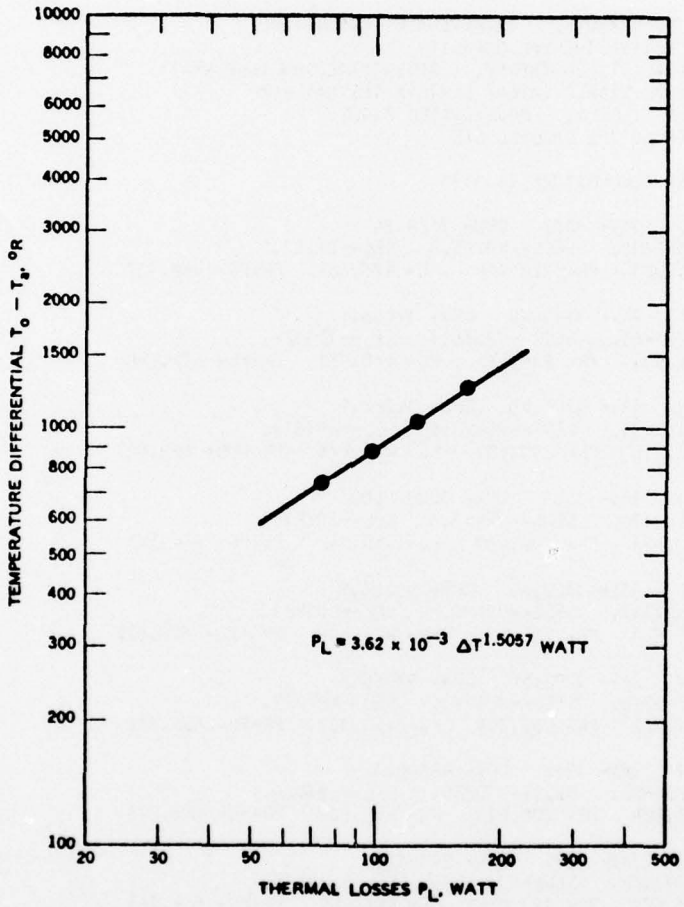

Figure 41. Thermal Losses from the Hi-Cap Thermal Energy Storage Unit in Its Initial Performance Testing Configuration

60335

BEST AVAILABLE COPY

```
11:11  JUN 07  TES2...                Run #10        2 June 1977

POWER LOSSES PL= 3.62000E-03X(T0-TR )XX 1.50570 WATT
SENSIBLE HEAT OF AIR CP=0.553+3.333E-5X(T1-TR) J/R-G
ELECTRICAL POWER INPUT PI= 0 WATT
FLOW RATE W= .667940 G/SEC
RADIATION CONSTANT R= 2.62000E-11 WATT/DEG.R**4
?T
?G
T=END TEMPERATURE,   TAV=AVERAGE TEMPERATURE
CPW=EFFECTIVE THERMAL CAPACITY
SEST=TOTAL STORED ENERGY,   SESS=TOTAL SENSIBLE HEAT
SESL=TOTAL STORED LATENT HEAT IN TES MATERIAL
PL=POWER LOSSES,   PR=RADIATED POWER
PG=POWER IN THE COOLING GAS

STARTING TEMPERATURE T= 1329

T= 1315   TAV= 1322   CPW= 7329.84
SEST=-102618.   SESS=-48225.8   SEL=-54391.9
PL= 167.021   PR= 221.444   PG= 466.682   PR+PG= 688.127

T= 1308   TAV= 1311.50   CPW= 14406.4
SEST=-203463.   SESS=-72338.7   SEL=-131124.
PL= 164.917   PR= 214.465   PG= 460.993   PR+PG= 675.458

T= 1301   TAV= 1304.50   CPW= 14286.9
SEST=-303471.   SESS=-96451.6   SEL=-207019.
PL= 163.518   PR= 211.417   PG= 458.466   PR+PG= 669.883

T= 1301   TAV= 1301   CPW= 100000000
SEST=-402730.   SESS=-96451.6   SEL=-306279.
PL= 162.821   PR= 208.401   PG= 455.942   PR+PG= 664.343

T= 1300   TAV= 1300.50   CPW= 96586.8
SEST=-501317.   SESS=-99096.3   SEL=-401421.
PL= 162.721   PR= 205.416   PG= 453.419   PR+PG= 658.835

T= 1299   TAV= 1299.50   CPW= 97960.6
SEST=-599278.   SESS=-103341.   SEL=-495937.
PL= 162.522   PR= 202.709   PG= 451.108   PR+PG= 653.816

T= 1297   TAV= 1298   CPW= 48690.1
SEST=-696658.   SESS=-110230.   SEL=-586428.
PL= 162.224   PR= 200.271   PG= 449.008   PR+PG= 649.278

T= 1293   TAV= 1295   CPW= 24191.7
SEST=-793425.   SESS=-124009.   SEL=-669416.
PL= 161.627   PR= 197.854   PG= 446.909   PR+PG= 644.763

T= 1281   TAV= 1287   CPW= 7976.26
SEST=-889140.   SESS=-165346.   SEL=-723795.
PL= 160.041   PR= 194.033   PG= 443.553   PR+PG= 637.586

T= 1265   TAV= 1273   CPW= 5898.11
SEST=-983510.   SESS=-220461.   SEL=-763049.
PL= 157.277   PR= 189.566   PG= 439.571   PR+PG= 629.138

T= 1249   TAV= 1257   CPW= 5805.24
SEST=-1.07639E+06   SESS=-275576.   SEL=-800818.
PL= 154.138   PR= 184.719   PG= 435.175   PR+PG= 619.895
```

Figure 42. Run No. 10 (Sheet 1 of 3)

```
T= 1231    TAV= 1240    CPW= 5048.36
SEST=-1.16726E+06    SESS=-337581.    SEL=-829684.
PL= 150.826    PR= 177.733    PG= 428.695    PR+PG= 606.428

T= 1215    TAV= 1223    CPW= 5529.90
SEST=-1.25574E+06    SESS=-392696.    SEL=-863047.
PL= 147.538    PR= 169.224    PG= 420.558    PR+PG= 589.782

T= 1200    TAV= 1207.50    CPW= 5740.84
SEST=-1.34186E+06    SESS=-444366.    SEL=-897489.
PL= 144.562    PR= 160.814    PG= 412.229    PR+PG= 573.043

T= 1185    TAV= 1192.50    CPW= 5586.70
SEST=-1.42566E+06    SESS=-496037.    SEL=-929619.
PL= 141.701    PR= 152.718    PG= 403.919    PR+PG= 556.637

T= 1170    TAV= 1177.50    CPW= 5435.31
SEST=-1.50719E+06    SESS=-547707.    SEL=-959478.
PL= 138.860    PR= 144.927    PG= 395.626    PR+PG= 540.553

T= 1156    TAV= 1163    CPW= 5665.01
SEST=-1.58650E+06    SESS=-595933.    SEL=-990562.
PL= 136.132    PR= 137.435    PG= 387.351    PR+PG= 524.786

T= 1140    TAV= 1148    CPW= 4825.65
SEST=-1.66371E+06    SESS=-651048.    SEL=-1.01266E+06
PL= 133.328    PR= 130.586    PG= 379.506    PR+PG= 510.092

T= 1123    TAV= 1131.50    CPW= 4418.38
SEST=-1.73882E+06    SESS=-709608.    SEL=-1.02921E+06
PL= 130.268    PR= 123.992    PG= 371.678    PR+PG= 495.670

T= 1106    TAV= 1114.50    CPW= 4298.97
SEST=-1.81190E+06    SESS=-768168.    SEL=-1.04373E+06
PL= 127.139    PR= 117.811    PG= 364.070    PR+PG= 481.882

T= 1090    TAV= 1098    CPW= 4448.94
SEST=-1.88308E+06    SESS=-823283.    SEL=-1.05980E+06
PL= 124.127    PR= 112.176    PG= 356.889    PR+PG= 469.065

T= 1070    TAV= 1080    CPW= 3463.99
SEST=-1.95236E+06    SESS=-892177.    SEL=-1.06019E+06
PL= 120.869    PR= 106.742    PG= 349.720    PR+PG= 456.463

T= 1050    TAV= 1060    CPW= 3368.12
SEST=-2.01973E+06    SESS=-961071.    SEL=-1.05865E+06
PL= 117.283    PR= 101.505    PG= 342.565    PR+PG= 444.070

T= 1031    TAV= 1040.50    CPW= 3446.56
SEST=-2.08521E+06    SESS=-1.02652E+06    SEL=-1.05869E+06
PL= 113.822    PR= 96.4587    PG= 335.424    PR+PG= 431.883

T= 1010    TAV= 1020.50    CPW= 3031.69
SEST=-2.14888E+06    SESS=-1.09886E+06    SEL=-1.05002E+06
PL= 110.309    PR= 91.7355    PG= 328.500    PR+PG= 420.236

T= 992    TAV= 1001    CPW= 3435.72
SEST=-2.21072E+06    SESS=-1.16086E+06    SEL=-1.04986E+06
PL= 106.919    PR= 87.0529    PG= 321.386    PR+PG= 408.439

T= 973    TAV= 982.500    CPW= 3157.34
SEST=-2.27071E+06    SESS=-1.22631E+06    SEL=-1.04440E+06
PL= 103.736    PR= 82.2957    PG= 313.880    PR+PG= 396.176

T= 956    TAV= 964.500    CPW= 3419.78
SEST=-2.32885E+06    SESS=-1.28487E+06    SEL=-1.04397E+06
PL= 100.671    PR= 77.6109    PG= 306.187    PR+PG= 383.798
```

Figure 42. Run No. 10 (Sheet 2 of 3)

BEST AVAILABLE COPY

BEST_AVAILABLE COPY

```
T= 939    TAV= 947.500    CPW= 3315.92
SEST=2.38522E+06    SESS=-1.34343E+06    SEL=-1.04178E+06
PL= 97.8038    PR= 73.2396    PG= 298.713    PR+PG= 371.952

T= 921    TAV= 930    CPW= 3036.65
SEST=2.43988E+06    SESS=-1.40544E+06    SEL=-1.03444E+06
PL= 94.8818    PR= 69.1616    PG= 291.454    PR+PG= 360.616

T= 905    TAV= 913    CPW= 3311.50
SEST=2.49286E+06    SESS=-1.46055E+06    SEL=-1.03231E+06
PL= 92.0719    PR= 65.2515    PG= 284.210    PR+PG= 349.462

T= 891    TAV= 898    CPW= 3669.44
SEST=2.54423E+06    SESS=-1.50878E+06    SEL=-1.03545E+06
PL= 89.6163    PR= 61.5047    PG= 276.981    PR+PG= 338.485

        OUT OF DATA
>SYS

!EDIT T
EDIT HERE
*TY 1-3
   1.000 1329,1315,1308,1301,1301,1300,1299,1297,1293,1281,1265,1249
   2.000 1231,1215,1200,1185,1170,1156,1140,1123,1106,1090,1070,1050
   3.000 1031,1010,992,973,956,939,921,905,891
*EDIT G
*TY 1-3
   1.000 1260,1240,1233,1228,1221,1216,1210,1206,1200,1190,1181,1169
   2.000 1150,1130,1110,1090,1070,1050,1032,1012,995,977,960,942
   3.000 925,908,890,871,852,834,816,798,780
*
```

Figure 42. Run No. 10 (Sheet 3 of 3)

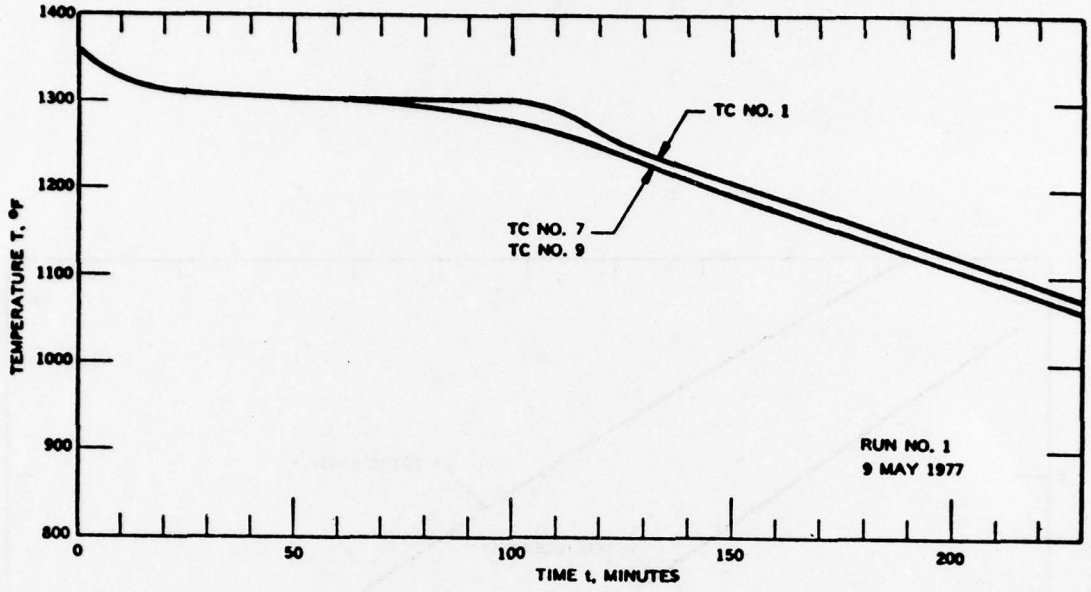

Figure 43. Measured Temperatures During Discharge of Hi-Cap TES Unit

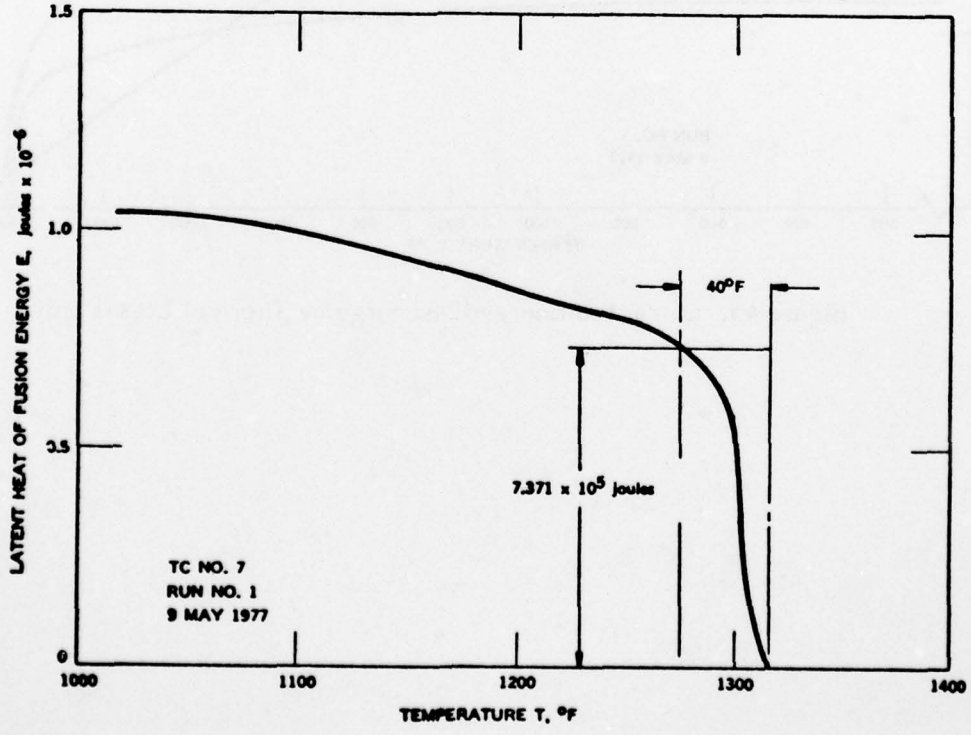

Figure 44. Latent Heat of Fusion Release During Discharge of Hi-Cap Thermal Energy Storage Unit (Thermal Losses only)

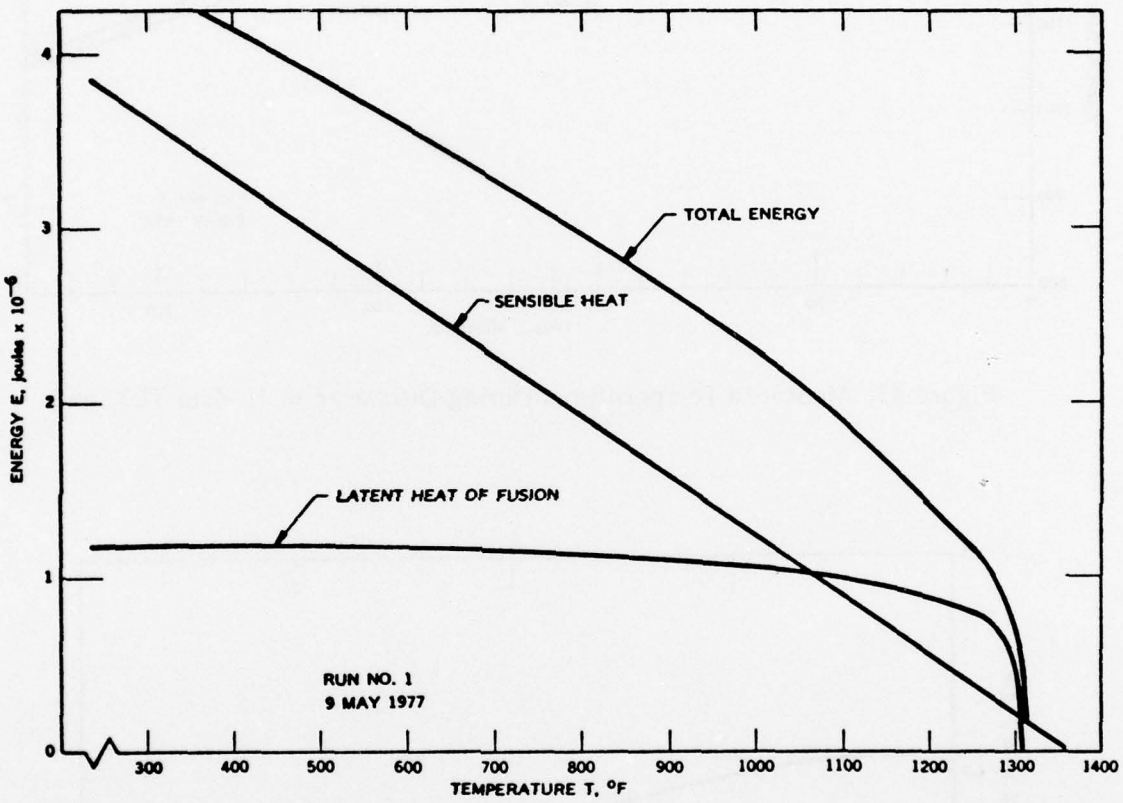

Figure 45. Extracted Energy (Discharge by Thermal Losses only)

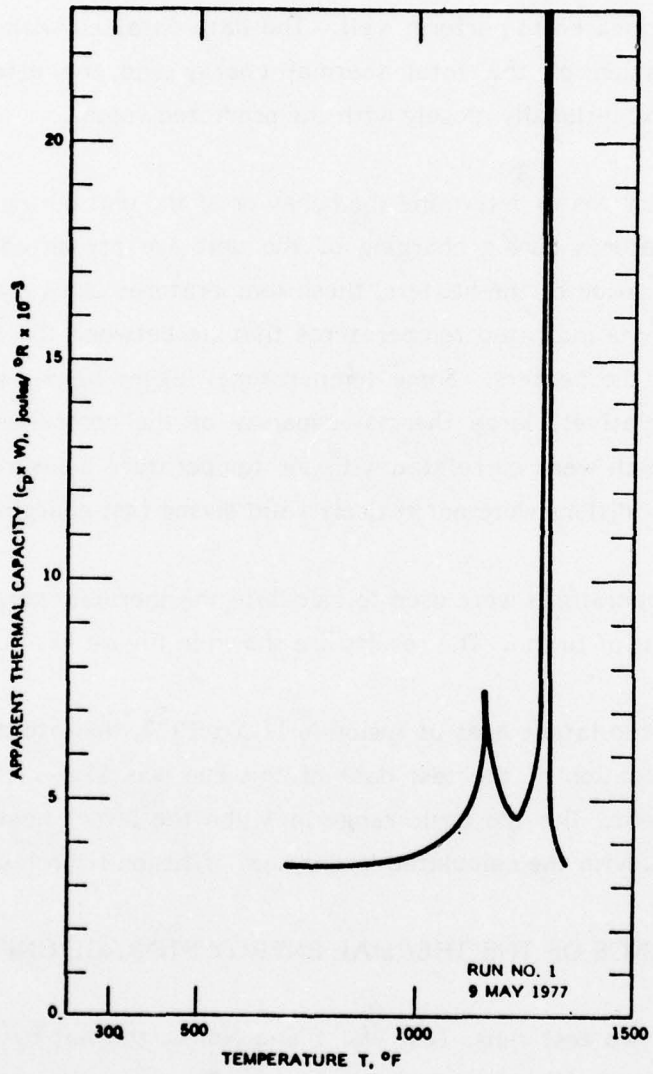

Figure 46. Apparent Thermal Capacity of Hi-Cap TES Unit

60323

The results from the first test run verified the design of the TES unit with respect to the thermal storage capacity of the TES material. The desired amount of thermal energy was released over the predicted temperature range of 40°F. The instrumentation appeared to perform well. The data obtained with it and entered into the computation of the total thermal energy and the effective thermal capacity agreed exceptionally closely with the predicted values.

The second test run was to determine the behavior of the unit during charging. The measured temperatures during charging of the unit are presented in Figure 47. Because of the location of the heaters, these temperatures can vary widely. Some of the measurements indicated temperatures that lie between the temperature of the TES unit and the heaters. Some temperatures lagged behind during charging because of the relatively large thermal capacity of the components. Thus, the thermal losses which were correlated with the temperature measured by TC No. 7 at steady-state conditions were not entirely valid during fast charging of the unit.

The transient temperatures were used to calculate the thermal energy stored in the form of latent heat of fusion. The results are shown in Figure 48.

While the calculated latent heat of fusion is 11.5×10^5J, the latent heat of fusion based on the evaluation of the test data of this run was 12.5×10^5J which is in error by 8.7 percent. But the basic range in which the latent heat of fusion was stored agreed well with the calculated latent heat of fusion from test run No. 1.

4.3.3 PERFOMANCE OF THE THERMAL ENERGY STORAGE UNIT

During the first two test runs, Test No. 1 and No. 2, the hot cylinder was fully insulated with Flexible Min-K insulation material. The losses from the hot cylinder were therefore minimal and insignificant compared to the overall losses. Following the first two tests were a series of tests designed to establish the performance of the TES unit during simulated operation of the Vuilleumier cooler by extracting power from the hot cylinder. A gas flow insert was built which permitted the

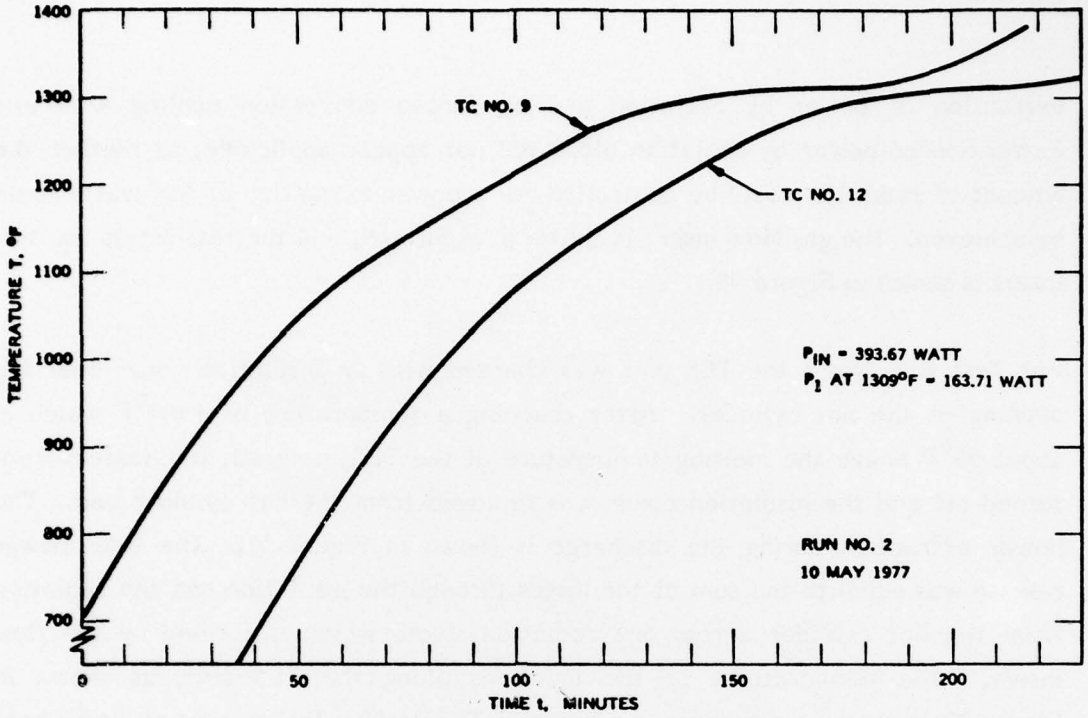

Figure 47. Temperature of Thermal Energy Storage Unit During Charging

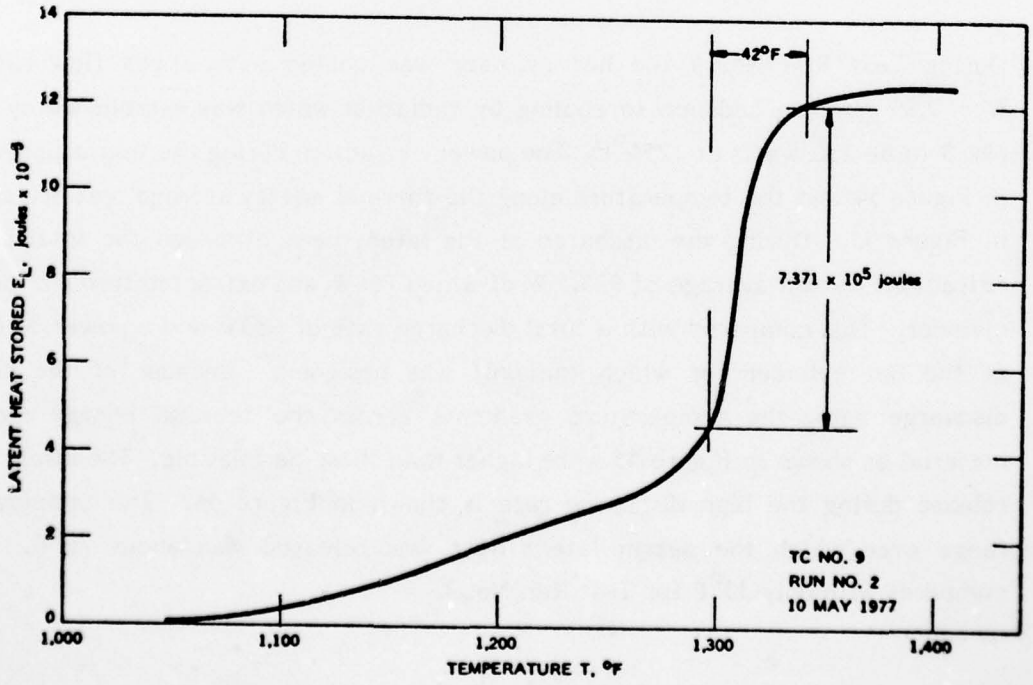

Figure 48. Latent Heat Storage in Thermal Energy Storage Material During Charging (Heater Power $P_{in.}$ = 393.67 watt)

AD-A054 466 XEROX CORP/ELECTRO-OPTICAL SYSTEMS PASADENA CALIF F/G 13/1
THERMAL ENERGY STORAGE DEMONSTRATION UNIT FOR VUILLEUMIER CRYOG--ETC(U)
OCT 77 R RICHTER F33615-75-C-2045
UNCLASSIFIED 2340-F AFAPL-TR-77-65 NL

2 OF 2
AD
A054466

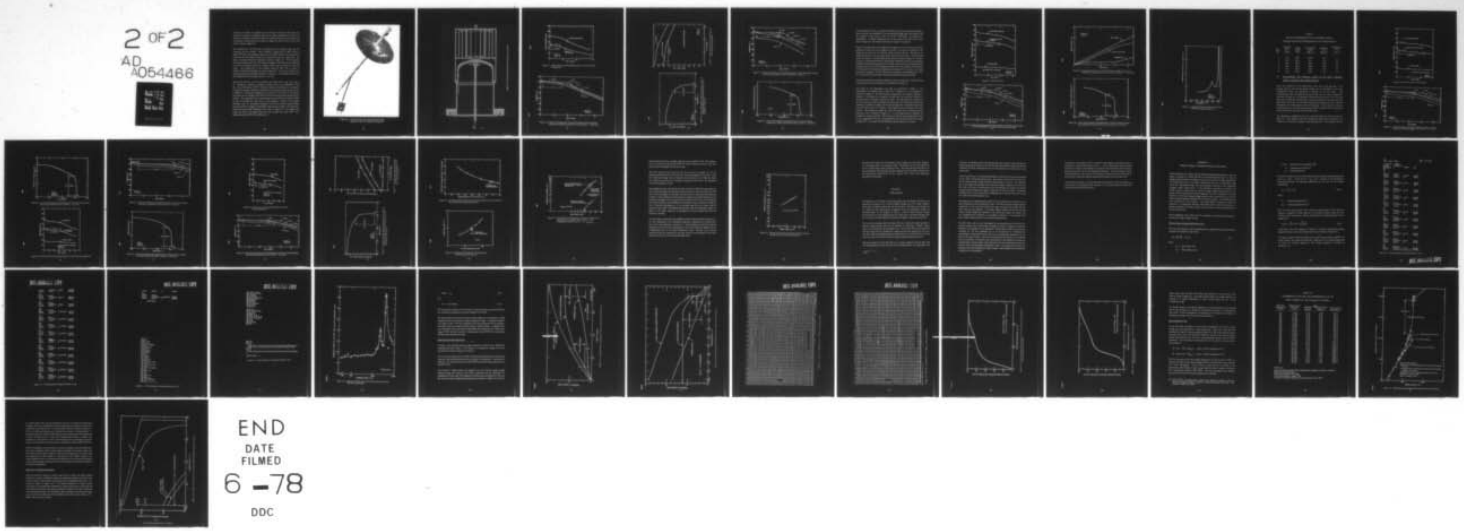

END
DATE
FILMED
6 -78
DDC

extraction of power by radiation and by forced convection cooling with air. Extraction of power by radiation alone did not appear applicable, as neither the amount of radiation could be controlled nor a power extraction of 650 watts could be achieved. The gas flow insert is shown in Figure 49, and the test set up for this insert is shown in Figure 50.

For Test Run No. 3 the TES unit was charged with an insulation cover over the opening of the hot cylinder. After reaching a temperature of 1360°F which is about 50°F above the melting temperature of the TES material, the heaters were turned off and the insulation cover was removed from the hot cylinder end. The power extraction during the discharge is shown in Figure 51. The total power release was equal to the sum of the losses through the insulation and the radiation from the hot cylinder across one radiation shield which is formed by the flow insert. The temperatures at the locations along the TES unit, as shown in Figure 33, during the discharge are shown in Figure 52. The amount of latent heat released during the discharge is plotted in Figure 53. The measured total latent heat agreed well with the theoretical of 11.5×10^5 J.

During Test Run No. 4 the hot cylinder was cooled with a gas flow rate of $\dot{W}$ = 0.89 g/sec in addition to cooling by radiation which was established by Test No. 3 to be 230 watts at 1255°F. The power extraction during the test is presented in Figure 54 and the temperature along the thermal energy storage unit are shown in Figure 55. During the discharge of the latent heat of fusion the total power extraction was an average of 923.5 W of which 764W was extracted through the hot cylinder. This compared with a total discharge rate of 685W and a power of 650W at the hot cylinder for which the unit was designed. Because of the higher discharge rate, the temperature gradients across the thermal energy storage material as shown in Figure 55 were higher than those permissible. The latent heat release during the high discharge rate is shown in Figure 56. The temperature range over which the design latent heat was released was about 70°F. This compares with only 33°F for Test Run No. 3.

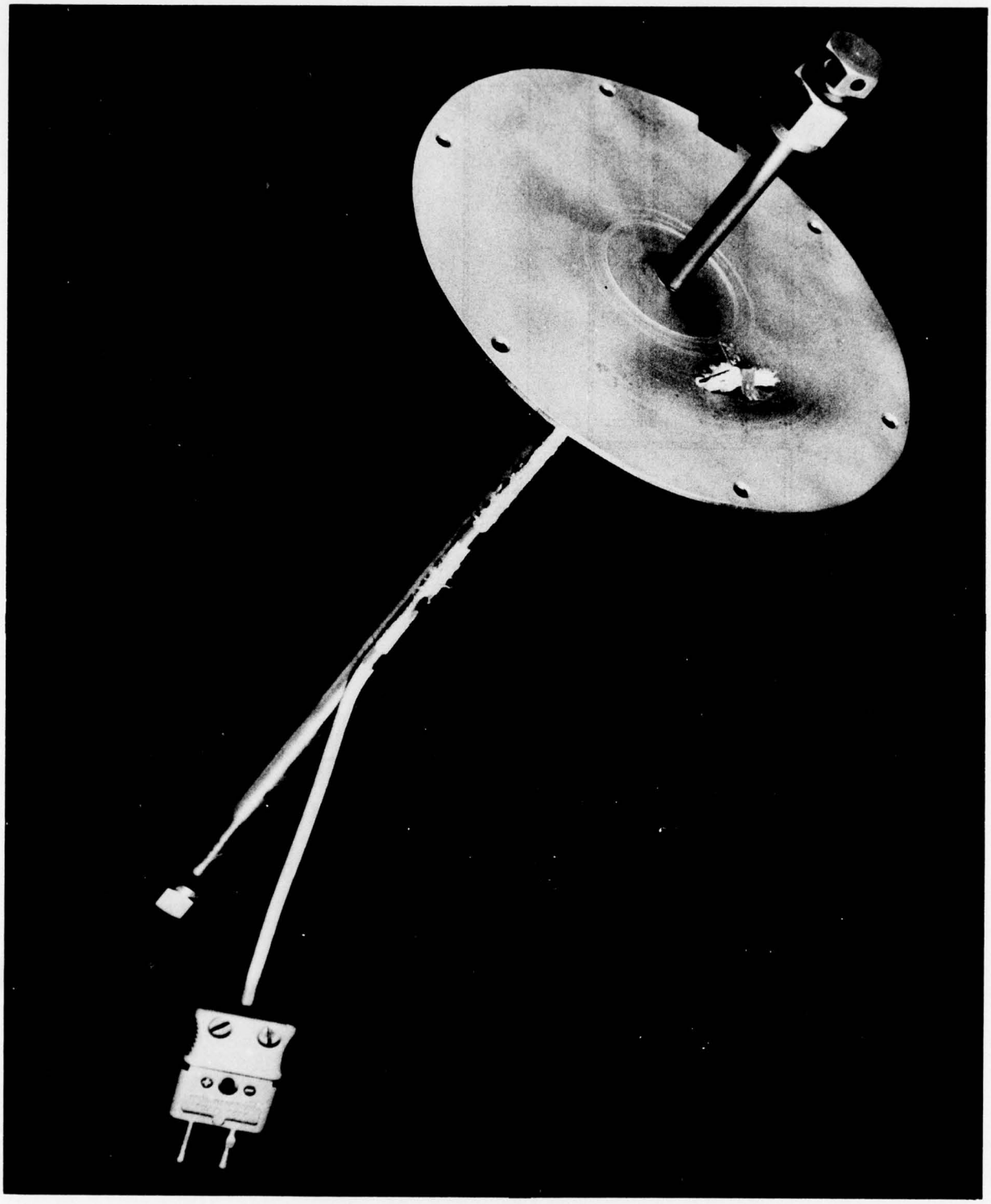

Figure 49. Gas Flow Insert for Simulating V/M Cooler Operation with Air Cooling and Radiation

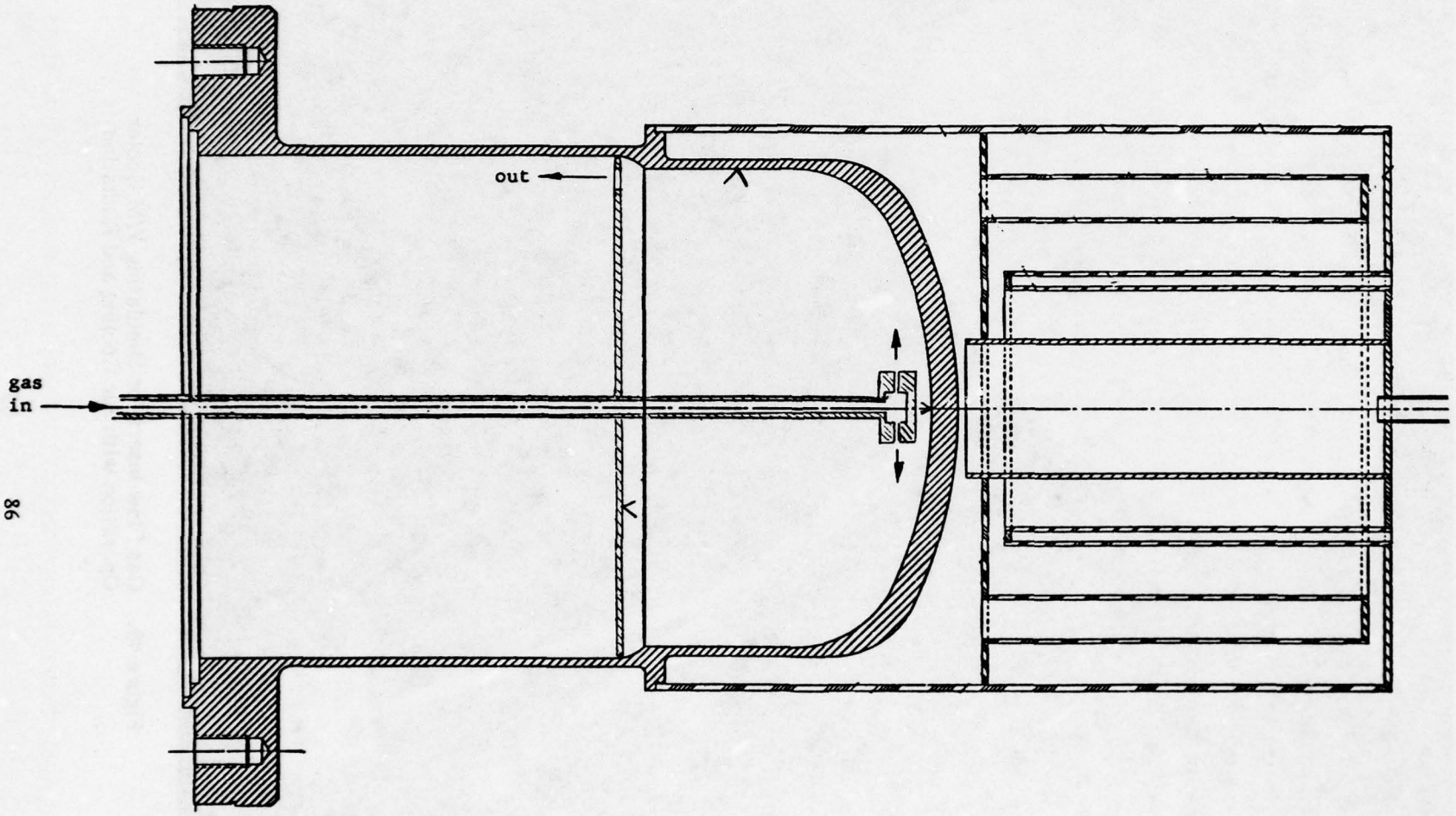

Figure 50. Position of Flow Insert in Hot Cylinder for Testing

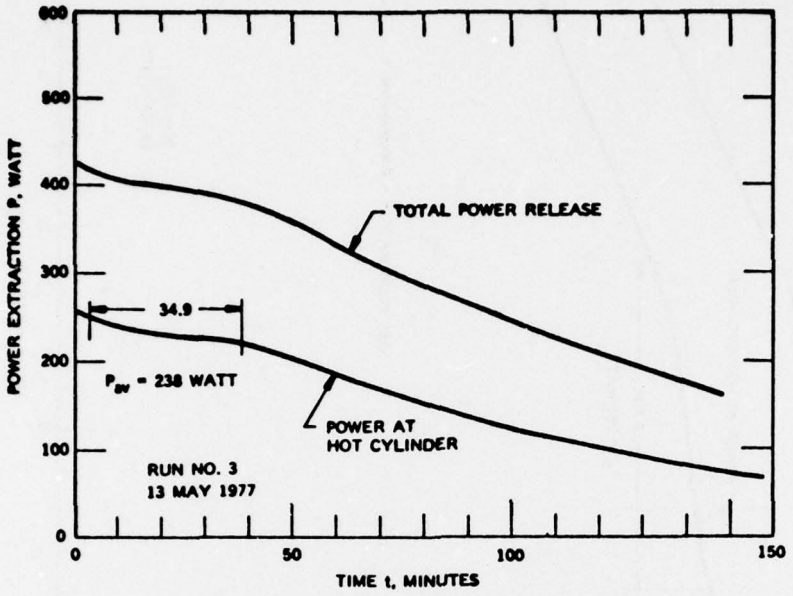

60300

Figure 51. Power Extraction During Discharge of Thermal Energy Storage Unit

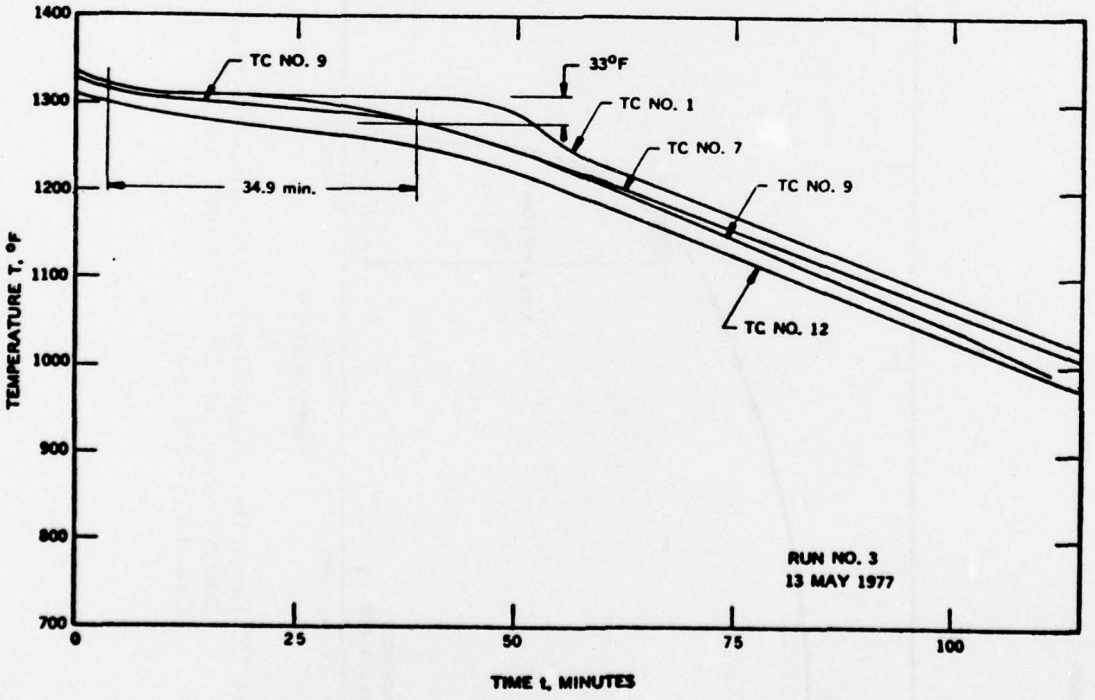

60349

Figure 52. Measured Temperatures During Discharge of Thermal Energy Storage Unit (Power Extraction at Hot Cylinder P = 238 watt)

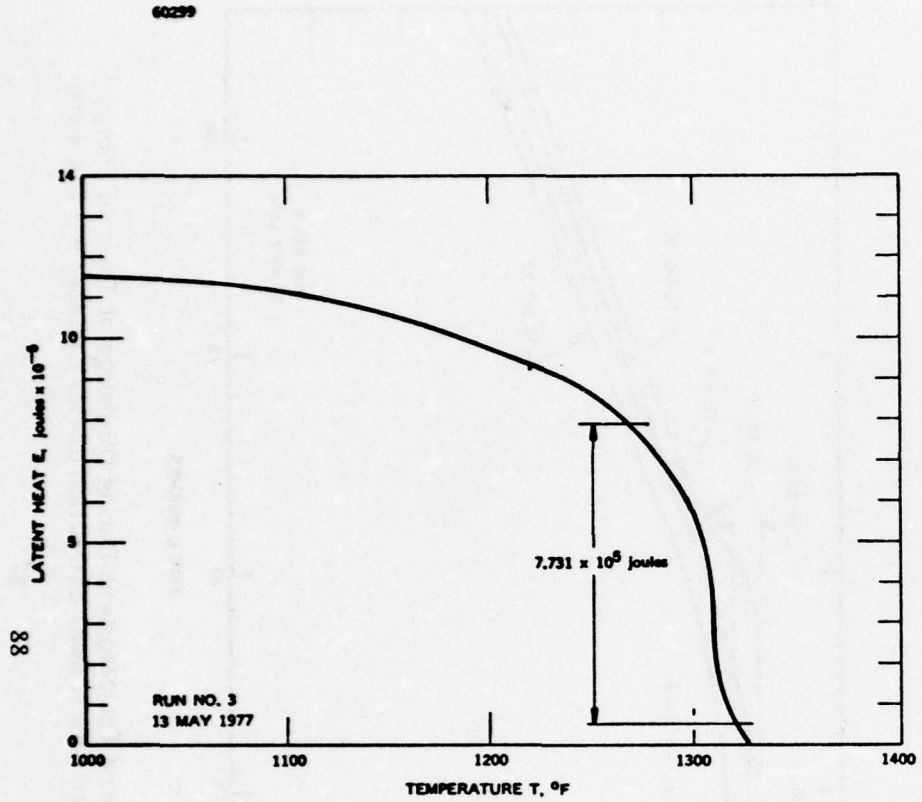

Figure 53. Latent Heat Release During Discharge of Thermal Energy Storage Unit (Power Extraction at Hot Cylinder P = 238 watt)

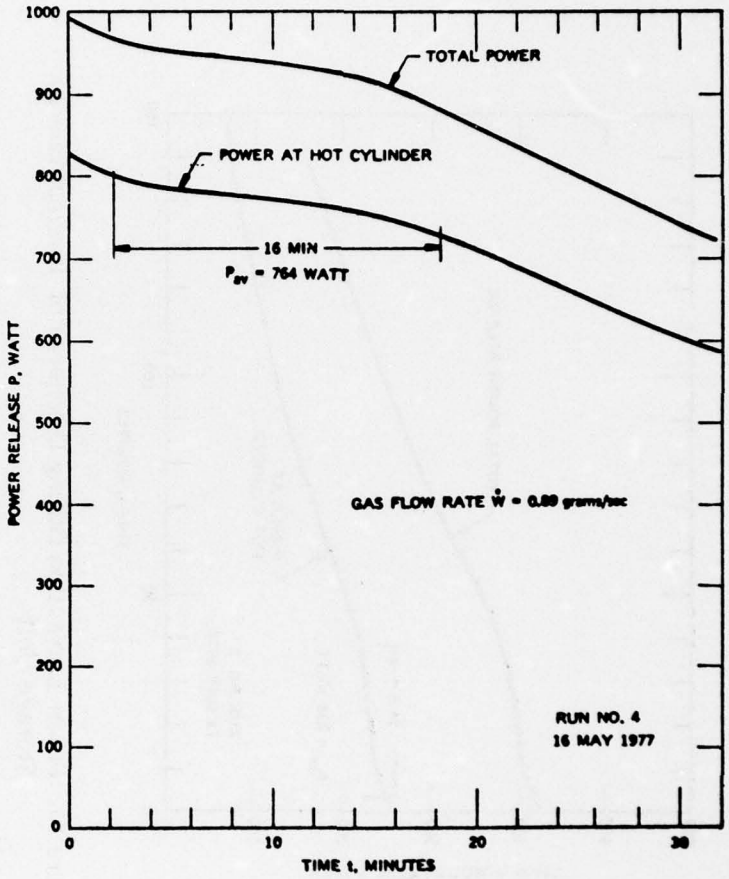

Figure 54. Power Extraction During Discharge of Thermal Energy Storage Unit

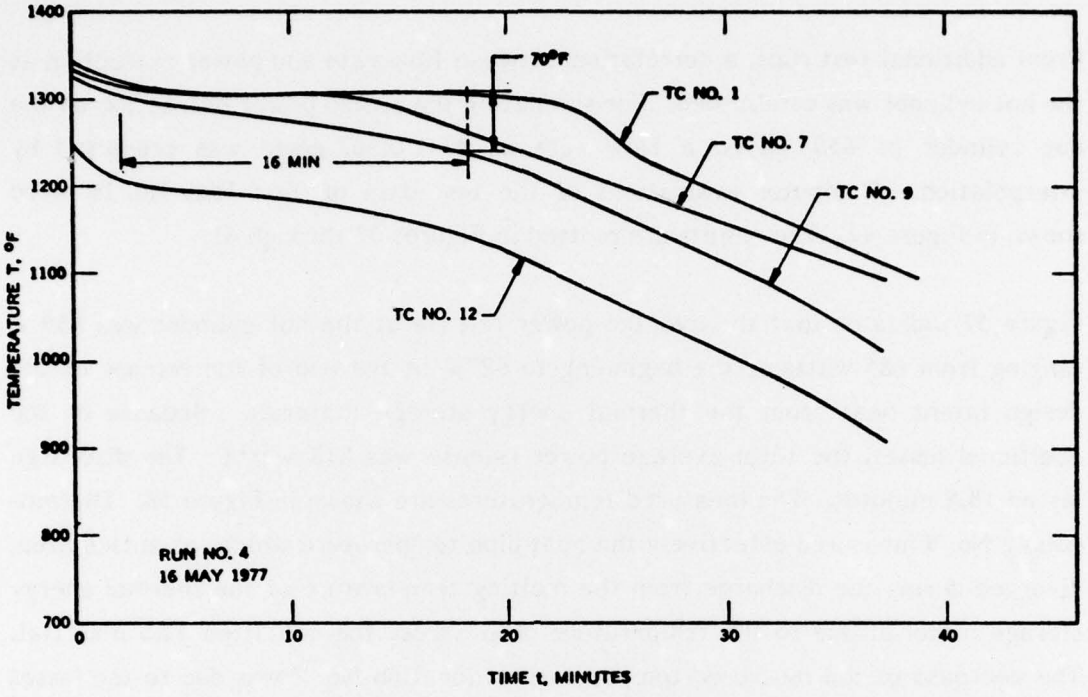

Figure 55. Measured Temperatures During Discharge of Thermal Energy Storage Unit (Power Extraction at Hot Cylinder P = 764 watt)

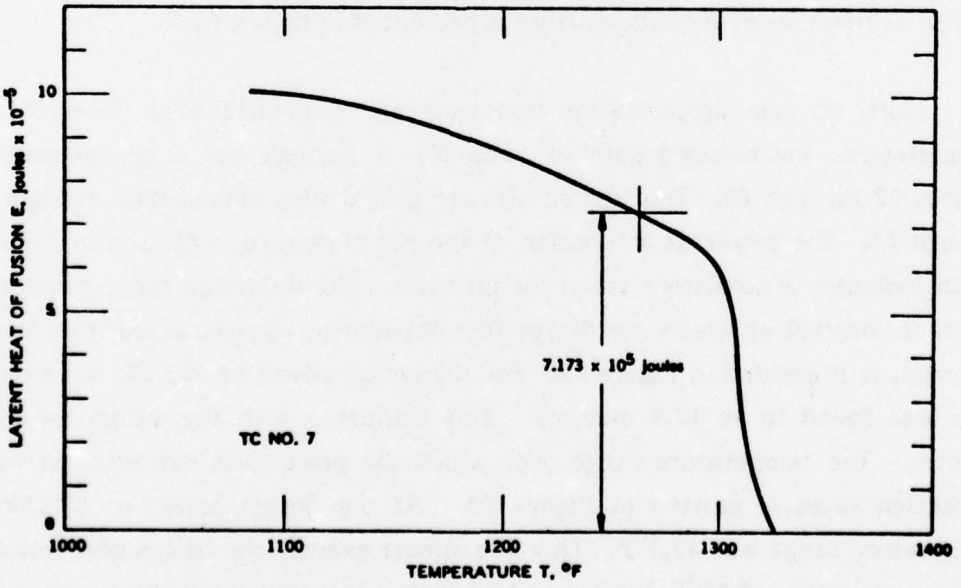

Figure 56. Latent Heat Release During Discharge of Thermal Energy Storage Unit (Power Extracted at Hot Cylinder P = 764 watt)

From additional test runs, a correlation between flow rate and power extraction at the hot cylinder was established. For simulating the design power extraction at the hot cylinder of 650 watts, a flow rate of $\dot{W}$ = 0.667 g/sec was predicted by interpolation. Computer evaluations of the test data of Test Run No. 10 were shown in Figure 42. The results are plotted in Figures 57 through 61.

Figure 57 indicates that the average power release at the hot cylinder was 659 W ranging from 685 watts at the beginning to 627W at the end of the release of the design latent heat from the thermal energy storage material. Because of the additional losses, the total average power release was 818 watts. The discharge lasted 18.8 minutes. The measured temperatures are shown in Figure 58. Thermocouple No. 9 measured effectively the heat pipe temperature which, as anticipated, diverged during the discharge from the melting temperature of the thermal energy storage material due to the temperature drop across the solidified TES material. The decrease of the measured temperature at location No. 7 was due to the losses through the insulation. If these losses were eliminated, thermocouples No. 7 and No. 1 should have indicated about the same temperatures during discharge.

The energy distribution during the dicharge is shown in Figure 58. The latent heat release as function of the temperature is presented in Figure 60.

The results of the performance test runs are summarized in Table 7. For completeness, the reduced data of tests No. 5 through No. 8 are presented in Figures 62 through 70. The test results are graphically summarized in Figures 71 through 73. The power as a function of the gas flow rate is plotted in Figure 71 which indicates a consistent trend for all tests. The discharge time, computed as the time interval at which the design thermal energy was extracted from the TES material, is presented in Figure 72. For the design power of 682.5W the discharge time was found to be 17.9 minutes. This compares with the design time of 18 minutes. The temperature range over which the power was extracted at various extraction rates is plotted in Figure 73. At the design power of 682.5W, the temperature range was 49.3°F. This was almost exactly the design goal which was set at a maximum of 50°F, but it was higher than the calculated temperature range of about 42°F. The reason for this difference cannot be given at this time.

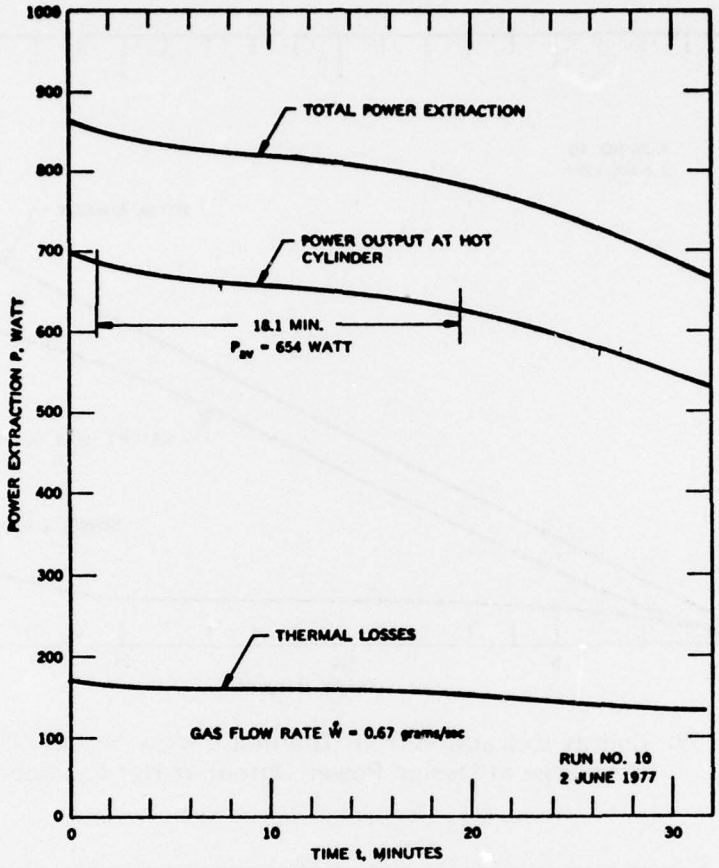

Figure 57. Power Extraction

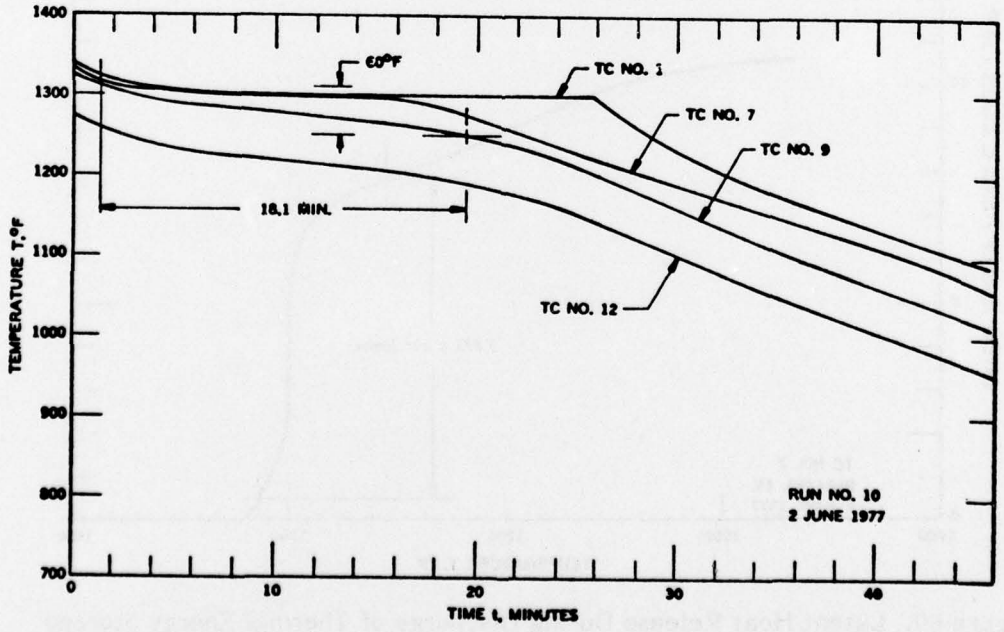

Figure 58. Measured Temperatures During Discharge of Thermal Energy Storage Unit at Design Power Extraction at Hot Cylinder (654 watt)

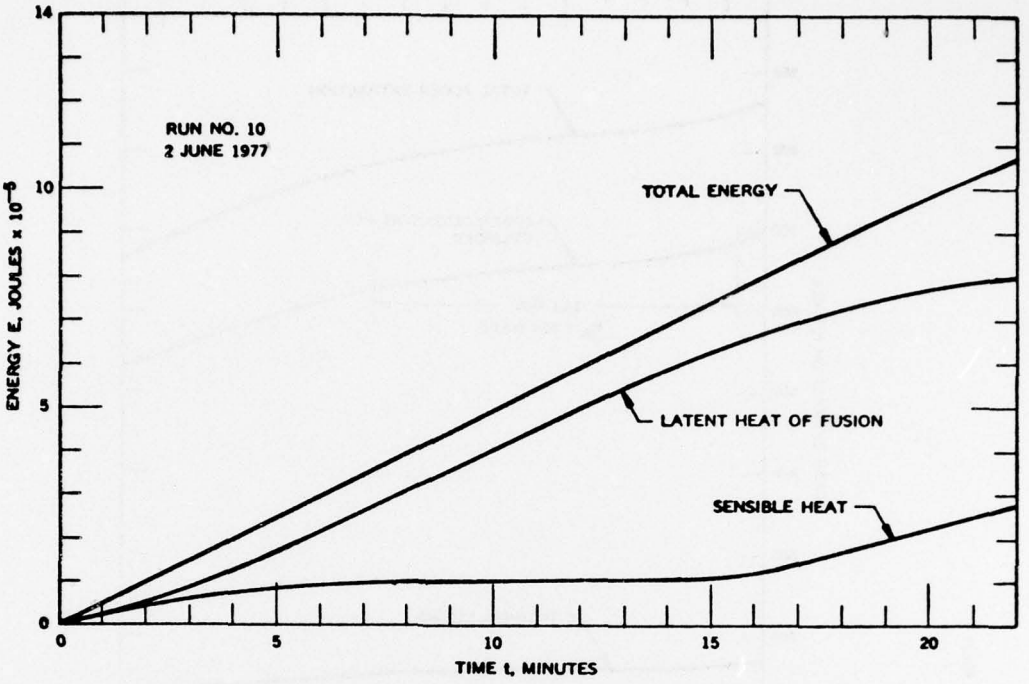

60294

Figure 59. Energy Extraction from Thermal Energy Storage Unit During Discharge at Design Power Output at Hot Cylinder (P = 654 watt)

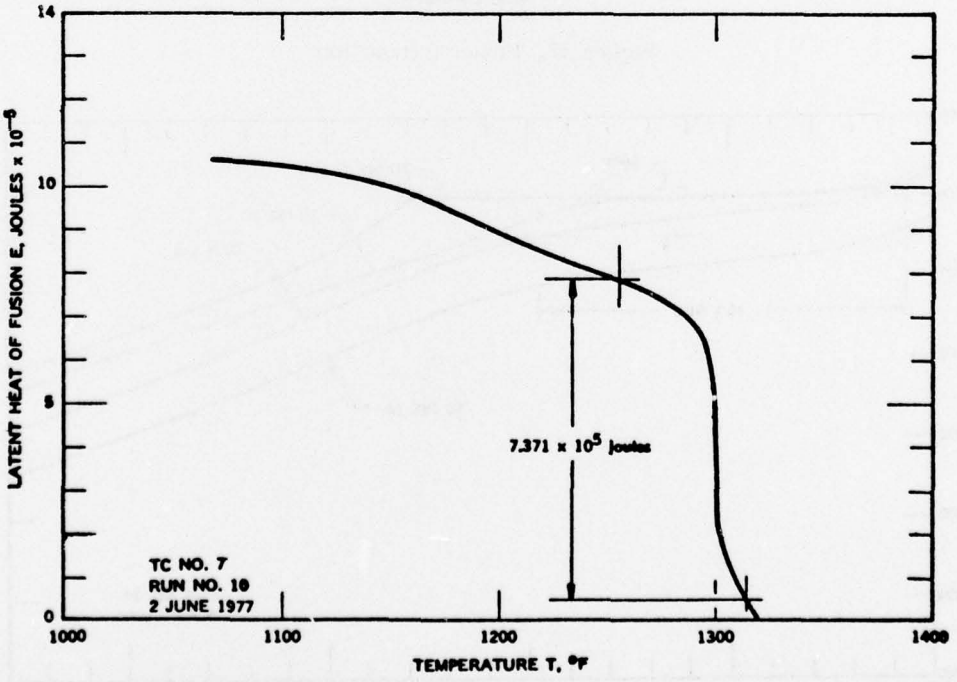

60292

Figure 60. Latent Heat Release During Discharge of Thermal Energy Storage Unit Design Power Extraction at Hot Cylinder (P = 654 watt)

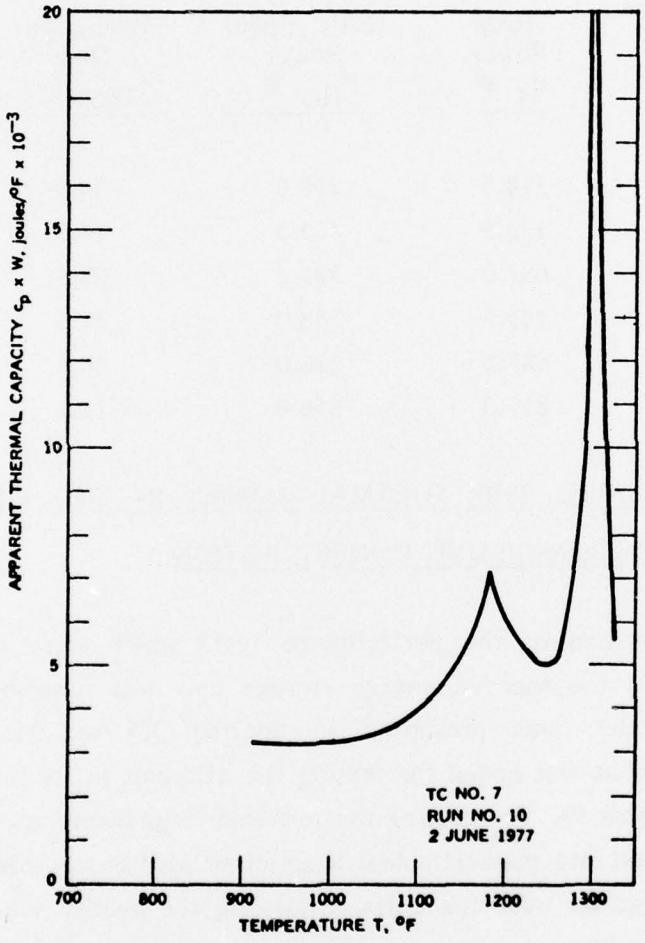

Figure 61. Apparent Thermal Capacity of Hi-Cap Thermal Energy Storage Unit

TABLE 7

TEST DATA OBTAINED WITH HI-CAP THERMAL ENERGY STORAGE UNIT IN THE PERFORMANCE TEST CONFIGURATION

Run No.	Gas Flow Rate $\dot{W}$, g/s	Total Power P_T, W	Hot Cylinder Power P_{HC}, W	Discharge Time t_{TES}, min	Temperature Drop T_9, ^oF
3	0.00	398.5	238.0	34.9	33
4	0.89	923.5	763.5	16.0	70
5	0.45	687.0	525.0	20.8	45
6	0.23	545.5	383.0	27.6	40
8	0.14	487.5	326.0	30.4	40
10	0.67	817.0	654.0	18.1	60

4.4 ESTABLISHING THE THERMAL LOSSES IN THE FINAL THERMAL ENERGY STORAGE UNIT CONFIGURATION

After the completion of the performance tests which were described in the previous sections, the thermal energy storage unit was assembled in the final configuration which was presented in Section 3.5 of this report. The instrumentation that was added for testing the TES unit in its final configuration was shown in Figure 39. For cooling the terminal ring, twenty-two 1-1/2 inch long bolts were screwed into the bolt holes. A small air blower was installed on the test table which forced air over the bolts extracting the energy that was conducted through the hot cylinder barrel to the terminal ring. It was essential to maintain the temperature of the terminal ring below 200^oF to protect the "O" ring which seals the insulation container and the terminal ring.

The temperature differences that were measured during the tests are shown in Figure 74. The average of the four temperatures which were measured on the outside of the insulation container never exceeded 91^oF. This indicated that the

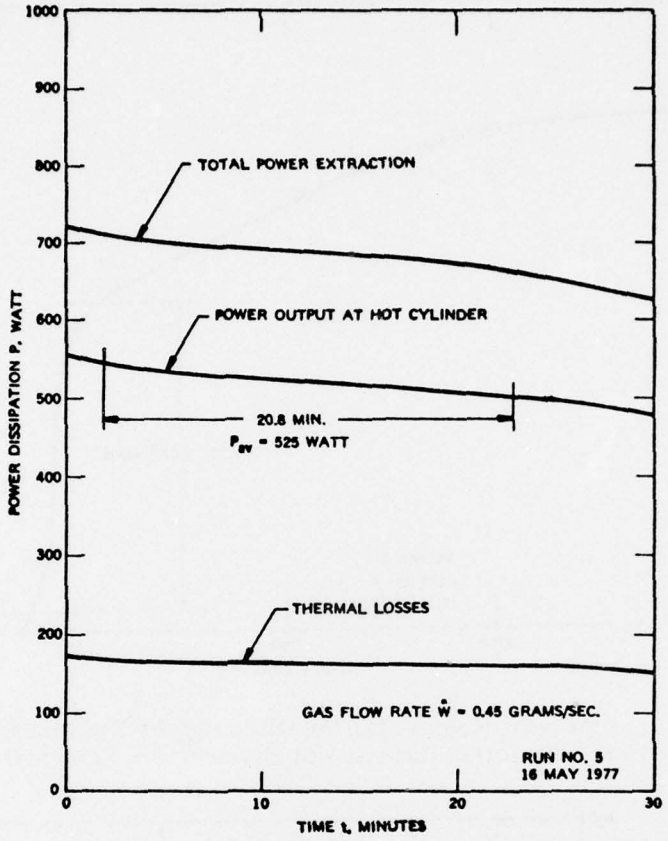

Figure 62. Power Extraction During Discharge

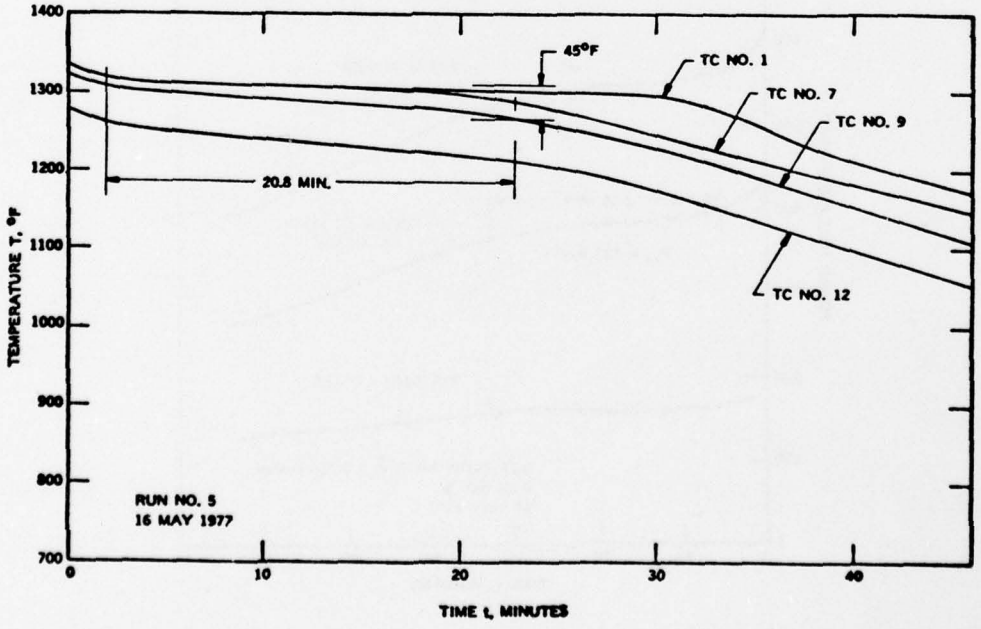

Figure 63. Measured Temperatures During Discharge of Thermal Energy Storage Unit (Extraction Rate at Hot Cylinder P = 525 watt)

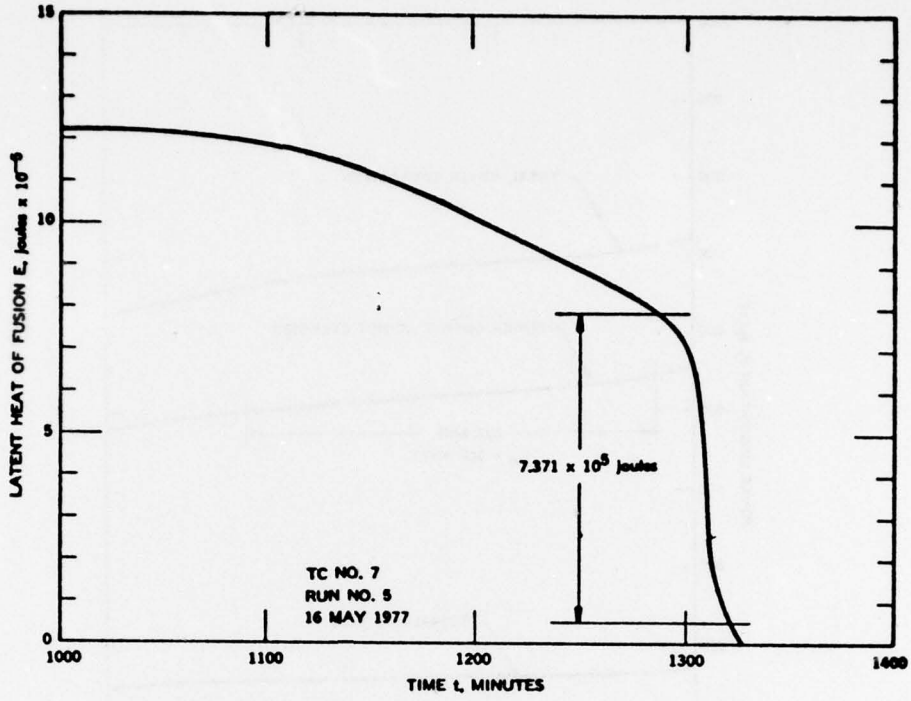

Figure 64. Latent Heat Release During Discharge of Thermal Energy Storage Unit (Extraction Rate at Hot Cylinder P = 525 watt)

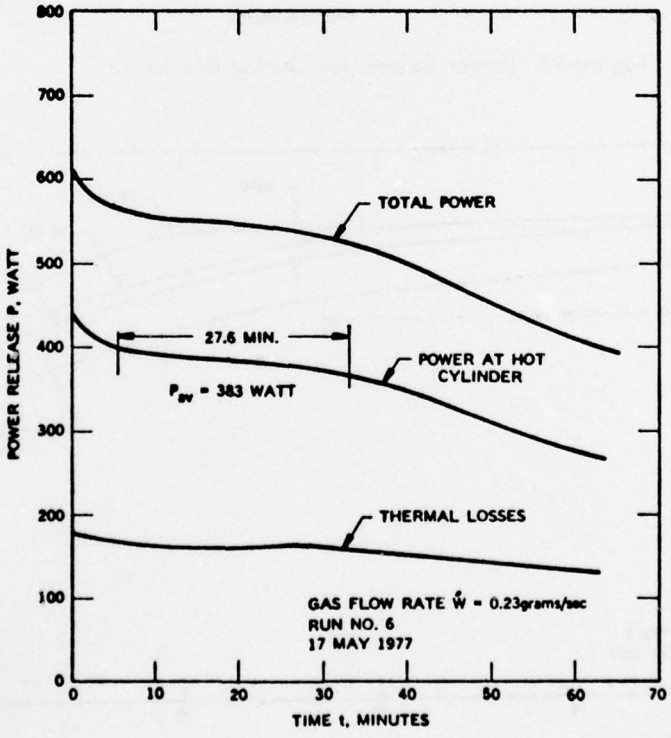

Figure 65. Power Extraction During Discharge of Thermal Energy Storage Unit

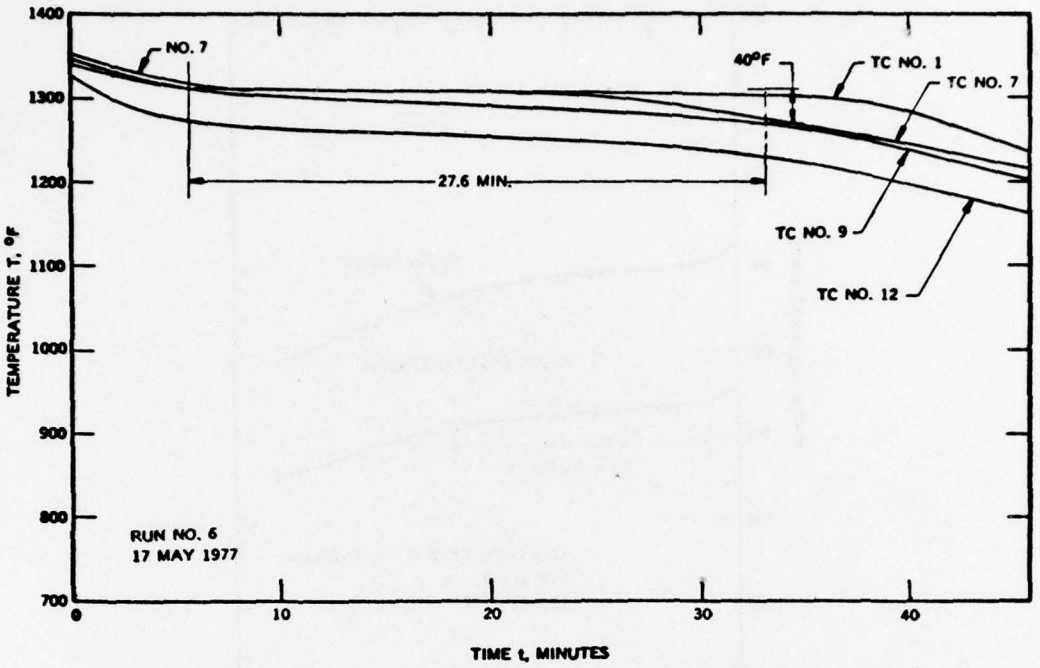

60346

Figure 66. Measured Temperatures During Discharge of the Thermal Energy Unit (Power Extraction at Hot Cylinder P = 383 watt)

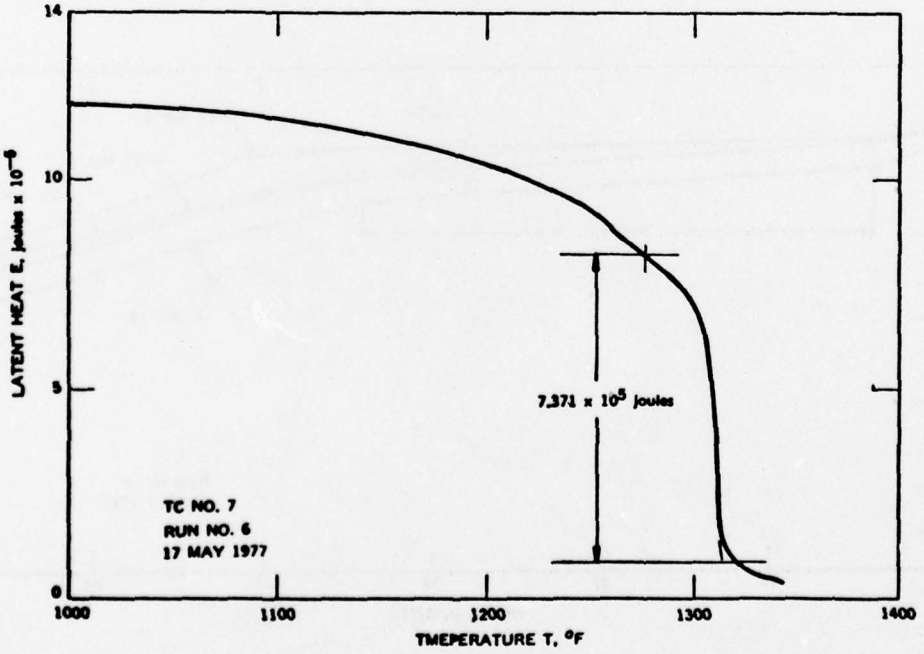

60287

Figure 67. Latent Heat Release During Discharge of Thermal Energy Storage Unit (Power Extraction at Hot Cylinder P = 383 watt)

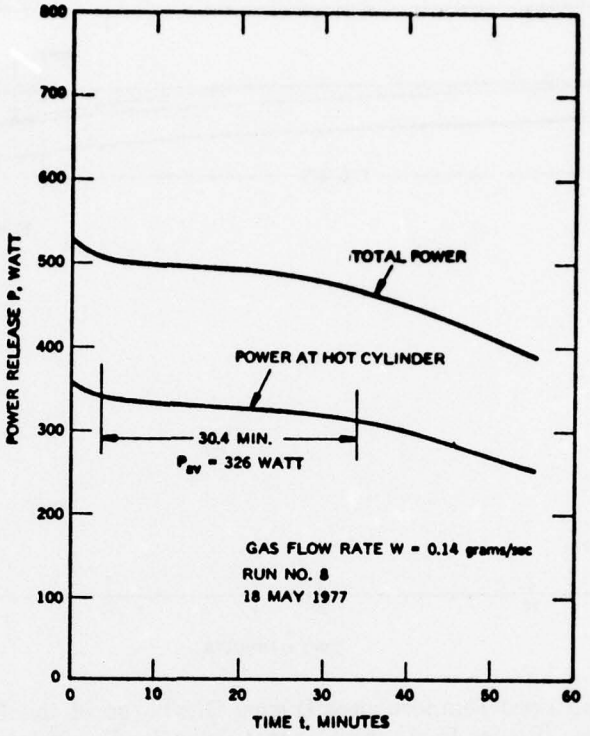

60284

Figure 68. Power Extraction During Discharge of Thermal Energy Storage Unit

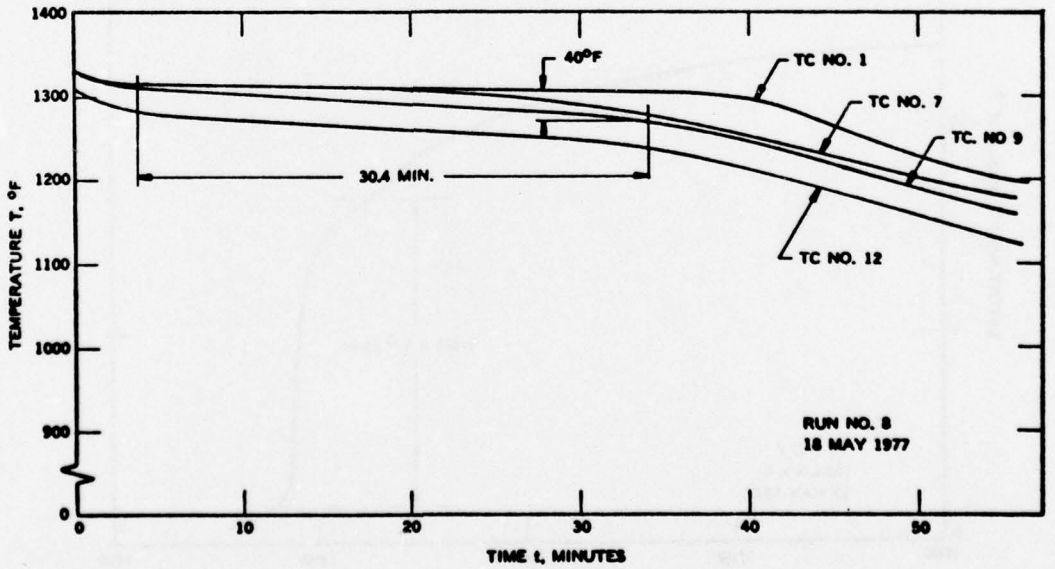

60350

Figure 69. Measured Temperatures During Discharge of Thermal Energy Storage Unit (Power Extracted at Hot Cylinder P = 326 watt)

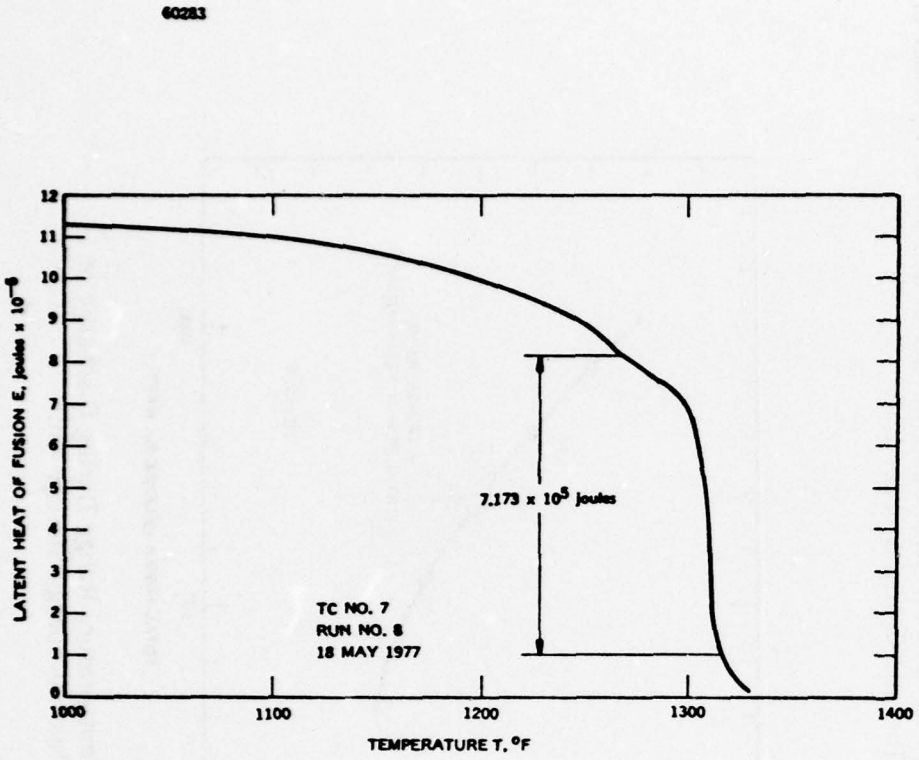

Figure 70. Latent Heat Release During Discharge of Thermal Energy Storage Unit (Power Extracted at Hot Cylinder P = 326 watt)

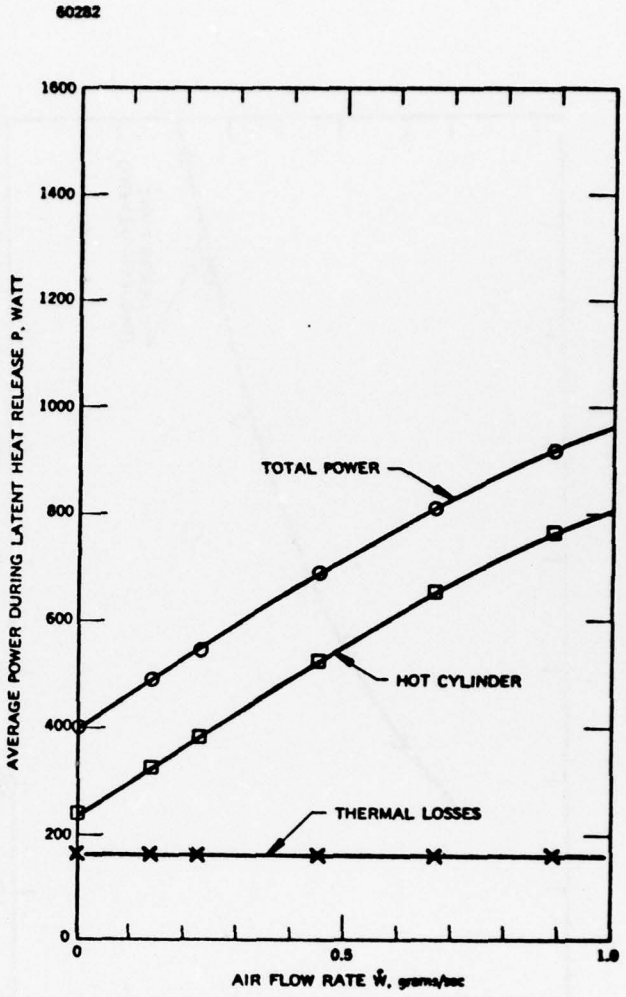

Figure 71. Average Power During Discharge of Thermal Energy Storage Unit (E = 7.173 x 10^5 joules)

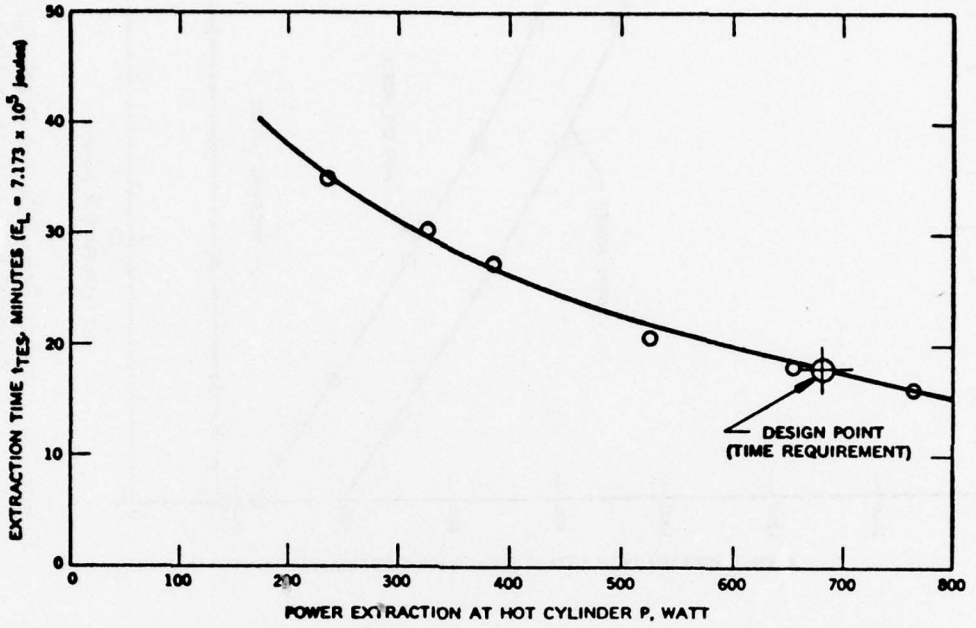

60281

Figure 72. Discharge Time as Function of Power Extraction at Hot Cylinder of Hi-Cap Thermal Energy Storage Unit

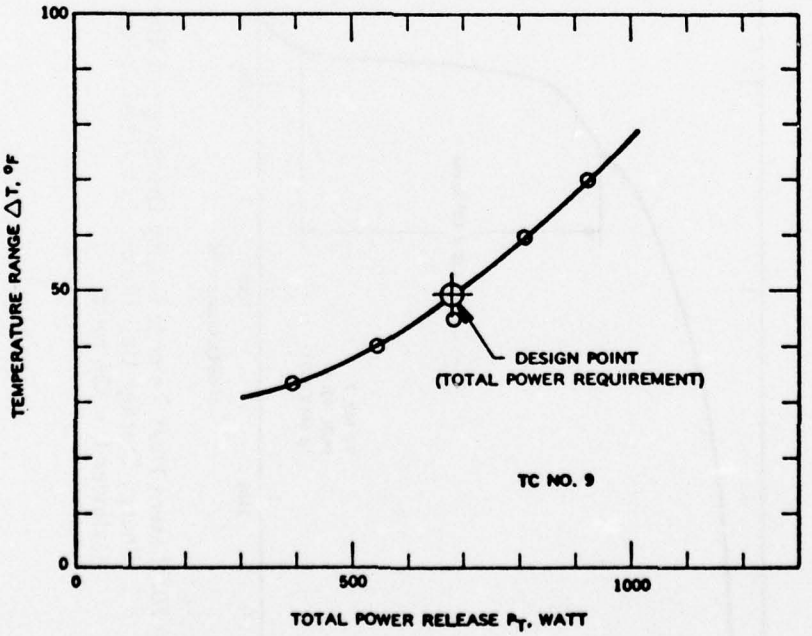

60280

Figure 73. Temperature Range During Discharge of Thermal Energy Storage Unit

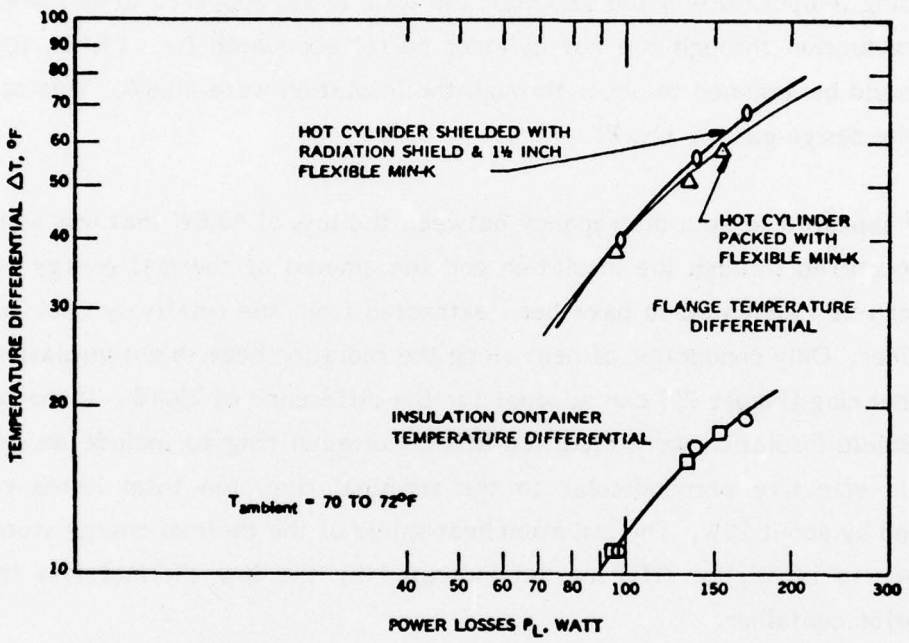

60334

Figure 74. Terminal Ring and Insulation Container Temperature Differential at Steady State Power Losses (Temperature Differential $\Delta T = T - T_{ambient}$)

thermal losses from that container could not have exceeded 11.2W. The temperature in the terminal ring reached 140°F with heavy cooling by forced air flow over 22 bolts and the exposed surfaces of the ring.

The total thermal losses from the TES unit are shown in Figure 75. At the operating temperature of the TES unit, the total losses appeared to be 154W. Since the conduction through the hot cylinder barrel accounted for 113.4W, the losses that could be assumed to occur through the insulation were 40.6W. This compared with the design goal of 32.5W.

There appeared to be a discrepancy between the loss of 40.6W that was assumed to have occurred through the insulation and the amount of thermal energy of 11.2W that can be calculated to have been extracted from the relatively cool insulation container. Only conduction of heat along the radiation heat shield insulation to the terminal ring (Figure 24) can account for the difference of 29.4W. If the radiation heat shield insulation were modified at the terminal ring to include an insulation that is effective perpendicular to the terminal ring, the total losses could be reduced by about 20W. The radiation heat shield of the thermal energy storage unit appears to be highly effective as indicated by the low thermal loss from the insulation container.

The performance tests that were repeated with the thermal energy storage unit in its final configuration were essentially repetitious, duplicating the performance tests which were presented in Section 4.3. Those temperature data that could be obtained with the limited instrumentation in the final configuration agreed with the corresponding data of the initial performance tests. Because of the limited instrumentation, the reduction of the data could not be performed in the same detail as was done for the initial performance tests.

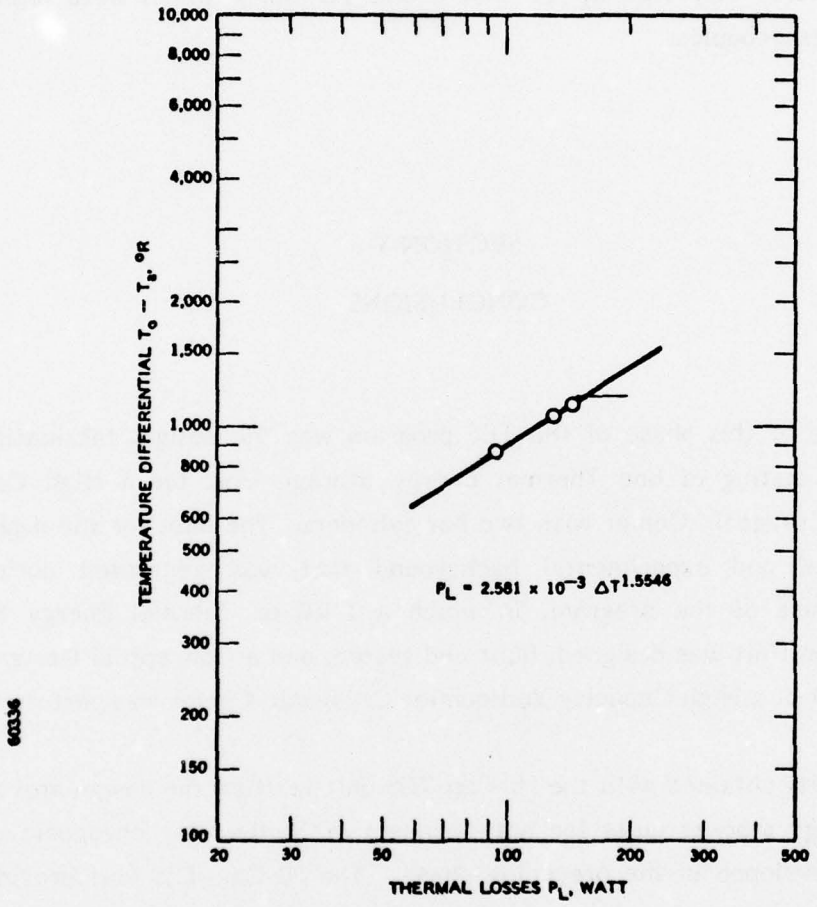

Figure 75. Thermal Losses from the Hi-Cap Thermal Energy Storage Unit in Its Final Configuration

During the first heat up of the thermal energy storage unit in its final configuration, the single RTD in the assembly failed. Fortunately, the RTD was backed up by two thermocouples which performed well. The temperatures indicated by the 1/8-inch diameter thermocouples, however, appeared to be low when compared with the temperatures indicated by TC No. 6 and TC No. 7 which were unsheathed grounded thermocouples.

SECTION V

CONCLUSIONS

The objective of this phase of the TES program was the design, fabrication, and performance testing of one Thermal Energy Storage Unit for a High Capacity Vuilleumier Cryogenic Cooler with two hot cylinders. The base for the design was the analytical and experimental background that was generated during the preceding phase of the program, in which a 1 kW-hr Thermal Energy Storage Demonstration Unit was designed, built and tested, and a Conceptual Design Study for a TES unit of a High Capacity Vuilleumier Cryogenic Cooler was performed.[1]

The test results obtained with the Hi-Cap TES unit verified the design approach to thermal energy storage units for hot cylinders of Vuilleumier cryogenic coolers which was developed in the preceding phase. The Hi-Cap TES unit provided the thermal energy over the temperature range that had been specified for the unit. The TES material exhibited the same characteristics in the Hi-Cap TES unit that were measured in the 1 kW-hr Thermal Energy Storage Demonstration Unit.

During the design of the Hi-Cap TES unit, it became apparent that the basic TES unit configuration that had evolved in the preceding phase is not applicable to all

---

1 Ibid

TES units. Fortunately, check calculations, that were made for the verification of the operating characteristics of the Hi-Cap TES unit, brought to light the need for modifying the basic configuration prior to the initiation of the fabrication of the current unit.

The Hi-Cap TES unit is a three-annulus design in contrast to the two-annulus design of the 1 kW-hr TES Demonstration Unit. The number of annuli refers to the number of thermal energy storage material compartments in the unit. The modification in the design was necessary to increase the energy transfer area in the unit. The size of the area is determined by the ratio between the amount of thermal energy material stored and the power requirement of the hot cylinder. The energy to power ratio of the Hi-Cap TES unit happened to be only one third the ratio of the 1 kW-hr TES Demonstration Unit.

The application of superinsulation proved to be very beneficial with respect to the power requirement of the Vuilleumier cooler. The thermal energy storage capacity requirement of the final Hi-Cap TES unit might actually be lower than that for which this unit was designed. The present design included the effects of high thermal losses through the insulation in the electrically heated hot cylinder unit (i.e., shredded Min-K insulation at atmospheric pressure). It is estimated that about 100W is being saved with the improved superinsulation.

The effort that went into the investigation of the instrumentation of the TES unit basically showed that commercially available resistance temperature detectors (RTD's) are not suitable for this application. RTD's made of platinum and having a resistance of 100 ohm, appeared not to be appropriate for measuring and controlling the temperature of the TES unit, as the operating temperature is too high for this type of sensor. This fact was consistently pointed out by every vendor that was contacted. Fortunately, the instrumentation was modified to include two chromel-alumel thermocouples which performed well and permitted the control of the unit within the permissible temperature range. The single RTD unit that was installed in the final configuration failed, though it had undergone four temperature cycles prior to its installation.

The phase of the program which is covered by this report was completed with a performance tested Hi-Cap TES unit No. 1. All its design goals were achieved except for he thermal loss through the insulation which exceeds by 8W the design goal that had been set for this operating parameter. This shortcoming can be corrected easily at a later date by modifying the insulation at the terminal ring to prevent heat conduction along the radiation heat shield into the terminal ring.

The insulation container is still provided with the evacuation valve to facilitate, at a later date, the evacuation of the container if the vacuum should have been lost during the shelf time of the TES unit.

APPENDIX A

THERMAL ENERGY STORAGE MATERIAL EVALUATION

During testing of the 1 kW-hr Thermal Energy Storage Demonstration in the first phase as reported in AFAPL-TR-76-110 it became apparent that the thermal energy storage material consisting of a eutectic mixture of LiF, MgF_2 and KF does not release latent heat at a constant temperature, but over a temperature range which was considerably larger than the operating conditions of the Vuilleumier cryogenic cooler would permit. It was, therefore, mandatory to establish the actual material constants for the thermal energy storage material prior to the design of the Hi-Cap thermal energy storage unit. For the investigation of the real behaivor of the thermal energy storage material, the test results from the 1 kW-hr Thermal Energy Storage Demonstration Unit were available. Two additional tests were conducted on the material. The Perkin-Elmer Corporation tested the material in a Differential Scanning Calorimeter DSC-2 and the University of Dayton established the energy content of the material at various temperatures in the drop calorimeter.

Three independent test results were thus available for evaluating the behavior of the thermal energy storage material.

Thermal Energy Storage Demonstration Unit

From the heat balance, it can be established that, neglecting internal heat transfer resistance and temperature gradients,

$$(c_p \times W) \frac{\Delta T}{\Delta t} = P_I - P_L \qquad (A.1)$$

where

P_I = Input Power, watt

P_L = Power Losses, watt

$c_p \times W$ = Effective thermal capacity, J/°F

ΔT = Temperature increase, °F

Δt = Time interval, sec

The power losses from the unit were determined from steady state operating conditions, i.e., $\Delta T/\Delta t = 0$ and thus $P_I = P_L$, to be a function of the temperature differential between the operating temperature of the unit and the ambient temperature.

$$P_L = A(T_o - T_a)^n \tag{A.2}$$

where

T_a = Ambient temperature, °F

T_o = Operating temperature, °F

With the input power known from electrical measurements of the electrical heaters, the apparent thermal capacity of the thermal energy storage unit as a function of the temperature could be calculated from temperature data and the elapsed time.

$$(c_p W) = \left\{P_I - A(T - T_a)^n\right\} / \frac{\Delta T}{\Delta t} \tag{A.3}$$

Calculations which are presented in Figure A-1 produced correlations between apparent thermal capacity and temperature which are shown in Figure A-2.

The thermal capacity shows two peaks, one at 1162°F and the other at 1290°F. For a pure eutectic, one would have expected a single peak at the melting temperature at which the thermal capacity of the melting substance is infinite by definition, i.e.,

```
RUN
15:55 .' JUN 19  TES3...                                    . June 4, 1976

 3.56372E-03   1.54000
  .552780      3.33300E-05
 7726          0              1040.50        600
711
766

271
229.500        -7458.12
619024.         619024.       -22234.0       641258
1040.50         8.79336       0              1031.71

346
308.500        -8193.28
614496.         1.23352E+06   12912.4        1220708
1040.50         16.3394       0              1024.16

413
379.500        -9099.34
609656.         1.84318E+06   104926.        1738350
1040.50         24.4074       0              1016.09

490
451.500        -7845.33
604090.         2.44727E+06   114014.        2333252
1040.50         33.6826       0              1006.92

569
529.500        -7561.85
597386.         3.04465E+06   101047.        2943606
1040.50         44.8563       0              995.644

641
605            -8198.35
590281.         3.63493E+06   135056.        3499878
1040.50         56.6981       0              983.802

711
676            -8329.78
583084.         4.21802E+06   177320.        4040698
1040.50         68.6928       0              971.807

778
744.500        -8592.45
575694.         4.79371E+06   235372.        4558340
1040.50         81.0095       0              959.491

842
810            -8878.71
568238.         5.36195E+06   309146.        5052804
1040.50         93.4373       0              947.063

905
873.500        -8899.36
560660.         5.92261E+06   393068.        5539542
1040.50         106.067       0              934.433

969
937            -8636.73
552751.         6.47536E+06   441354.        6034006
1040.50         119.242       0              921.251
```

Figure A-1. TES Computer Correlations (Sheet 1 of 4)

BEST AVAILABLE COPY

BEST AVAILABLE COPY

```
544787.      7.02015E+06   530307.      6469840
1040.50      132.522       0            907.978

1075
1051.50      -11440.2
537650.      7.55784E+06   704876.      6852962
1040.50      144.349       0            896.151

1119
1097         -12078.0
531430.      8.08927E+06   896362.      7192906
1040.50      154.783       0            885.717

1149
1134         -17540.9
526228.      8.61550E+06   1.19081E+06  7424696
1040.50      163.453       0            877.047

1174
1161.50      -20891.9
522297.      9.13779E+06   1.51996E+06  7617836
1040.50      170.004       0            870.496

1208
1191         -15235.9
518021.      9.65581E+06   1.77529E+06  7880520
1040.50      177.132       0            863.368

1247
1227.50      -13144.8
512645.      1.01685E+07   1.98663E+06  8181834
1040.50      186.091       0            854.409

1265
1256         -28243.5
508384.      1.06768E+07   2.35594E+06  8320902
1040.50      193.194       0            847.306

1279
1272         -36140.5
505967.      1.11828E+07   2.75374E+06  8429066
1040.50      197.222       0            843.278

1293
1286         -35988.4
503837.      1.16966E+07   3.14942E+06  8537230
1040.50      200.771       0            839.729

1309
1301         -31346.3
501541.      1.21882E+07   3.52734E+06  8660846
1040.50      204.598       0            835.902

1350
1329.50      -12125.3
497137.      1.26853E+07   3.70771E+06  8977612
1040.50      211.938       0            828.562

1382
1356         -41082.8
492994.      1.31783E+07   4.10800E+06  9070324
1040.50      218.844       0            821.656

1411
```

Figure A-1. TES Computer Correlations (Sheet 2 of 4)

BEST AVAILABLE COPY

```
 1040.50        224.239        0              816.261

-1422
 1406.50       -15,644.2
 484569.        1.41530E+07    4.61916E+06    9533884
 1040.50        232.218        0              808.282

        OUT OF DATA
>
```

```
 SAVE TES6
ILLEGAL
>SAVE ON TES6
>LIST 10-990
 10 REM TES PROGRAM
 20 PRINT
 30 A=3.56372E-3
 40 N=1.54
 50 B=0.55278
 60 C=3.333E-5
 70 C1=7726
 80 W1=0
 90 P1=1040.5
 100 D1=600
 120 PRINT A,N
 130 PRINT B,C
 140 PRINT C1,W1,P1,D1
 150 INPUT T
 160 OPEN T TO:1,INPUT
 170 INPUT G
 180 OPEN G TO:2,INPUT
 190 S1=0
 200 INPUT :1,X
 220 T0=X
 230 T1=X
 240 INPUT :2,Y
 250 T6=Y
 260 INPUT :1,X
 280 IF X=0 THEN 190
 300 T2=X
 310 INPUT :2,Y
```

Figure A-1. TES Computer Correlations (Sheet 3 of 4)

BEST AVAILABLE COPY

```
340  T4=(T1+T2)/2
350  T3=(T6+T7)/2-70
360  T5=T4-70
370  L1=A*T5**N
380  L2=M1*T8*(B+C*T9)
386  P2=P1-L1-L2
390  E1=P2*D1
400  S1=S1+E1
410  S3=(T2-T0)*C1
420  S2=S1-S3
430  T9=T1-T2

440  C2=1E8
450  IF T9=0 THEN 470
460  C2=E1/T9
470  PRINT T2
480  PRINT T4,C2
490  PRINT E1,S1,S2,S3
500  PRINT P1,L1,L2,P2
600  T1=T2
610  T6=T7
620  GO TO 260
990  END
>
```

```
!EDIT TT
EDIT HERE
*TY1-3
   2.000 188,271,346,413,490,569,641,711,778,842,905,969,1028,1075,1119
   3.000 1149,1174,1208,1247,1265,1279,1293,1309,1350,1362,1391,1422
*EDIT GG
*TY1-3
   1.000 0,0,0,0,0,0,0,0,0,0,0,0,0,0,0,0,0,0,0,0,0,0,0,0,0,0,0,0,0,0,0,0,0
,0

--EOF HIT AFTER    1.
*
```

Figure A-1. TES Computer Correlations (Sheet 4 of 4)

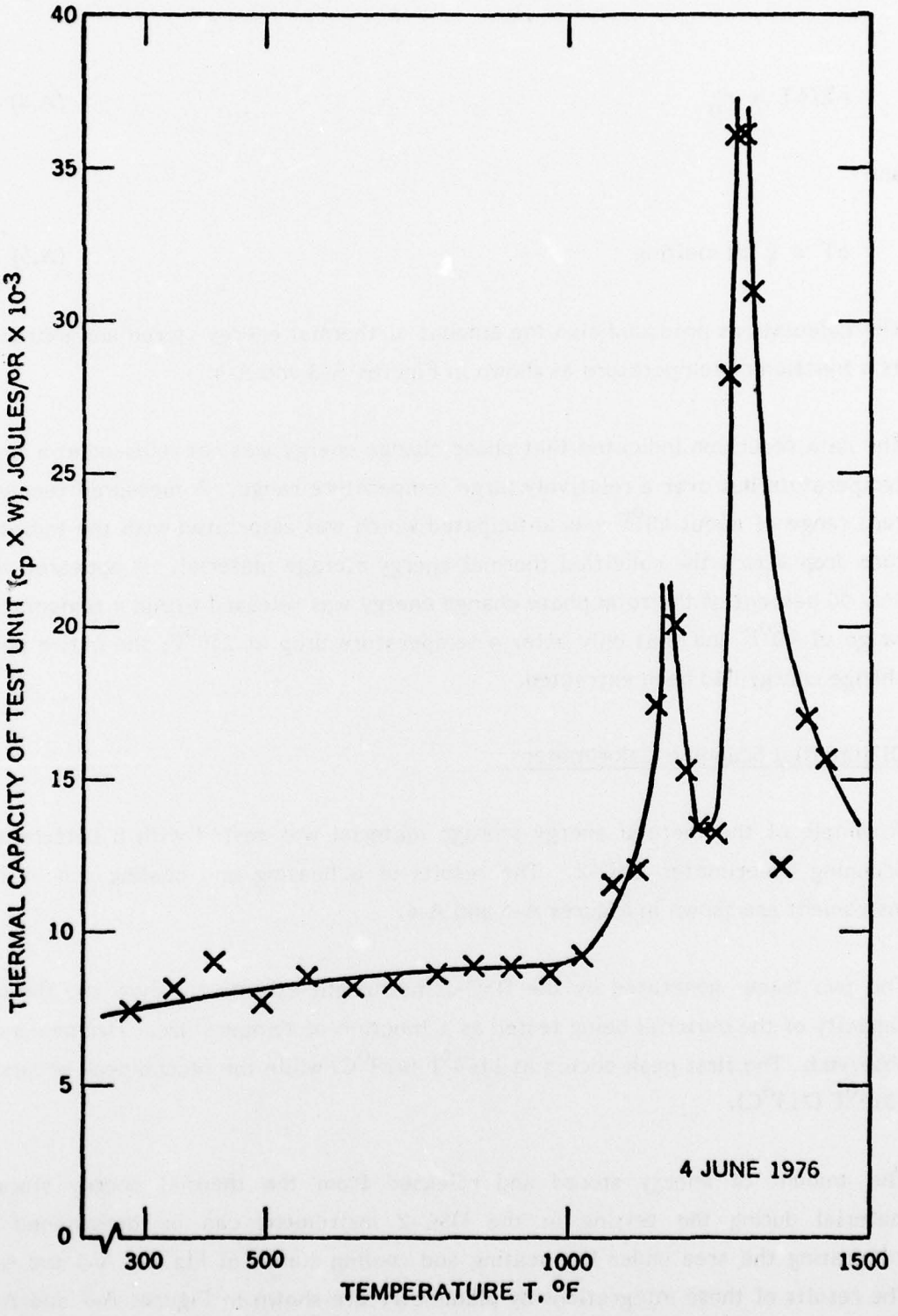

Figure A-2. Apparent Thermal Capacity of Thermal Energy Storage Unit During Discharge

$$\Delta E/\Delta T = c_p \qquad (A.4)$$

and

$$\Delta T = 0 \text{ at melting} \qquad (A.5)$$

The calculations produced also the amount of thermal energy stored and extracted as a function of temperature as shown in Figures A-3 and A-4.

The data reduction indicated that phase change energy was not released at a single temperature but over a relatively large temperature range. A measured temperature range of about $40^{\circ}F$ was anticipated which was associated with the temperature drop across the solidified thermal energy storage material. It appeared that only 50 percent of the total phase change energy was released within a temperature range of $40^{\circ}F$ and that only after a temperature drop of $250^{\circ}F$, the entire phase change energy had been extracted.

Differential Scanning Calorimeter

A sample of the thermal energy storage material was tested with a Differential Scanning Calorimeter DSC-2. The results of a heating and cooling run in this instrument are shown in Figures A-5 and A-6.

The two traces generated by the DSC-2 instrument effectively show the thermal capacity of the material being tested as a function of temperature. Two peaks are observed. The first peak occurs at $1164^{\circ}F$ ($629^{\circ}C$) while the second peak occurs at $1315^{\circ}F$ ($713^{\circ}C$).

The amount of energy stored and released from the thermal energy storage material during the testing in the DSC-2 instrument can be determined by integrating the area under the heating and cooling curves of Figures A-5 and A-6. The results of these integrations by planimetry are shown in Figures A-7 and A-8.

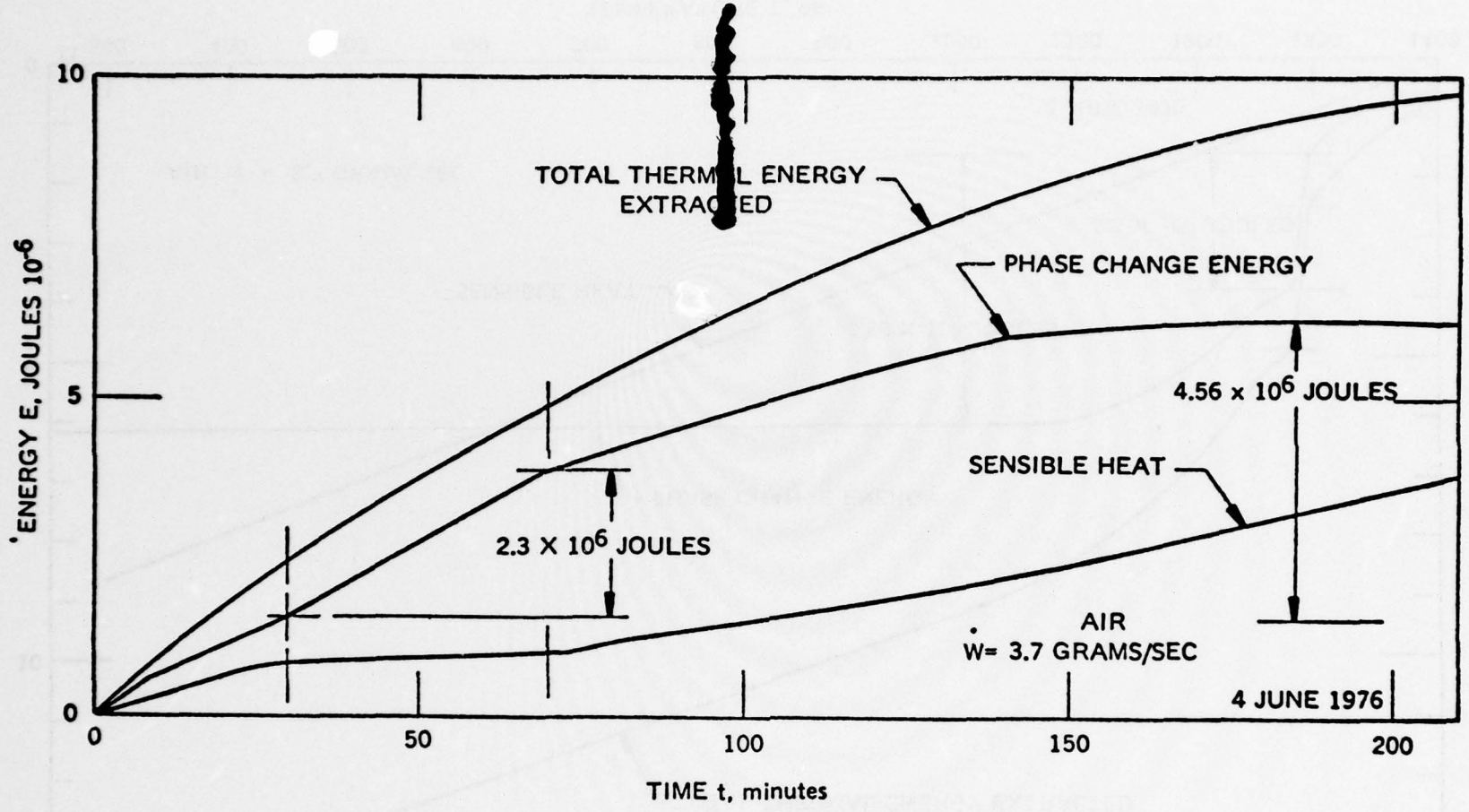

Figure A-3. Extracted Energy (Cooling by Thermal Losses and by Flowing Air

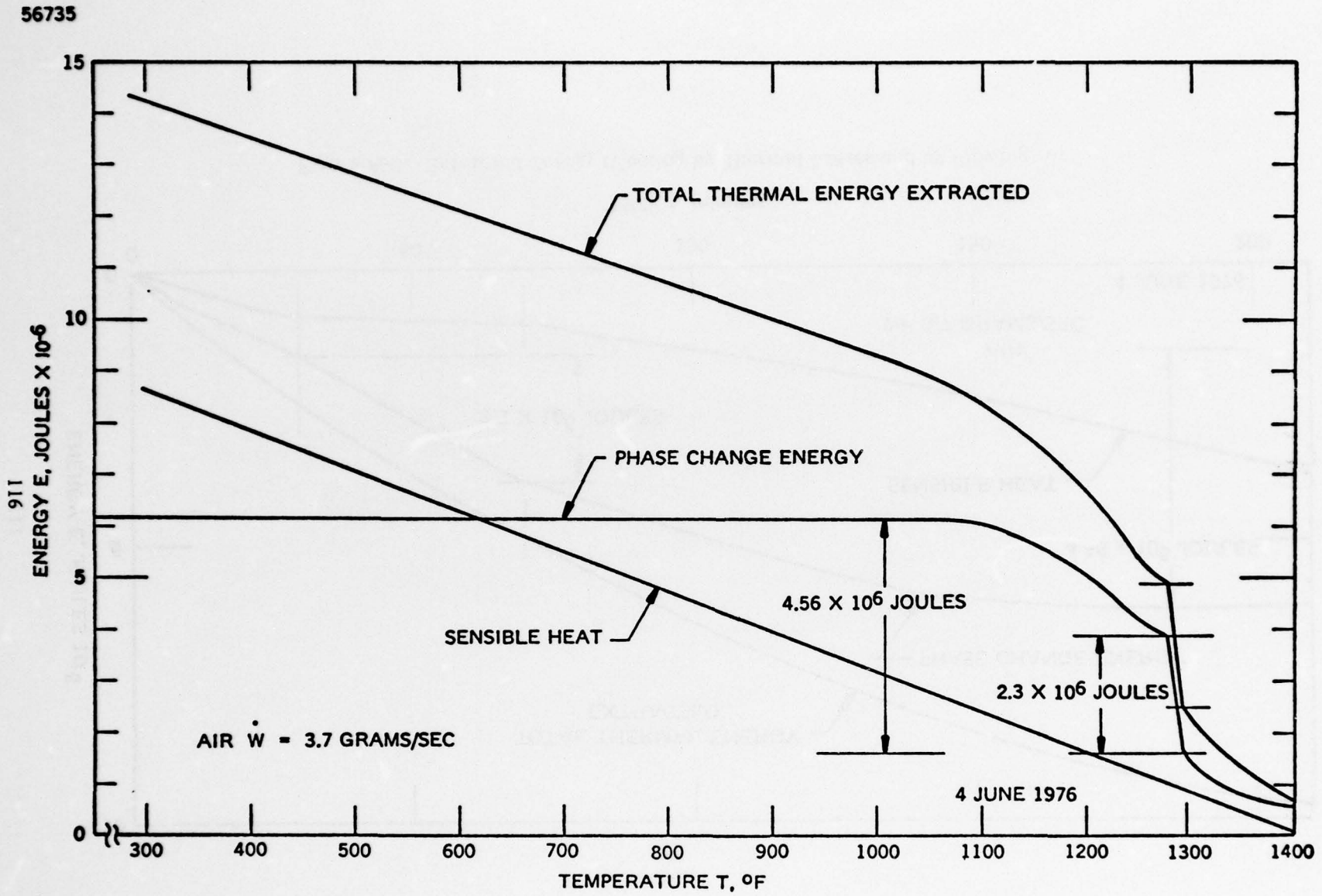

Figure A-4. Extracted Energy (Cooling by Thermal Losses and by Flowing Gas

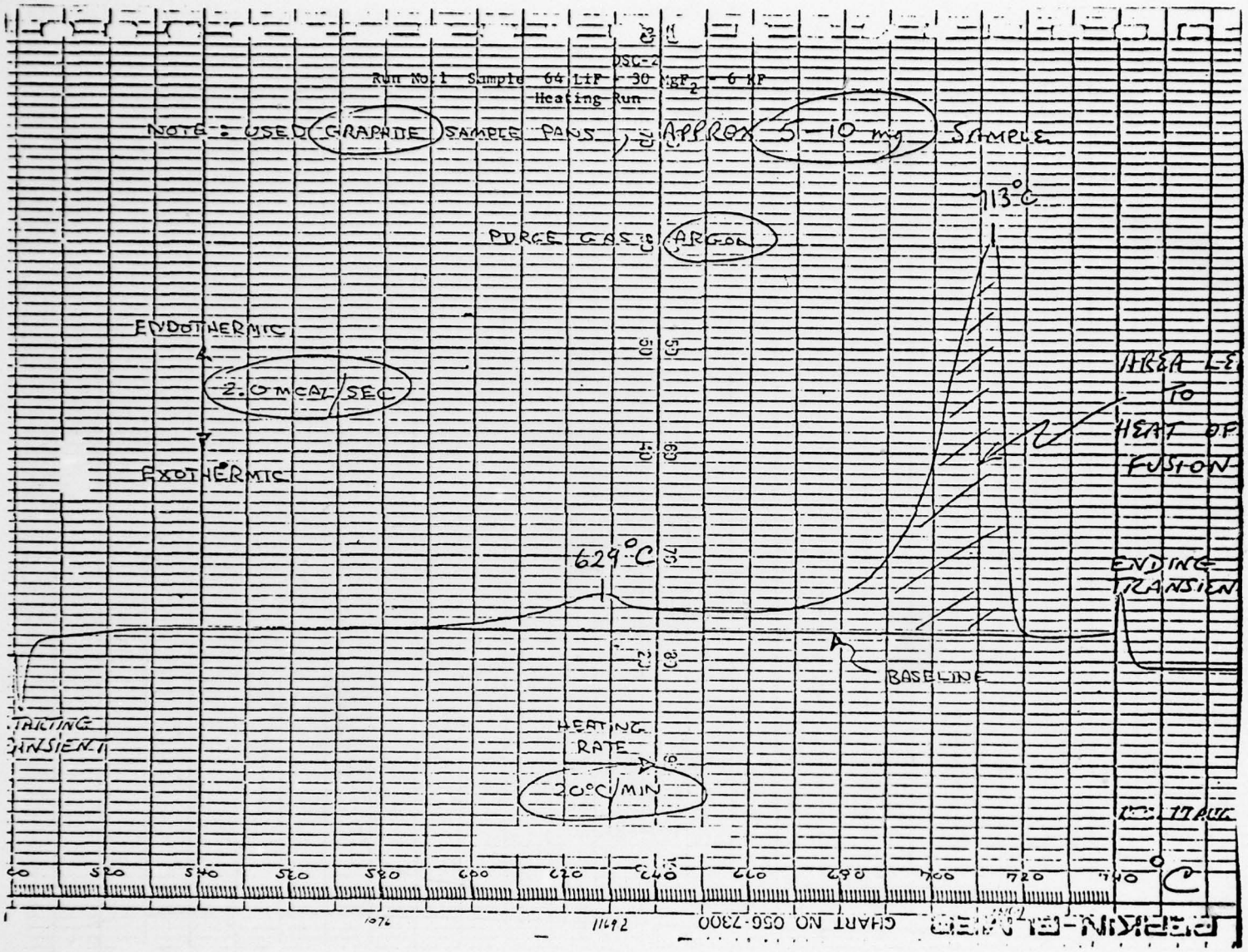

Figure A-5. Run No. 1 Sample 64 LiF - 30 MgF_2 - 6 KF Heating Run

BEST AVAILABLE COPY

BEST AVAILABLE COPY

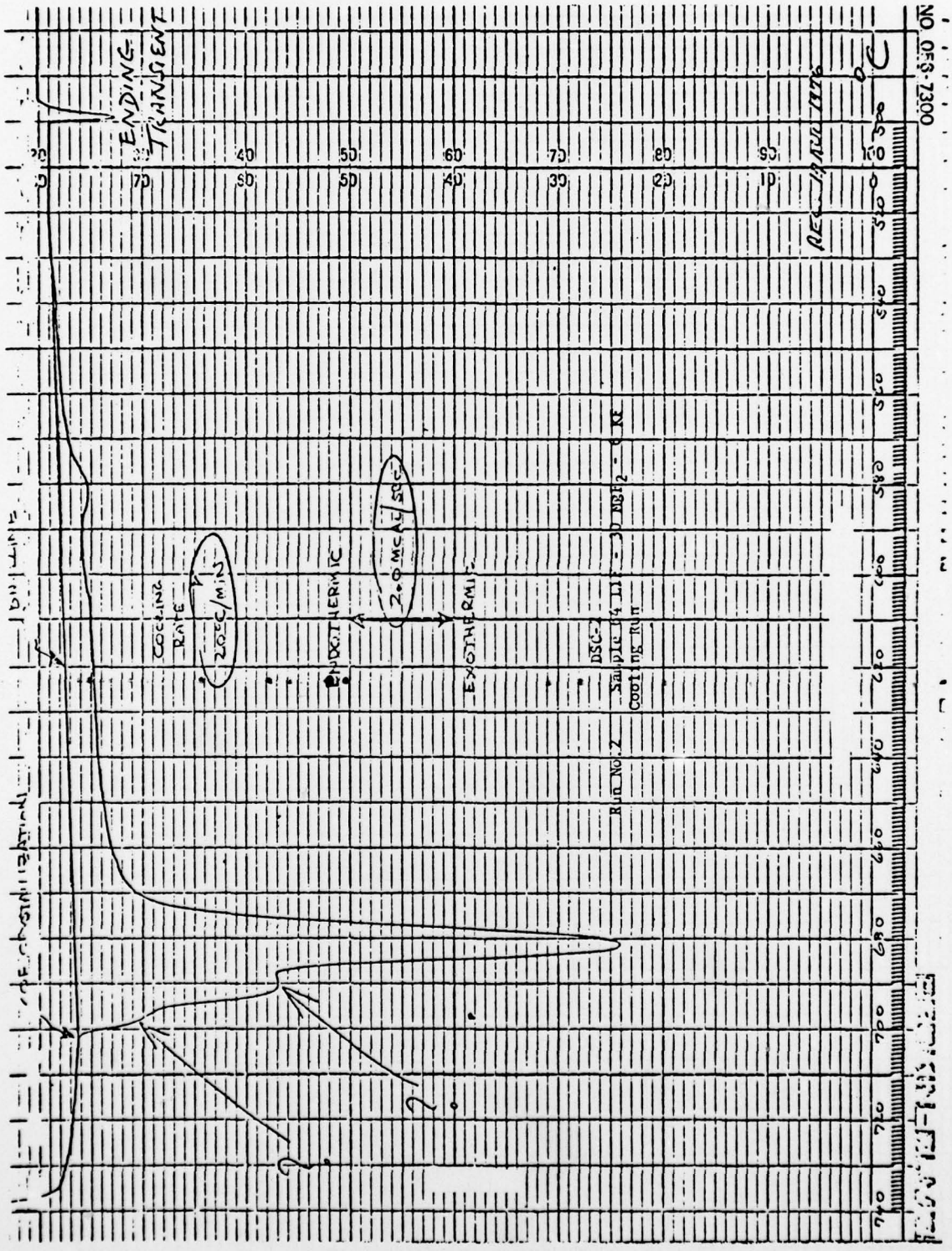

Figure A-6. Run No. 2 Sample 64 Lif - 30 MgF_2 - 6 KF Cooling Run

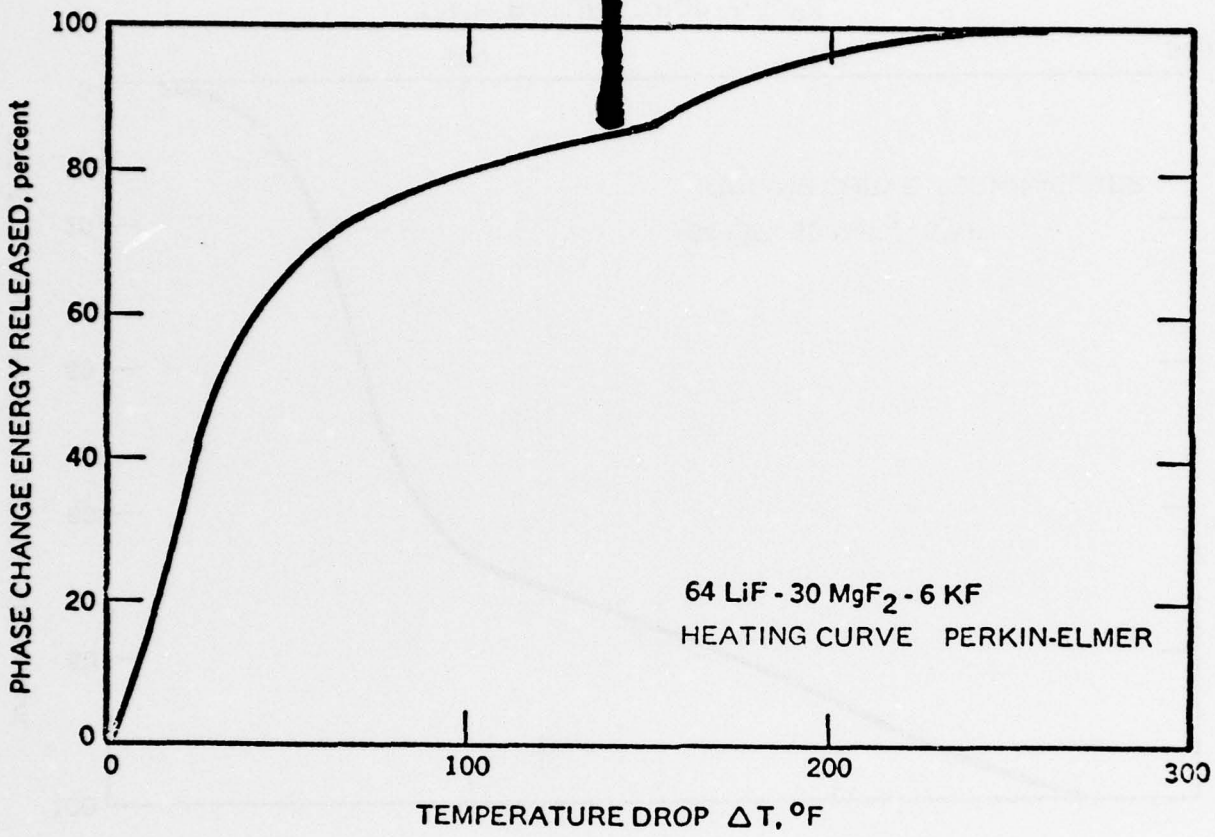

Figure A-7. Relative Energy Extraction from Thermal Energy Storage Material (Starting Temperature 1328°F)

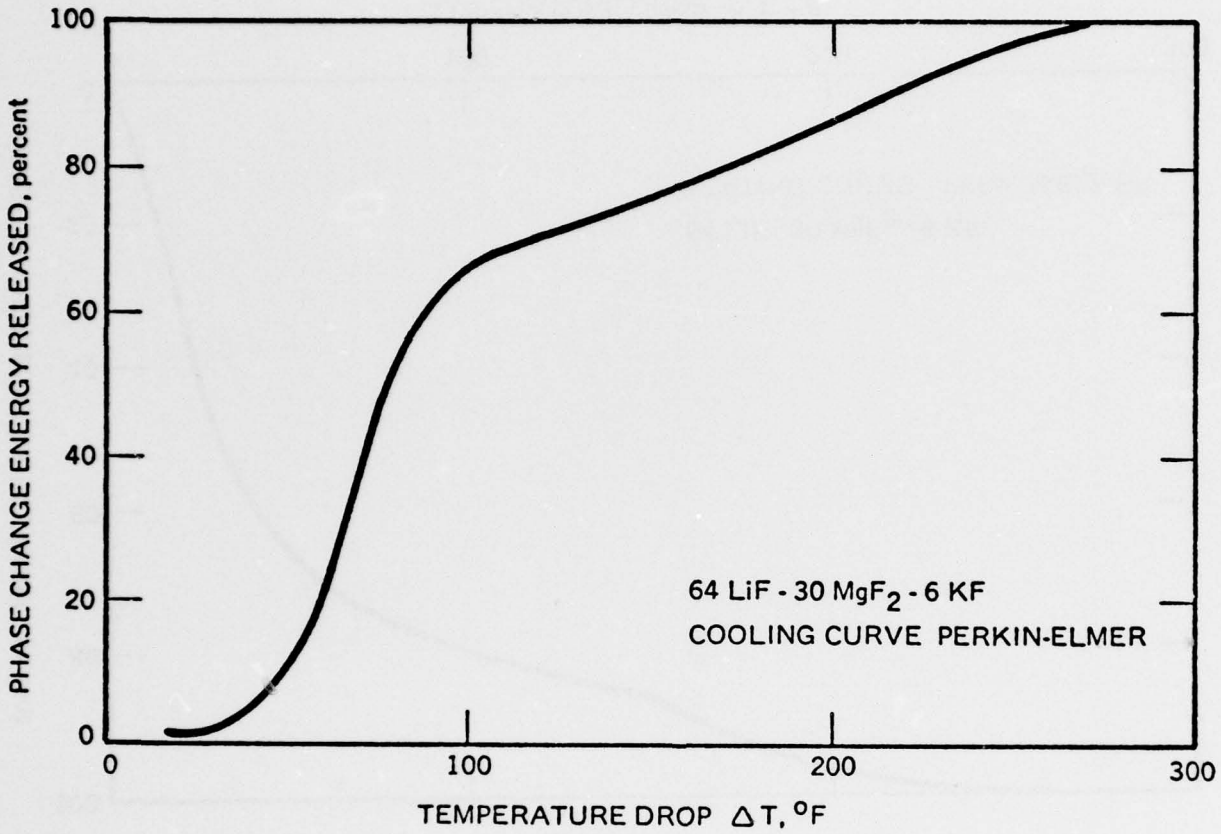

Figure A-8. Relative Energy Extraction From Thermal Energy Storage Material (Starting Temperature 1328°F)

These curves show the same trend which was observed for the test data of the thermal energy storage unit. The phase change energy was neither absorbed nor released at a single temperature or over a narrow band, but over a wide temperature range.

The energy storage in the eutectic appeared to be nearly identical for the cooling and for the heating curve, though the temperatures seemed to be displaced by about 48°F. Further investigation into subcooling of the material and the effect of heating and cooling rates has to clarify this difference.

Drop Calorimeter Test

At the University of Dayton, a calorimetric investigation of the same energy storage salt was conducted in a drop calorimeter. Data from these tests are reproduced in Table A-1 and are plotted in Figure A-9. The results clearly indicate the same trend which was discovered during the testing of the thermal energy storage demonstration unit and which were graphically produced by the DSC-2 instrument. Two relations for the specific heat of the eutectic, solid and liquid were presented.

(a) Solid $H(T) - H(T_{ref}) = -312.8 + 2.025T$ joules/gram ($T\ ^{o}C$)

(b) Liquid $H(T) - H(T_{ref}) = 1219.6 + 0.9769T$ joules/gram ($T\ ^{o}C$)

With the assumption that the melting temperature of the eutectic is 705°C, as stated in the report (*), the fusion energy would be calculated from these relations to be 793.5 joules/gram. If this value is traced down on the graph of the experimental data (Figures A-9), it is seen that the "fusion" energy is extracted over a temperature range of 50°C (90°F). The total calculated fusion energy is also only 84.1 percent of the fusion energy based on ideality.

(*) EVALUATION OF INORGANIC OXIDES FOR THERMAL ENERGY STORAGE, BiMonthly Progress Report, University of Dayton, Research Institute. Contract No. F33615-76-C-2096.

TABLE A-1

EXPERIMENTAL DATA FOR THE DETERMINATION OF THE

HEAT CONTENT OF THE LiF-MgF_2-KF SPECIMEN

Specimen Temperature (°C)	Potentiometer Deflection (cm)	Mass		Heat Content (joules/gram)
		Fluoride (grams)	Stainless Steel (grams)	
165	2.461	8.54	5.46	115.5
276	6.350	9.29	6.95	285.1
341	7.144	8.54	6.95	314.5
389	10.636	9.29	6.95	520.0
408	10.478	9.29	6.95	493.9
435	11.192	9.29	6.95	526.9
436	9.604	8.54	5.46	549.7
474	10.676	8.54	5.46	617.4
476	13.256	9.29	6.95	650.9
488	11.351	8.53	5.46	669.7
537	12.422	8.54	5.46	726.9
539	14.764	9.29	6.95	716.0
559	15.081	9.29	6.95	724.4
562	14.049	8.54	5.46	860.3
591	16.113	9.29	6.95	777.5
598	13.970	8.53	5.46	819.6
622	16.193	8.53	5.46	1012.6
636	20.082	9.29	6.95	1047.3
644	17.145	8.53	5.46	1084.7
681	18.574	8.53	5.46	1189.4
715	18.455	6.87	3.81	1806.6
720	26.789	7.06	6.00	1890.7
723	28.178	7.06	6.00	2017.7
733	19.249	6.87	3.81	1898.2
739	26.392	9.15	5.31	1920.3
740	26.988	9.21	5.31	1976.6
754	26.194	10.29	5.04	1891.9
755	20.241	6.87	3.81	2013.7

Reference:

EVALUATION OF INORGANIC OXIDES FOR THERMAL ENERGY STORAGE
BiMonthly Progress Report
Contract No. F33615-76-C-2096
For Period Ending 15 August 1976
University of Dayton Research Institute, Dayton, Ohio 45469

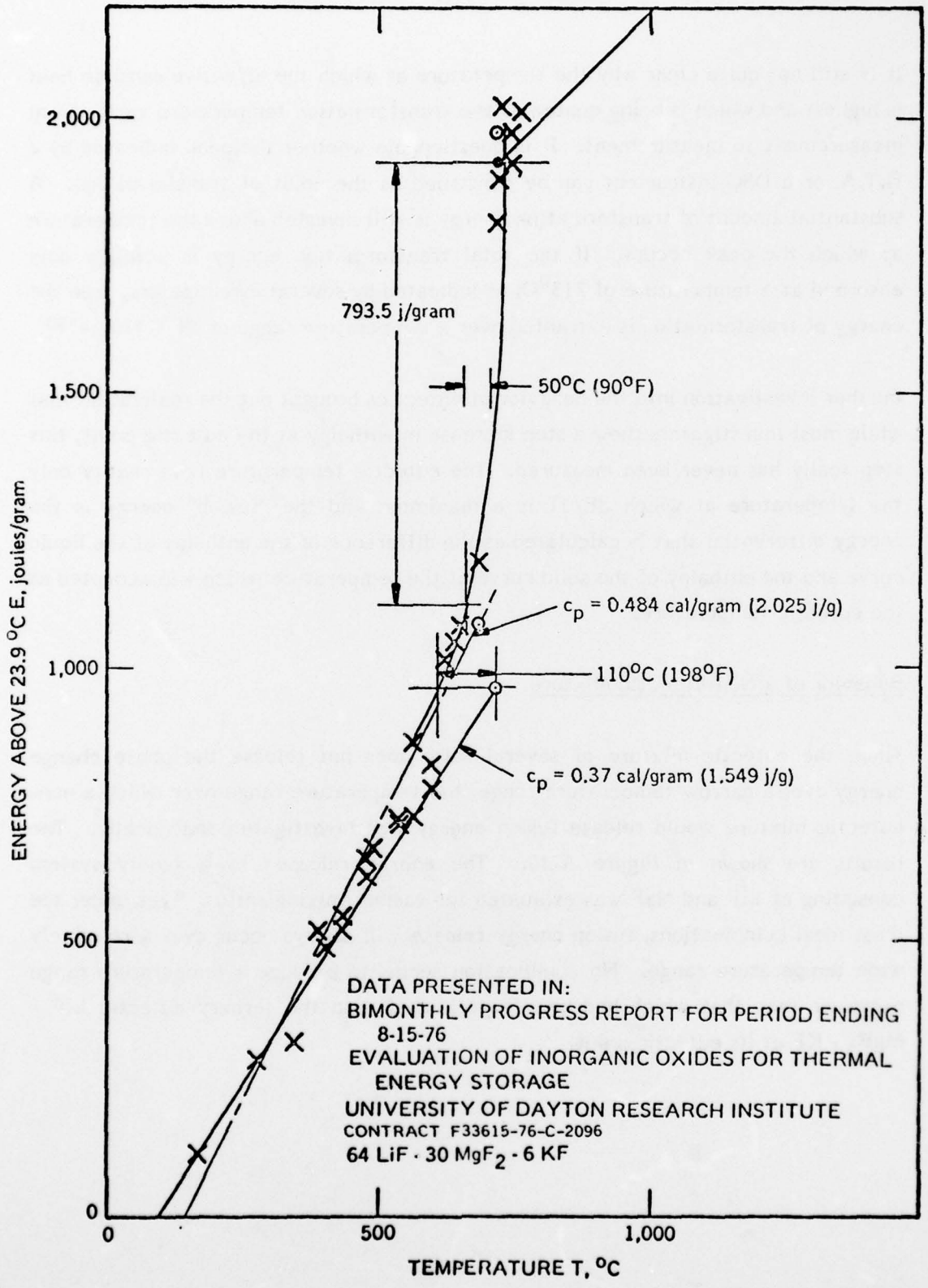

57322

Figure A-9. Thermodynamic Data Obtained by Drop-Calorimeter Technique

It is still not quite clear why the temperature at which the effective sensible heat is highest and which is being quoted as the transformation temperature varies from measurement to measurement. It is questionable whether the peak indicated by a D.T.A. or a DSC instrument can be construed as the point of transformation. A substantial amount of transformation energy is still invested above the temperature at which the peak occurs. If the total transformation energy is actually only absorbed at a temperature of 713°C, as indicated by several investigators, then the energy of transformation is extracted over a temperature range of 58°C (104.4°F).

Further investigation into the behavior of eutectics brought out the realization that while most investigators show a step increase in enthalpy at the eutectic point, this step really has never been measured. The eutectic temperature is in reality only the temperature at which dE/dT is a maximum and the "fusion" energy is the energy differential that is calculated as the difference of the enthalpy of the liquid curve and the enthalpy of the solid curve at the temperature which was accepted as the eutectic temperature.

Behavior of a Non-Eutectic Mixture

Since the eutectic mixture of several salts does not release the phase change energy over a narrow temperature range, the temperature range over which a non-eutectic mixture would release fusion energy was investigated analytically. The results are shown in Figure A-10. The energy released by a binary system consisting of LiF and NaF was evaluated for various mixing ratios. Even under the most ideal combinations, fusion energy release will always occur over a relatively wide temperature range. No combination seems to produce a temperature range narrower than that which had been experienced with the ternary eutectic LiF - MgF_2 - KF at its eutectic point.

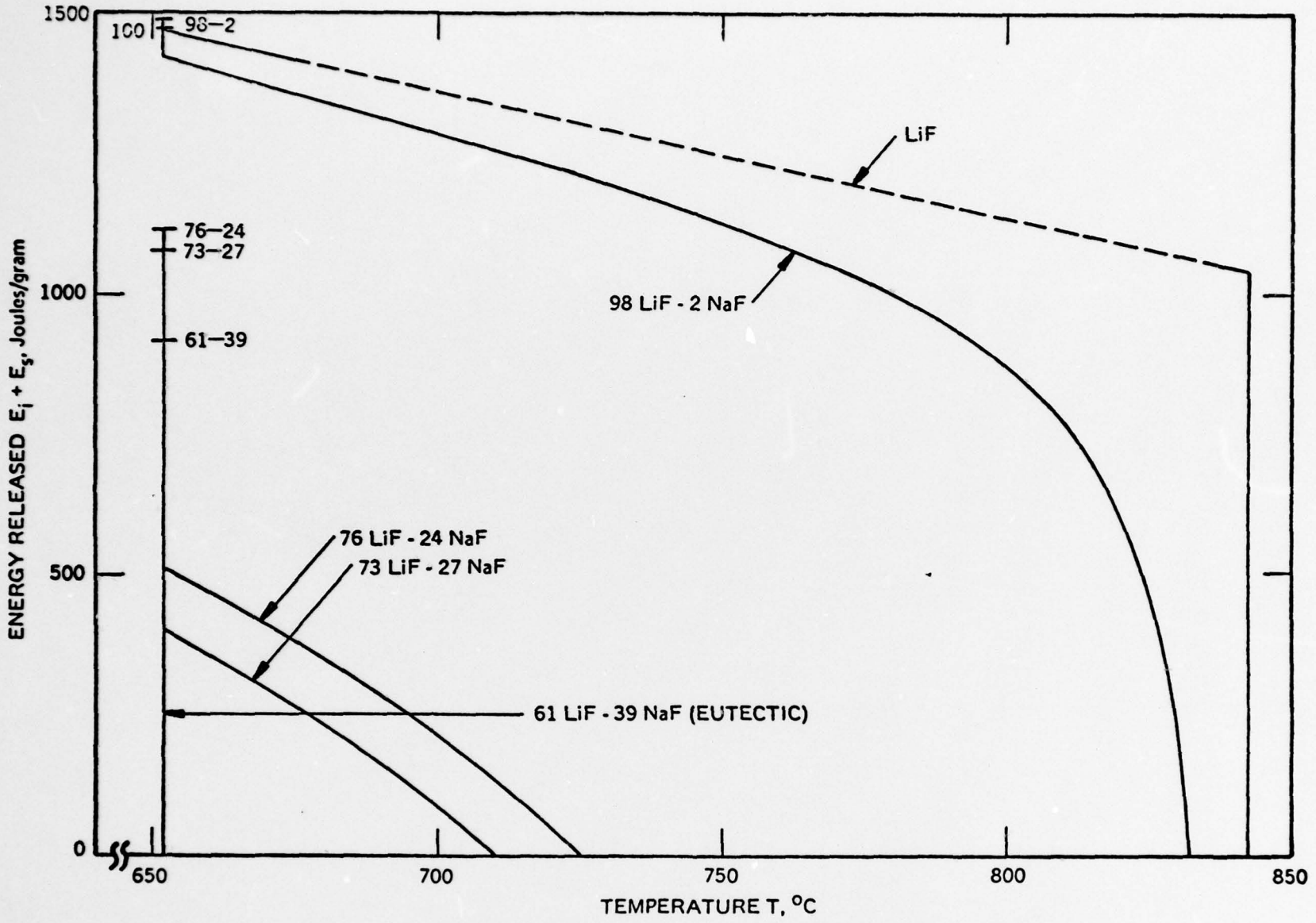

Figure A-10. Effect of Composition of the Energy Release Between Liquids and Solidus

*U.S. Government Printing Office: 1978 — 757-080/503